EROSION AND RELEASE FROM BIODEGRADABLE POLYANHYDRIDES

by

Lisa Y. Shieh

B.S. Chemical Engineering, Purdue University (1989)

Submitted to the Harvard-MIT Division of Health Sciences and Technology
in partial fulfillment of the requirements for the degree of

Doctor of Philosophy
at the
Massachusetts Institute of Technology

February 1995

Signature of Author.....
Harvard-MIT Division of Health Sciences and Technology
January 13, 1995

Certified by .....
Robert Langer
Germeshausen Professor of Chemical and Biomedical Engineering
Thesis Supervisor

Accepted by.....
Roger Mark
Chairman, Department Graduate Committee

EROSION AND RELEASE FROM BIODEGRADABLE POLYANHYDRIDES

by
Lisa Y. Shieh

Submitted to the Harvard-MIT Division of Health Sciences and Technology on January 13, 1995 in partial fulfillment of the requirements for the degree of Doctor of Philosophy

ABSTRACT

Degradable polymers are becoming increasingly useful in consumer and medical applications. Some advantages of using polymers for controlled release applications include the ability to localize and sustain desired concentrations at the chosen site, thus avoiding systemic side effects. The polymer may also protect the encapsulated drug until released, thus increasing the half-life of potentially very unstable drugs. Finally, with biodegradable polymers, there is no need for additional surgery for device removal.

It has been suggested that hydrophobic polyanhydrides might be a promising class of erodible polymers. They are one of few synthetic degradable systems with regulatory approval from the FDA for use in human clinical trials. In this thesis, we describe studies investigating the erosion and release from Poly (Fatty Acid Dimer: Sebacic Acid) polyanhydride, p(FAD:SA), which has been approved for clinical trials in the treatment of osteomyelitis.

Polymer hydrophobicity, crystallinity, and monomer diffusion out of the polymer (all controlled by copolymer composition), played a role in the erosion of p(FAD:SA). Increasing the hydrophobic monomer (FAD) content up to 50 wt% in the copolymer resulted in longer erosion, whereas further increases up to 70 wt% decreased the erosion period. Much faster degradation was found in p(FAD:SA) 70:30 compared to the more crystalline copolymers of higher SA content. P(FAD:SA) also displayed certain surface eroding characteristics, such as material loss from the outside to the inside of the matrix (erosion zone), erosion rate that was not dependent on the matrix volume, thicker samples with longer lifetimes, and low water uptake into the polymer interior.

Another objective was to investigate the factors controlling drug release from polyanhydride systems. By reducing drug particle size within the matrix, we could decrease a drug's initial "burst" during release from 25% to 4% of total drug incorporated. Acid Orange release followed SA erosion, and released faster than the more hydrophobic dye, Rhodamine B Base.

Finally we investigated the potential of p(FAD:SA) to release proteins. Fabrication procedures only reduced 10-20% of the incorporated protein's activity. Peroxidase was released over a one week period, and enzyme activity was retained over the first half of release. However, activity dropped from 80% of initial activity down to 0% from 5 - 8 days. Size exclusion chromatography indicated the presence of aggregated protein during this time. Polymer hydrophobicity and acidic environment within the polymer during release may have contributed to the loss of protein activity.

Thesis Supervisor: Professor Robert Langer
Title: Germeshausen Professor of Chemical and Biomedical Engineering

Acknowledgements

I would like to thank everyone in the lab over the past five years who have made my experience in Langer Labs a really great one. I think our lab is unique in that we have so many people from different backgrounds all with diverse areas of expertise (not to mention fun and interesting personalities!) Hopefully we will all continue to meet throughout our careers and future.

I would like to thank Bob Langer for his guidance, support, generosity, and enthusiasm over the years. He has provided many opportunities for me that would never have been available without his support. I would also like to thank the members of my thesis committee Edward Merrill and Alan Grodzinsky, who have been very supportive and understanding. Also lab would not be the same without the help of Pam Brown, who was always there with a friendly helping hand! I also appreciate the support of Roger Mark and Keiko Oh of HST.

There are many visiting scientists, post docs, graduate students, and undergraduates who have helped contribute to my work throughout the years. Janet Tamada helped me start my thesis project. I am grateful to Avi Domb and Manoj Maniar who, while at Nova Pharmaceuticals, synthesized the polymers that were used in this thesis. Ruxandra Gref was always generous with her help and suggestions. Many thanks go to Michael Cardamone (also my gel mentor and biochemistry tutor), Steve Schwendeman, Rick Costantino, and Masa Chiba for their contribution to the protein work of my thesis. I greatly appreciate the help of several undergraduates who have worked with me: Irene Chen, Judy Pang, Julie Chang, and Francine Wang.

I would also like to acknowledge the financial support of a NSF Graduate Fellowship and NIH Grant CA5257.

Finally I would like to thank my parents, my sister Mae-Mae, and Bernard, for their constant support and encouragement throughout my work on this thesis.

Table of Contents

List of Figures

List of Tables

CHAPTER 1

INTRODUCTION

1.1 Motivation

Degradable polymers are becoming increasingly useful in consumer and medical applications. Designing consumer products (such as garbage bags and diapers) with polymers that degrade would reduce environmental waste build-up. Biocompatible degradable polymers are being considered for use in such medical applications as scaffolds for tissue regeneration, resorbable sutures, stents, and drug delivery systems. Advantages of using polymeric drug delivery devices include the ability to localize and sustain desired concentrations at the chosen site, thus avoiding systemic side effects and improving the patient's quality of life. Barriers can be bypassed (e.g. blood brain barrier) by implanting devices directly at the desired site. The polymer also protects the encapsulated drug until released, thus increasing the half-life of potentially very unstable drugs. Smaller drug doses are needed, which would be advantageous if the drug is expensive or scarce. Finally, with biodegradable polymers, there is no need for additional surgery for device removal.

Currently, the most widely used implantable degradable polymer are the poly α-esters, in particular poly(glycolic acid) and poly (lactic acid) and their copolymers poly(lactic/glycolic) acid {P(LGA)}. These FDA approved polymers are used in resorbable sutures and injectable drug delivery systems. P(LGA) polymers display bulk erosion characteristics [1] (i.e.. polymer mass is lost uniformly throughout the matrix, erosion rates are dependent on the volume of the matrix rather than its thickness, and the lifetimes of different thickness samples are the same [2]). In contrast, surface eroding systems display material loss from the outside to the inside of the matrix, erosion rate is dependent on the surface area rather than the volume of the polymer matrix, and thicker samples have longer lifetimes [2]. For controlled drug delivery applications, a surface eroding device is often desirable. Polymers undergoing surface erosion can provide easily controllable and zero-order drug release rates (when a thin slab geometry is used), and protect the drug from the harsh in vivo environment.

1.2 Choice of polymer

Polyanhydrides are a class of bioerodible polymers that were developed specifically for controlled release drug applications and display certain features characteristic of surface erosion [3]. It has been suggested that hydrophobic polyanhydrides might be a promising class of erodible polymers. They are one of few synthetic degradable systems with regulatory approval from the Food and Drug Administration for use in human clinical trials. Probably the most well studied polyanhydride being developed for clinical use is the (1) Poly[1,3-bis(p-carboxyphenoxy)propane:Sebacic acid] {p(CPP:SA)} copolymer (see Figure 1.1). A phase III clinical study using P(CPP:SA) incorporated with carmustine (BCNU) to treat recurrent malignant gliomas has just been completed, and the effect of treatment was found to be statistically significant [4].

The poly (Fatty acid dimer:Sebacic acid) {p(FAD:SA)} copolymer [5] (see Figure 1.1) is a much newer polyanhydride that has some advantages over the p(CPP:SA) copolymer. The monomers of p(FAD:SA) are readily available and naturally occurring [6]. The p(FAD:SA) copolymer is simpler and less expensive to synthesize than the p(CPP:SA) [6]. It also has some more suitable physical properties for fabrication (more flexible, lower melting point, higher solubility in some organic solvents, higher mechanical strength [5]) than p(CPP:SA), and can be easily processed and shaped into desired delivery devices such as slabs, microspheres, films, and rods. P(FAD:SA) also degrades into liquid materials (as opposed to hard, sharp materials), which is important when in contact with sensitive tissue [6]. The biocompatibility of p(FAD:SA) has been evaluated[7], and the Food and Drug Administration has approved p(FAD:SA) for human clinical trials in the treatment of osteomyelitis..

1.3 Specific Aims

The polyanhydrides, with their potential as surface eroding polymers, are thus interesting and useful polymers to study. Many [1, 3, 8, 9] have carefully

P(FAD-SA)

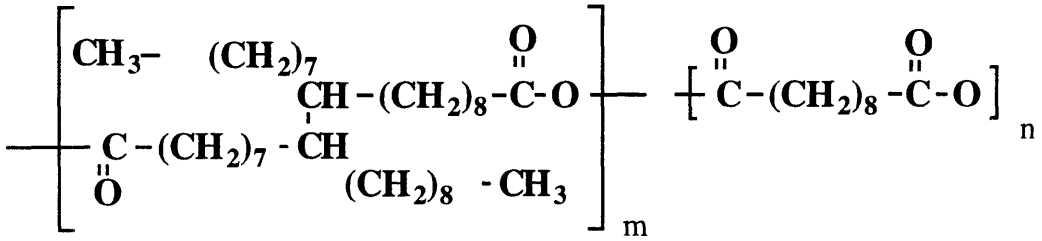

fatty acid dimer (FAD) sebacic acid (SA)

P(CPP-SA)

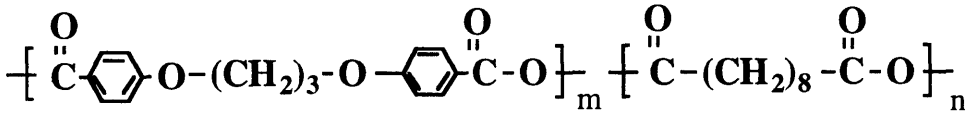

bis(p-carboxyphenoxy) propane (CPP) sebacic acid (SA)

Figure 1.1 Chemical structure of p(FAD:SA) and p(CPP:SA)

studied the erosion and drug release from p(CPP:SA) (see Section 2.2). However, there have been few fundamental studies investigating the erosion and drug release from the recently developed p(FAD:SA) system. We wanted to understand what effect substitution of the FAD monomer for the CPP monomer had on copolymer erosion properties and how applicable previous p(CPP:SA) erosion findings are to p(FAD:SA). We wanted to investigate what type of erosion (such as surface, bulk, or both) was occurring in p(FAD:SA), and how we can control the erosion. We hypothesized varying copolymer composition would affect the copolymer physical properties. This would affect steps in the erosion process and thus affect overall erosion.

With a better understanding of the underlying erosion of p(FAD:SA), we can move on to investigate drug release from p(FAD:SA). The effect of drug incorporation method, copolymer composition, initial drug loading, and drug solubility will be investigated. Finally, we will study the potential of p(FAD:SA) in the delivery of proteins. The area of protein release from polymers is challenging in that proteins are extremely fragile, and thus fabrication and subsequent release of proteins often prove difficult.

1.4 Outline of thesis

The thesis begins with a brief background on bioerodible systems and previous work done with polyanhydrides, which is described in Chapter 2. Then the thesis objectives are outlined in Chapter 3. Chapters 4 - 6 describe the majority of the thesis work, which is divided into three main sections:

Chapter 4 Characterization of p(FAD:SA) erosion

Chapter 5 Release of model drugs from p(FAD:SA)

Chapter 6 Release of model proteins from p(FAD:SA)

Finally, Chapter 7 discusses the conclusions and future work.

CHAPTER 2

BACKGROUND

2.1 Bioerodible Systems

Degradation of polymers can vary from surface (heterogeneous) erosion to bulk (homogeneous) erosion. Most real systems erode by some combination of both mechanisms. Surface erosion occurs when the erosion takes place only at the surface of the polymer (analogous to peeling an onion layer by layer). Bulk erosion occurs when the entire polymer, including the interior, undergoes erosion.

Often it is desirable to have a polymer system that erodes purely by surface erosion. There are many advantages of a surface eroding system. Zero-order (constant) release of a drug can be obtained. The release kinetics of such a system would be easier to predict and control. The drug release would be proportional to the drug loading, and the lifetime of the system would be proportional to the thickness of the device. Unfortunately, polymeric systems that degrade by pure surface erosion are difficult to develop. Most polymeric systems erode by some combination of both surface and bulk erosion. Therefore both the erosion of the device and the diffusion of the monomer and drug through the polymer are determinants of drug release. Consequently, producing zero-order release is more difficult.

To be clinically useful the material must also satisfy other criteria. The polymer must be biocompatible with the body, with no adverse tissue reaction. It must also erode into non-toxic degradation products that are readily eliminated or metabolized in the body. From a physical standpoint, the device should be of high enough mechanical integrity to avoid any undesirable burst of its contents. It would also be desirable to develop a polymer that can be chemically altered to change its physical properties which could affect erosion characteristics. The polymer should also be easily synthesized, stable on storage, and reasonable in cost.

Examples of bioerodible systems include poly-lactic acid, polyaminoacids, polyorthoesters, and polyanhydrides. For drug delivery, it is often desirable to have

a system that undergoes surface erosion. Unfortunately most systems degrade by bulk erosion (eg. poly(lactide-co-glycoside) copolymers [10]). Other polymers do undergo surface erosion, but additives are needed (eg. polyorthoesters) [11].

The polyanhydrides appear to show many characteristics of a surface eroding polymer, and are interesting and useful to study. The polyanhydrides are one of few bioerodible systems with FDA regulatory approval for use in human clinical trials. Degradation of these polymers occurs by hydrolysis of the anhydride linkage. By changing the ratio of monomers (x:y) in these copolymers, the physical properties of the copolymer can be altered (eg. crystallinity, hydrophobicity). Theoretically the polymer degradation and release behavior from the polymer can also be varied. If the polymer is sufficiently hydrophobic and/or crystalline to inhibit water penetration into the interior, then surface erosion may be achieved. If water is allowed to penetrate the interior of the polymer, then bulk erosion will also occur.

The erosion of biodegradable polymers such as the polyanhydrides involves a number of steps, any of which can be rate limiting [12]. First there must be water contact with the labile polyanhydride bond. This can occur directly at the surface of the polymer, or by imbibition into the polymer interior. The polymer degrades into monomers or oligomers as the anhydride bonds are hydrolyzed. These degradation products then dissolve according to their aqueous solubility. If erosion has taken place in the interior of the polymer, the products must then diffuse out to the surface of the polymer. Degradation products at the surface are removed to the bulk solution by external mass transfer convection and diffusion. The combination of all these steps leads to the appearance of monomers in solution.

2.2 p(CPP:SA) copolymer characterization studies and development

Leong et al. [13] have conducted a number of characterization studies with a variety of p(CPP:SA) polyanhydrides. They found that the identity of polyanhydrides could be readily confirmed by infrared spectra (IR). The doublet occurring between 1670 cm^{-1} and 1800 cm^{-1} was characteristic of the carboxylic anhydride.

Ron [14] and Mathiowitz [15] determined copolymer composition and comonomer sequence distributions in polyanhydride copolymers using the techniques of nuclear magnetic resonance (NMR) spectroscopy. They also used X-ray powder diffraction combined with differential scanning calorimetry (DSC) to determine the degree of crystallinity of different copolymer compositions. The degree of crystallinity plays a major role in preventing water penetration into the polymer interior, thus preventing bulk erosion. Crystalline regions also are thought to erode more slowly than amorphous regions. They found a high degree of crystallinity at high mole ratios of either aliphatic or aromatic diacids, while copolymers with almost equal ratios of monomer were amorphous. [14]

Leong et al.[13] have also reported degradation studies of the CPP:SA polyanhydrides. They found they could obtain a wide range of degradation rates and lifetimes of polymeric devices (1 week to several years) by changing the monomer ratio of CPP to SA. The more hydrophobic polymers, p(CPP) and (CPP:SA) 85:15, displayed constant erosion kinetics over several months. The degradation rates increased with copolymerization of SA (an 800 times increase with 80% SA content). They also found that by changing the polymer backbone (by adding methylene groups) they were able to render the polymer more hydrophobic and decrease the reactivity of the anhydride linkage. This resulted in a substantial decrease in erosion rates. Degradation of these polyanhydrides was also determined to be pH sensitive. Erosion rates increased at high pH, and decreased under acidic conditions.

More recently, Tamada et al. have proposed a mechanism for the erosion of the p(CPP:SA) copolymer [12]. In erosion studies with p(CPP:SA), it was found that the SA-SA and SA-CPP bonds are more labile than the CPP-CPP bonds. The SA leaves more rapidly than the CPP, leaving behind a disk containing mainly CPP, which dissolves at a much slower rate. They also reported the presence of an erosion zone in these polyanhydride devices [16]. The erosion zone is a fragile, porous zone, which grows from the outside to the inside of the polymer. In the p(CPP:SA) system, the outer zone is mainly composed of CPP-CPP bonds, whereas the inner intact zone keeps the physical appearance of the original polymer.

Tamada et al. also compared the erosion of p(CPP:SA) with the polyester poly(lactic/glycolic) {P(LGA)}[16]. They did not find the presence of an erosion zone in the p(LGA) copolymer. In addition they found that erosion rate, but not total erosion time, was dependent on p(LGA) disk thickness. Discs twice as thick gave twice the erosion rate. Thus for p(LGA) it is not the surface area but the volume of the disc that controls the rate of erosion: behavior characteristic of bulk erosion. In contrast, p(CPP:SA) copolymers had nearly identical initial and maximum erosion rates for discs of different thicknesses. Thicker discs showed prolonged erosion at the peak rate, and discs twice as thick took twice as long to erode. The effect of geometry is similar to what would be expected for surface erosion: discs of the same surface areas give the same rates, but thicker discs erode over a longer time period.

Goepferich et al. [8] also did extensive work studying the mechanism of p(CPP:SA) erosion, concentrating on the influence of microstructure and monomer properties on erosion. They found that crystalline parts of the polymer were more resistant to erosion than the amorphous areas. The matrices eroded into highly porous devices, where monomers crystallize inside the pores.. Goepferich et al.[17] have also developed an erosion model for p(CPP:SA), which describes such changes in polymer matrix microstructure, movement of erosion fronts, creation of pores, and weight loss during erosion. In their approach, the polymer matrix was represented as a sum of small individual polymer matrix parts. The factors that determine erosion were combined, and the erosion of each matrix piece was regarded as a random event. Once such a matrix piece had come into contact with water, an individual life expectation was assigned to it using Monte Carlo techniques.

Drug release from p(CPP:SA) polyanhydrides have also been studied. Leong et al. [13] found that the release behavior depended on the formulation procedure. Best results were obtained with injection molded samples. The drug release (p-nitroaniline) profile followed that of the polymer degradation over a period of 8 months for p(CPP). There was an initial lag phase before a period of constant erosion and release. The more hydrophilic devices (p(CPP:SA) 21:79) still maintained the correlation between erosion and release over the lifetime of the device (around two weeks). However, these more hydrophilic matrices suffered the problem of mechanical disintegration (at around 60%). Fortunately, there was no sudden burst of drug release, and the release profiles were reproducible [13].

Laurencin et al. [18] have investigated the release of different drugs from p(CPP:SA) 9:91. Both the solubility and the loading of the drug were found to have an effect on the release from the polymer. At low drug loading and solubility, generally constant release kinetics were observed. With more soluble drugs, the release appeared to include a significant diffusional component. Higher drug loadings also resulted in release deviating from zero order. The degradation of the p(CPP:SA) 9:91 seemed to be unaffected by the solubility of the drug incorporated, whereas increased loadings of a drug resulted in increased rate of polymer degradation [18].

In drug release studies, another important factor to take into consideration is the possibility of drug-polymer interaction. Many fabrication procedures require the use of heat or high pressures, which could promote chemical interactions. Because the polyanhydride polymers contains a hydrolytically reactive linkage, there is even more legitimate concern that this labile bond may react with strong nucleophiles (eg. primary amines) other than water. Also many potential drugs to be used in controlled release applications often contain reactive groups.

Leong et al. [19] examined the drug-matrix interaction potential by incorporating several amino-containing compounds into polyanhydrides by injection molding (which requires raising temperatures above the melting point of the polymer). Using infrared spectroscopy, they found that many of the amino-containing compounds formed amide bonds if fabricated by injection molding (such as *p*-bromoaniline, *p*-anisidine, *p*-phenylenediamine). With *p*-nitroaniline, there was no apparent amide formation. However, when applying IR to compression molded samples of the same drugs, they found no evidence of any reaction. Evidently, elevated temperatures play a big role in polymer-drug interactions.

Leong et al. [19] also tested the possibility of any interaction occurred during the degradation process. In analyzing the release of *p*-anisidine from compression molded samples, they retrieved only free drug. From HPLC analysis, no additional peaks indicative of interaction products were evident at any time during the release process.

Ron et al. have studied the effects of both polymer hydrophobicity and addition of stabilizers on the release and integrity of polymer-encapsulated proteins were studied. By using p(CPP:SA) with sucrose as an excipient, both recombinant bovine somatotropin and zinc insulin were released intact over 3 weeks. The released proteins appeared to maintain their integrity as judged by acidic reverse-phase HPLC, size-exclusion HPLC, radioimmunoassay , and conformation-sensitive immunoassays. Their results also suggest that polymer hydrophobicity can be used to enhance protein stability [20].

CHAPTER 3

THESIS OBJECTIVES

The objectives of this thesis are to:

3.1 Gain a better understanding of the mechanism of polymer erosion of polyanhydride systems, using the p(FAD:SA) copolymer.

The erosion of polyanhydrides involves a number of steps [12], any or a combination of which can be the rate controlling mechanism. These steps can be divided into the following areas of study:

•Water contact at surface and penetration into polymer matrix.

How fast and how much water is penetrating the polymer? Where does the water penetrate? How does water uptake correlate with polymer degradation? Is this affected by such polymer properties as hydrophobicity and crystallinity?

•Polymer degradation (into monomers or oligomers) by hydrolysis of anhydride bond at surface and/or interior of polymer matrix.

Where is the degradation taking place? Is surface erosion or bulk erosion controlling? Or is it a combination of both? Is degradation affected by the polymer's hydrophobicity and crystallinity? How is the structure of the polymer changing with degradation? How does molecular weight change with erosion?

•Dissolution and diffusion of interior degradation products to surface of polymer matrix and removal to bulk solution by external mass transfer convection and diffusion.

Does the outer structure and composition of the polymer affect the diffusion of the interior degradation product to the surface? Once the product has reached the surface of the polymer, how does external mass transfer affect the release into the bulk environment?

The combination of all these above steps leads to the appearance of monomers in solution.

3.2 After gaining a better understanding of the underlying polymer erosion, we can then start to investigate the factors controlling drug release from polyanhydride systems.

We will investigate the effect of drug loading and the effect of different methods of drug incorporation on drug release. We will also examine how the properties of the copolymer (eg. hydrophobicity, crystallinity) and the drug (eg. solubility) affect drug release.

We would also like to correlate the drug release with the underlying polymer erosion. Does drug release follow polymer erosion? How does the outer structure of the polymer affect the diffusion of the drug to the surface? Does external mass transfer play a role in the release of the drug?

3.3 Finally we will investigate the potential of our system to release proteins.

Protein delivery is a challenging problem because one must maintain the protein's native structure through fabrication and release. Loss of native conformation not only leads to loss of biological activity, but also increases susceptibility to further problems such as covalent or non-covalent aggregation. In addition, the large variety of functional groups present in proteins amplifies the number of chemical processes (eg. oxidation, deamidation, β-elimination, disulfide scrambling, hydrolysis, isopeptide bond formation, and aggregation) [21] which may occur. We will determine whether our fabrication procedures affect the activity of the protein incorporated. We will also investigate the protein activity during the time course of it's release.

CHAPTER 4:

CHARACTERIZATION OF POLYMER EROSION[a]

[a] Results of this chapter are published in [22]

4.1 INTRODUCTION

In this chapter, we describe our polymer erosion characterization studies. We began by visualizing the p(FAD:SA) erosion process using light microscopy and scanning electron microscopy. We examined the overall SA erosion of different monomer composition p(FAD:SA) copolymers to determine what effect copolymer properties (such as hydrophobicity and crystallinity) had on polymer erosion. Differences in erosion patterns were explained by investigating factors which affect the erosion process. These include water penetration into the polymer matrix, degradation by anhydride bond hydrolysis, and dissolution and diffusion of interior degradation products (such as SA oligomers or monomers) to the polymer matrix surface. Monitoring SA release gives an idea of how a drug may release from the polymer as well. We also conducted studies to elucidate the type of erosion (surface vs. bulk) p(FAD:SA) was undergoing.

4.2 EXPERIMENTAL

4.2.1 MATERIALS

P(FAD:SA) copolymer discs were received as a gift from Scios-Nova Pharmaceuticals (Baltimore, MD). The polymers were of weight composition p(FAD:SA) 20:80 (M_w=30,000), p(FAD:SA) 50:50 (M_w=25,000), and p(FAD:SA) 70:30 (M_w=50,000). The synthesis of the copolymers were done elsewhere [5], and materials and experimental methods are briefly described here:

Polymer materials [5]: Fatty acid dimers (FAD) were a gift from Unichema Chemicals (Chicago, IL) as Pripol 1004 (dimer). FAD is a dimer derivative of erucic acid having a Mw of 720. It is a clear slightly yellow liquid, and contains 99% diacids. Sebacic acid (SA) was purchased from Aldrich (Milwaukee, WI (99%)) and were recrystallized twice from anhydrous ethanol before use. Analytically pure solvents were purchased from J. T. Backer and were used as received. All other reagents and chemicals were obtained from Aldrich.

Synthesis of Prepolymers [5]: The FAD monomer was purified by dissolving it in dichloromethane and extracting the impurities with deionized water. The dried purified monomer was then refluxed in acetic anhydride (100 g in 500 ml) for 20 minutes and left to cool to room temperature. The solution separated into two phases, and the upper layer (FAD prepolymer) was isolated and evaporated to dryness using an evaporator. The FAD prepolymers were light yellow liquids at room temperature. The prepolymers of sebacic acid (SA) was prepared from purified diacid monomer by refluxing it in excess acetic anhydride for 30 minutes and evaporating it to dryness. The hot clear viscous residue was dissolved in dichloromethane and the prepolymer was precipitated in a mixture of hexane/isopropyl ether (1:1). The solid was collected by filtration and dried by vacuum at room temperature.

Preparation of Polymer [5]: Polymers were synthesized in a small scale (up to 10 g) or large scale (40-2000g). The polymerization time for small-scale reactions were 90 minutes, large-scale polymerizations took from 3-5 hours, depending on the vacuum applied and the efficiency of mixing.

A typical large-scale polymerization was as follows: to a 3 L polymerization kettle equipped with an over-head stirrer and a vacuum line port, was added 500g of FAD prepolymer and 500g of SA prepolymer. The prepolymers were melted in a 180 ± 1°C heating mantle before connecting the systems to a vacuum line. The polymerization was continued for 4-8 hours under a vacuum of 0.1 - 1 mm of Hg with constant stirring (150 rpm). The polymerization was followed by viscosity measurements or by GPC analysis of samples withdrawn during polymerization. Small-scale polymerizations (up to 10g) were made in a Pyrex tube with a side arm and a magnetic stirrer.

4.2.2 METHODS

4.2.2.1 Erosion study

Erosion studies were conducted by placing each polymer disc in a glass vial containing 20 ml of 0.1 M pH 7.4 phosphate buffer at 37°C (Precision gravity convection incubator 4EG) with constant shaking at 120 RPM (Lab-line shaker). Monobasic potassium phosphate and dibasic potassium phosphate were purchased in analytical grade from Mallinckrodt, Paris, KY. Effect of copolymer composition was studied using discs (14.0 ± 0.1 mm diameter, 2.7 ± 0.1 mm thickness) of p(FAD:SA) 20:80, p(FAD:SA) 50:50, and p(FAD:SA) 70:30. Effect of device thickness on erosion rate was studied using p(FAD:SA) 50:50 discs of 0.68, 0.98, 1.40, and 1.67 ± 0.01 mm thickness (measured using a micrometer). Mass transfer studies were conducted at 0, 60, and 120 RPM (Lab-line shaker). The buffer was changed frequently enough (at least once a day) to approximate perfect sink conditions. The buffer solutions were analyzed by reversed phase ion-pair high performance liquid chromatography (Hewlett Packard 1090 Series II). The column used was a poly(styrene-divinylbenzene) reversed phase HPLC column (Hamilton, PRP-1), and the mobile phase consisted of acetonitrile (Mallinckrodt, HPLC grade) in aqueous 0.05 mol/L tetrabutylammonium phosphate (Waters, Pic A). All HPLC solutions were filtered (Millipore, type HV, 0.45 μm) and degassed. SA was determined by UV at λ=210 nm. The run time was 10 minutes at a flow rate of 1.2 ml/min and 100 μl injection volume.

4.2.2.2 Visualization studies

Cross sections of polymer were cut with a razor blade from p(FAD:SA) 20:80 discs (of 14.0 ± 0.1 mm diameter, 2.7 ± 0.1 mm thickness) at different erosion stages and examined under a light microscope (Wild Makroskop M420) at 25x. To better visualize the erosion zone, cross sections of polymer disc were also investigated by scanning confocal microscopy using an MRC 600 imaging system from Bio Rad, Hercules, CA. Fluorescein (Sigma Chemical) was added to the phosphate buffer medium (0.5 mg/ml). Fluorescein (MW = 376), a hydrophilic molecule, is unable to penetrate into the hydrophobic polymer. It is only able to penetrate into the aqueous-filled porous sections of the polymer matrix where SA has left the polymer.

The erosion zone was also identified by scanning electron microscopy (SEM). P(FAD:SA) 20:80 eroded samples were dropped in liquid nitrogen and freeze fractured to obtain cross sections. Samples were dried, mounted on metal stubs (Energy Beam Inc.), gold coated, and examined by SEM using a Stereoscan 250 MK3 microscope from Cambridge Instruments, Cambridge, MA.

4.2.2.3 Water uptake

Samples of p(FAD:SA) 20:80, p(FAD:SA) 50:50, and p(FAD:SA) 70:30 were placed in 0.1 M pH 7.4 phosphate buffer at 37°C ; one was removed every 24 hours. Each was then dropped into liquid nitrogen and stored frozen (-20°C) until time of analysis, where they were dissolved in chloroform (Mallinckrodt, analytical grade) titrated for water content (unreacted water) using a Mettler DL18 Karl Fischer titrator with Hydranal solvent (Riedel-deHaen). To monitor the extent of water uptake (reacted and unreacted water) with time, tritiated water (1.0 mCi/gr) was added to the phosphate buffer medium (at 0.5% concentration) and p(FAD:SA) polymer samples were taken out at 24 and 48 hours. These discs were then cut with a razor blade into 1 mm squares, embedded in Polyfreeze Tissue Fixing Medium (Polysciences), and sectioned at < -20°C into 12 μm slices with a microtome (International Equipment Company). The blade was wiped with an ethanol/water mixture after each cut to ensure no radioactivity was transferred between sections. Each section was dissolved in 15 ml scintillation fluid (Ecolume, ICN Biomedicals, Inc.) and counted with a Packard 2000 CA Tri-Carb Liquid Scintillation Analyzer.

4.2.2.4 Crystallinity

Thermal analysis of polymer samples of p(FAD:SA) 20:80, p(FAD:SA) 50:50, and p(FAD:SA) 70:30 was determined with a Perkin-Elmer DSC-7 Differential Scanning Colorimeter at a heating rate of 10°C/min. Copolymer crystallinity (X_c) was calculated from the heat of fusion using the following relation [23]:

$$X_c = \frac{\Delta H_{obs}}{W_a \Delta H_{a,pure} + W_b \Delta H_{b,pure}}$$

ΔH_{obs} is the heat of fusion for each copolymer, W_a and W_b are the mole fractions of

SA and FAD monomer respectively in each copolymer and

$$\Delta H_{a,pure} = \frac{\Delta H_{a,obs}}{X'_{a,c}}$$

where $X'_{a,c}$ is the % crystallinity of the homopolymers, and $\Delta H_{a,obs}$ is the heat of fusion for the homopolymer. $\Delta H_{b,pure}$ was estimated to equal zero since p(FAD) is a liquid at room temperature. The fraction of crystallities for p(SA) was taken from previous X-ray diffraction studies[15] and estimated to be 67%.

4.2.2.5 Hydrolysis of anhydride bond

The hydrolysis of three different copolymer compositions (p(FAD:SA) 20:80, p(FAD:SA) 50:50, p(FAD:SA) 70:30) was examined. Discs were 14.0 ± 0.1 mm diameter and 2.7 ± 0.1 mm thickness. At various time points, polymer samples were removed from release media, dissolved in chloroform (Mallinckrodt, analytical grade) and film cast onto NaCl plates. The outer "erosion zone" of the polymer was scraped with a spatula from the inner intact zone and analyzed separately. The IR analysis was done with a Nicolet Magna-IR Spectrometer 550. The anhydride bond has a characteristic doublet occurring at 1800-1850 and 1740-1790 cm^{-1}. The carboxylic acid peak is at 1700-1725 cm^{-1}.

4.2.2.6. Molecular weight study

p(FAD:SA) samples were placed in pH 7.4 phosphate buffer solution at 37°C. Samples were taken at various time points (1, 2, 4, 6, 12, 24 hours) and rinsed with deionized water. They were then frozen with liquid nitrogen and lyophilized (Lanconco, Freeze Dryer 8) overnight. Polymer molecular weight was determined on a Perkin-Elmer gel permeation chromatography (GPC) system consisting of the Series 10 pump and the 3600 data station with the LC-25 refractive index detector. Samples were eluted in chloroform through a PL gel 5-mm mixed column (Polymer Laboratories) at a flow rate of 0.9 ml/min at 23°C. Polymer molecular weights were determined relative to polystyrene standards (Polysciences).

4.3 RESULTS AND DISCUSSION

4.3.1 Erosion zone

Initial studies involved visualizing the p(FAD:SA) 20:80 erosion process. Light microscopy indicates the presence of an erosion zone, a distinct area where mass loss occurs (Figure 4.1a). This erosion zone moves linearly with time from the surface of the polymer matrix (which is in contact with the phosphate buffer) towards the interior (Figure 4.1b, Table A.1). As the erosion zone progresses, disc thickness also decreases. The erosion zone is thought to be formed when the copolymer degrades and SA monomers (or oligomers) dissolve and diffuse out of the polymer matrix, leaving a porous network behind. The presence of this erosion zone is further demonstrated by the penetration of fluorescein (Mw = 376) only into this eroded section but not into the interior of the polymer matrix (Figure 4.2a). The zone presumably also includes insoluble degradation products, such as FAD monomer.

SEM studies also confirm the presence of a distinct area where erosion has occurred (Figure 4.2b). As described by Goepferich [8], the non-eroded sections show Maltese crosses, which are typical of polymers containing spherulites [24]. The maltese crosses show circular arranged bands [25], which results from the arrangement of the crystalline regions within the spherulites. In the erosion zone, the spherulites have eroded and pores are present. In higher FAD content copolymers, FAD monomer may fill these pores. Both material loss from the outside to the inside of the matrix and disc thickness decreases with erosion are consistent with characteristics of a surface eroding polymer [2]. However, the insoluble FAD monomer presence in the erosion zone makes achieving perfect surface erosion difficult.

A similar erosion zone has also been identified in studies with the p(CPP:SA) polyanhydride [1]. However, no thickness change was observed during erosion [1]. It has also been shown in p(CPP:SA) that monomers crystallize during erosion inside the porous network of the eroded polymer matrix [8]. Likewise, the p(FAD:SA) copolymer could also have crystallized SA within the erosion zone. The erosion zone structure and properties are important because any interior degradation product must diffuse through this zone to reach the disc surface.

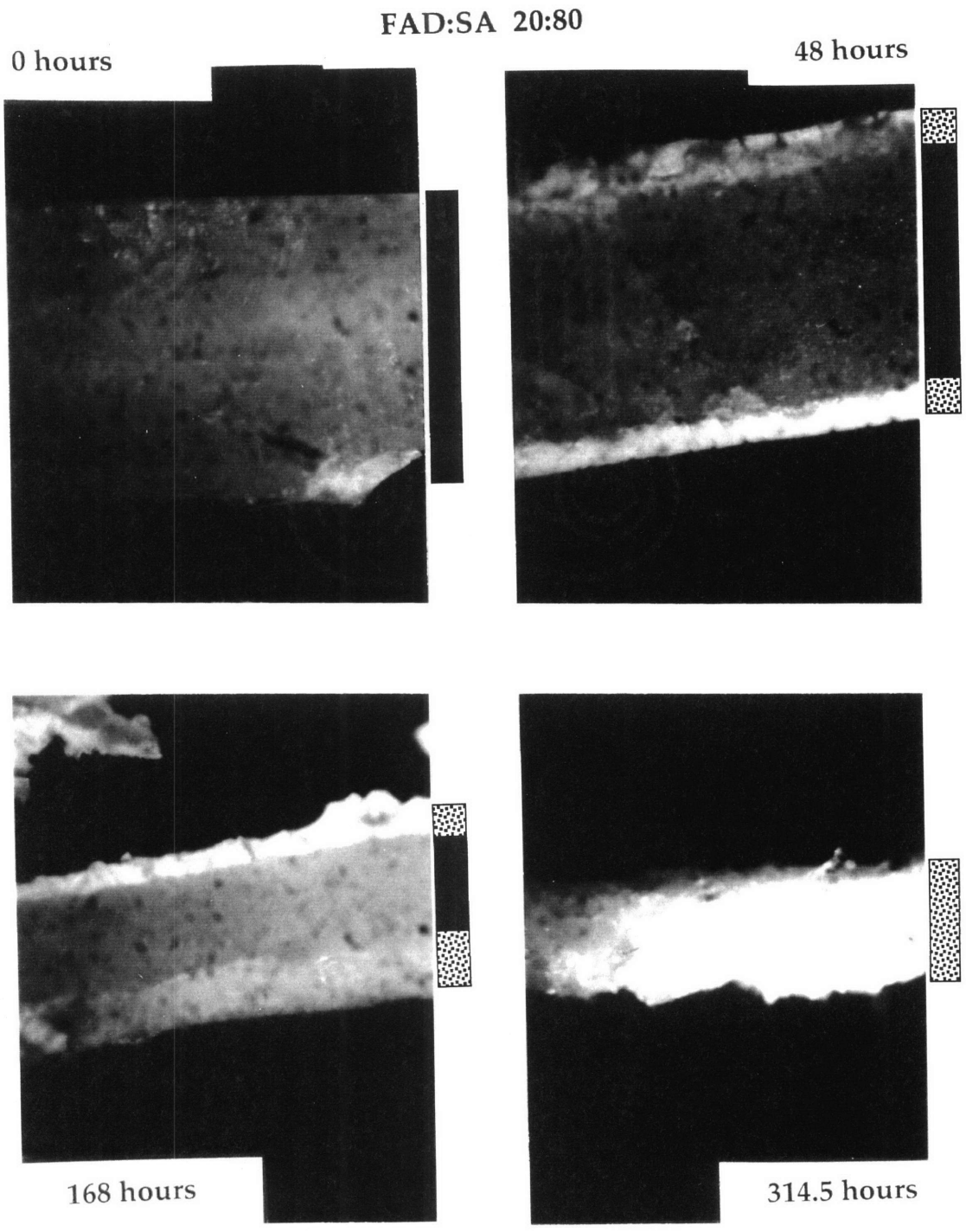

Figure 4.1a Time series of p(FAD:SA) 20:80 cross sections (initial thickness 2.7± 0.1mm) taken by light microscopy of 25x magnification. The solid bar at the right hand side indicates non-eroded polymer, the spotted bar indicates eroded polymer.

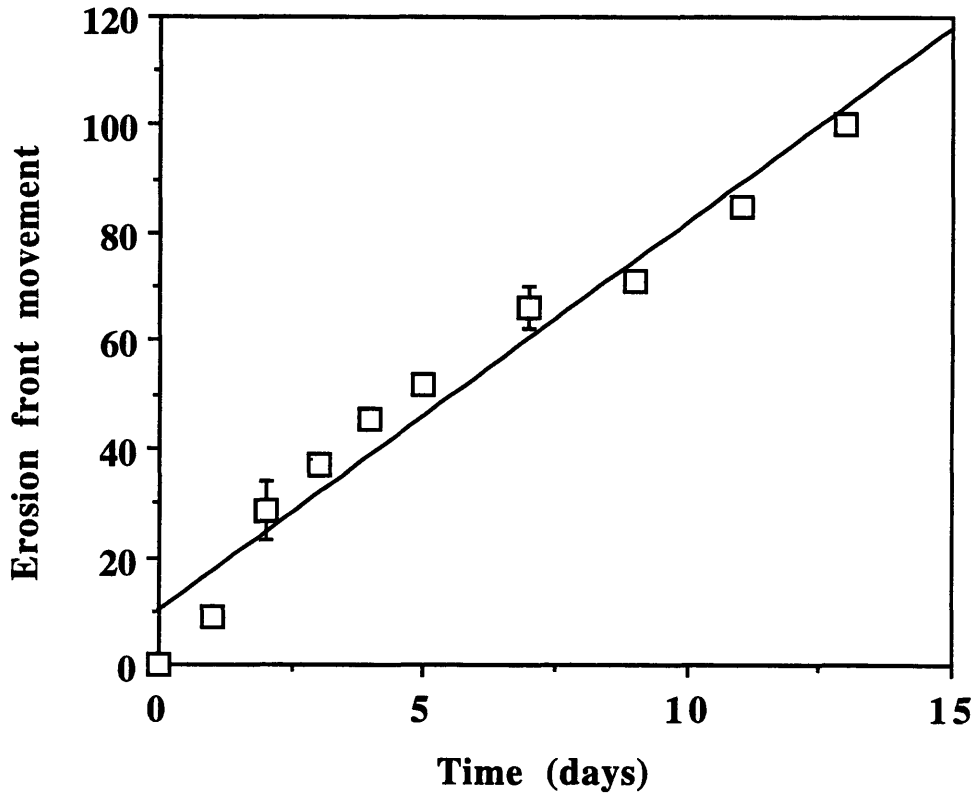

Figure 4.1b Erosion front progression of p(FAD:SA) 20:80. Erosion front movement is plotted as a percentage (thickness of erosion zone from initial polymer surface divided by entire disc thickness). Data with error bars represent an average of two measurements; error bars represent the spread of the data.

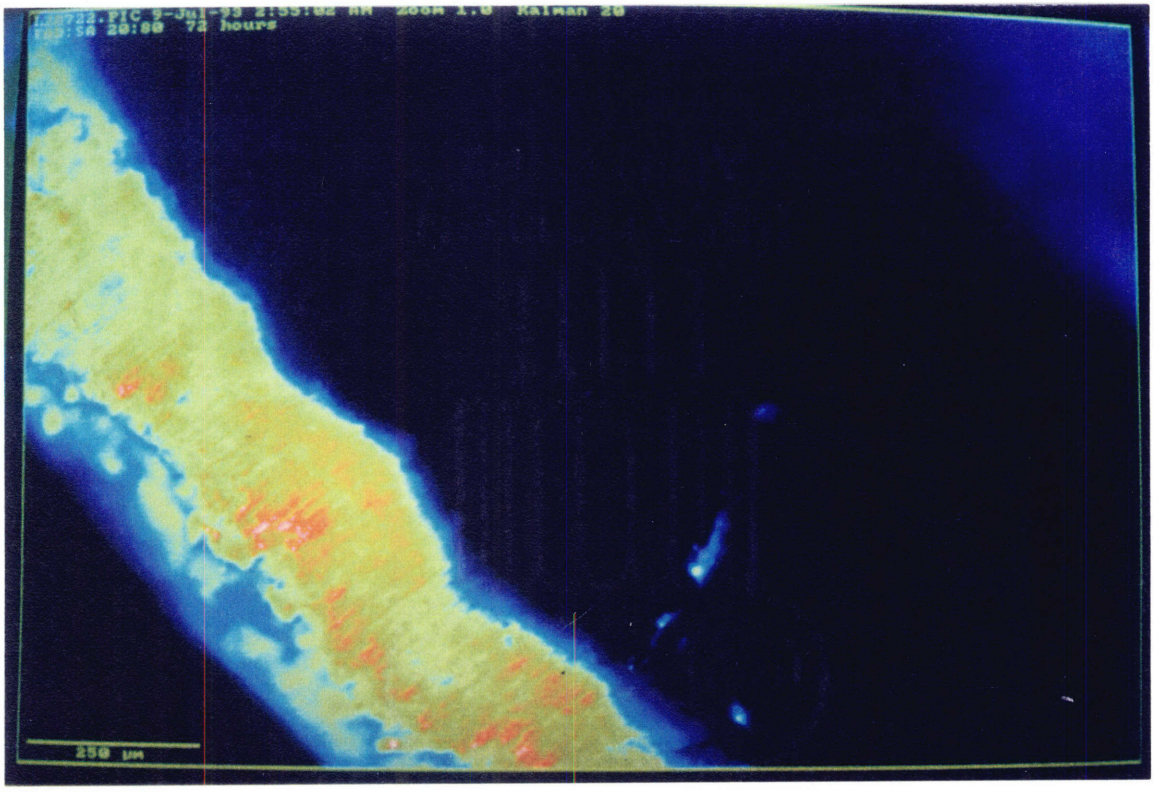

Figure 4.2a Cross sections of p(FAD:SA) 20:80 showing fluorescein dye penetration (yellow area) into polymer erosion zone after 3 days in phosphate buffer with 0.5 mg/ml fluorescein. Dark areas indicate non-eroded polymer, where there is no dye penetration. Only one of the two symmetrical erosion zones is shown. Picture is taken by confocal microscopy.

0 DAYS

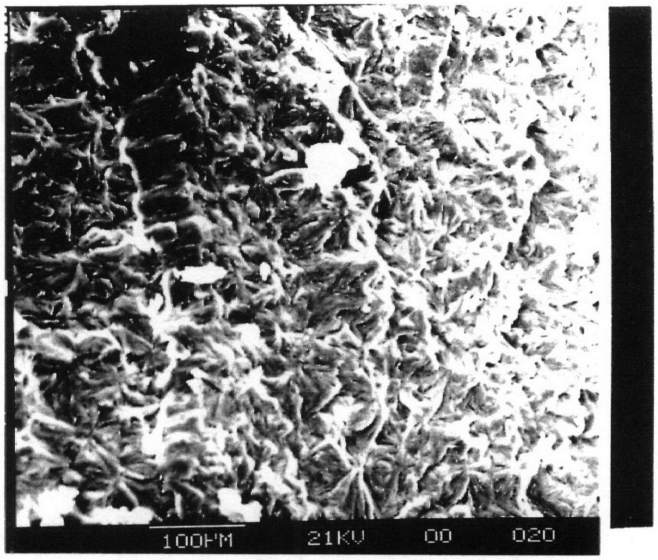

5 DAYS

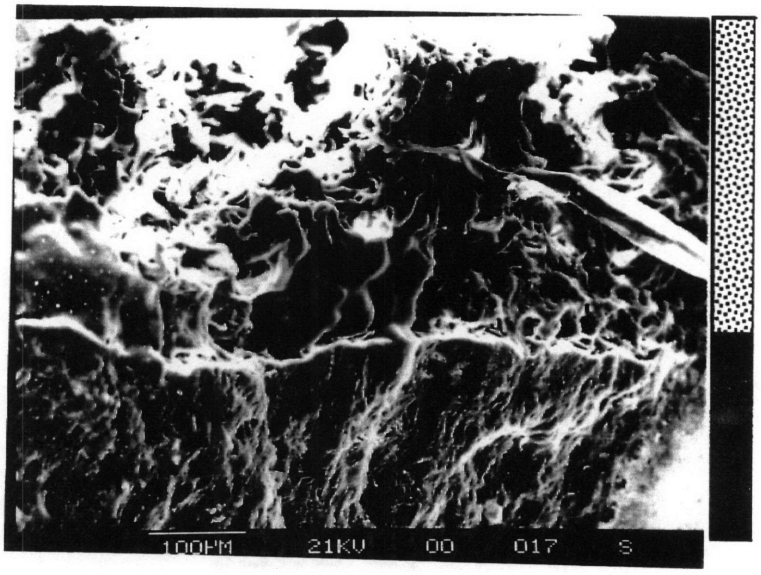

Figure 4.2b Freeze fracture cross sections of p(FAD:SA) 20:80 using scanning electron microscopy at 140x magnification. Top picture is initial non-eroded cross section; bottom picture is eroded polymer after 5 days in phosphate buffer solution. Erosion zone is more porous, indicated by spotted bar on right hand side. Non-eroded polymer interior is indicated by solid bar.

4.3.2 Erosion studies

The overall erosion of different monomer composition p(FAD:SA) copolymers was examined to determine whether and to what extent copolymer properties affected erosion. Erosion was measured by the cumulative appearance of sebacic acid (SA) in solution. The p(FAD:SA) 20:80, p(FAD:SA) 50:50, and p(FAD:SA) 70:30 erosion profiles (normalized by the cumulative experimental SA) are shown in Figure 4.3. (Data is shown in Table A.2) Monitoring SA release from the copolymer provides an idea of how a drug incorporated into the polymer matrix may release as well. The SA erosion of p(FAD:SA) 50:50 extends over a longer time period than p(FAD:SA) 20:80. To determine if longer erosion periods could be achieved by increasing the copolymer hydrophobic component, higher FAD content polymers were also examined. However, increasing up to p(FAD:SA) 70:30 did not result in a longer erosion period.

This is in contrast from what has been reported with the p(CPP:SA) polyanhydride. Leong et al. [13] have reported that they could obtain a wide range of CPP erosion rates (1 week to several years) by increasing the monomer ratio of CPP to SA. However, Goepferich et al. [8] have found that increasing CPP monomer content (although extending CPP release) does not actually affect SA release from p(CPP:SA). SA release from both p(CPP:SA) 20:80 and p(CPP:SA) 50:50 was about equal (over a time period of 7 days for 1 mm thick discs).

4.3.3 Crystallinity studies

A possible explanation for why FAD content increases beyond p(FAD:SA) 50:50 does not appear to prolong erosion periods may be due to the copolymer hydrophobicity and crystallinity. As the copolymer FAD component increases, the polymer not only becomes more hydrophobic but also more amorphous. Differential Scanning Colorimetry (DSC) studies confirm that the polymer degree of crystallinity decreases with increasing FAD monomer content (Figure 4.4, Table A.3). Hydrophobicity inhibits water penetration into the polymer matrix, but amorphous domains are more vulnerable to hydrolytic attack [8, 13], and therefore degrade more easily than crystalline regions. These two opposing copolymer properties may compromise the range of degradation rates that can be achieved by varying the monomer ratio in the p(FAD:SA) copolymer.

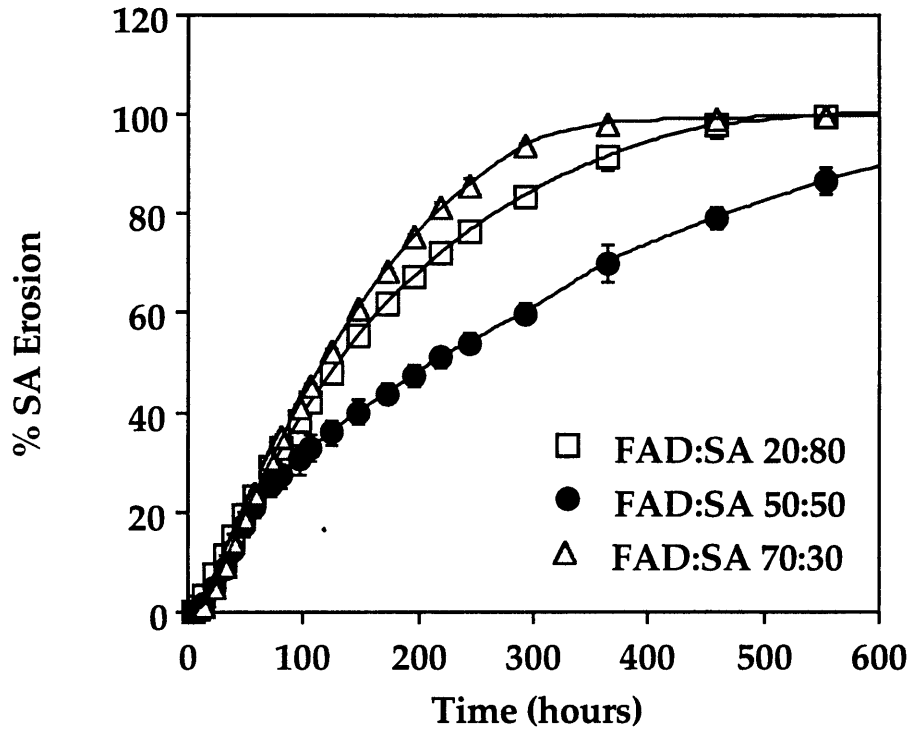

Figure 4.3 Effect of p(FAD:SA) monomer ratio on %SA erosion. Polymer discs are of initial 14.0 ± 0.1 mm diameter; 2.7 ± 0.1 mm thickness. Data with error bars represent an average of two measurements; error bars represent the spread of the data.

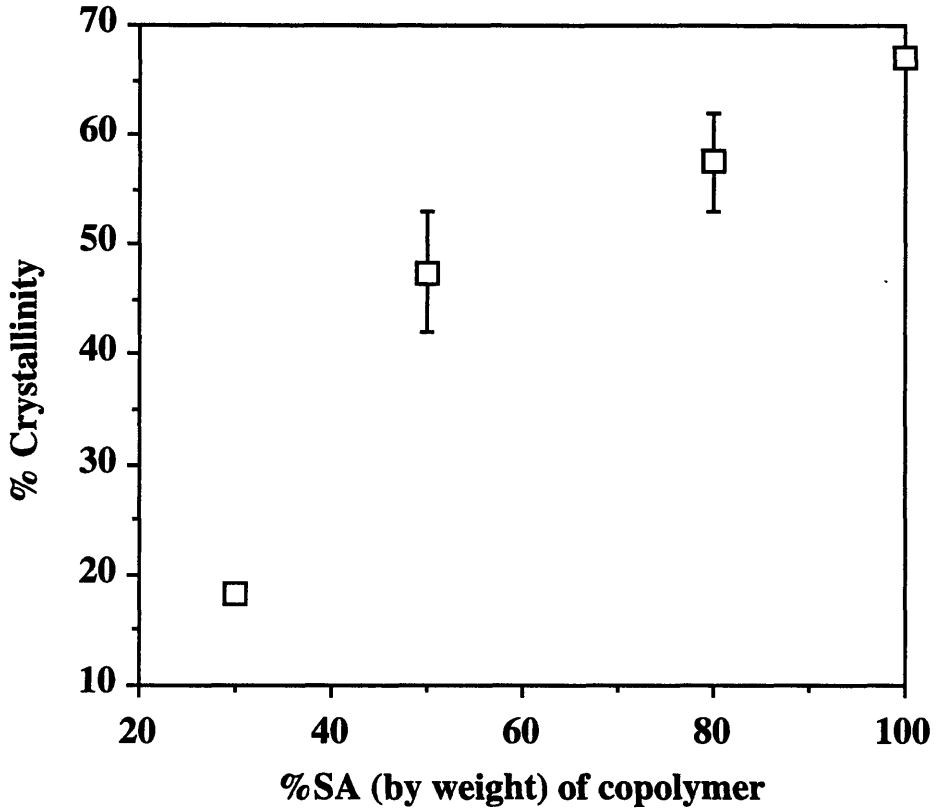

Figure 4.4 Effect of p(FAD:SA) monomer ratio on copolymer crystallinity. Crystallinity was calculated from the heat of fusion as described in Section 4.2.2.4. Data with error bars represent an average of two measurements; error bars represent the spread of the data.

The degree of crystallinity also changes with erosion. As the polymer erodes, SA monomer diffuses out before the FAD monomer, leaving behind a device with increasing FAD content (which is amorphous) relative to SA (which is more crystalline). Therefore there is a decrease in polymer crystallinity with erosion (Figure 4.5, Table A.4). The crystallinity decrease from increased FAD relative to SA appears to overshadow any increase in crystallinity due to attack and erosion of amorphous domains.

4.3.4 Degradation studies

We can test whether the more amorphous polymers are degrading faster by examining anhydride bond hydrolysis by infrared spectroscopy. As the anhydride bond is hydrolyzed, the anhydride characteristic doublet occurring at 1800-1850 and 1740-1790 cm^{-1} becomes smaller and the carboxylic acid peak at 1700-1725 cm^{-1} grows larger. We have plotted the ratio of the anhydride peak to acidic peak with time for the p(FAD:SA) copolymers, separating the outer erosion zone from the inner intact zone (Figure 4.6, Table A.5). The time series of the IR spectra for the p(FAD:SA) 50:50 is shown in Figure 4.7a. The anhydride peak in the p(FAD:SA) 20:80 and p(FAD:SA) 50:50 interior (or inner zone) remain present for about 13 days and 11 days respectively, while p(FAD:SA) 70:30 is completely hydrolyzed in 5 days. The most crystalline copolymer, p(FAD:SA) 20:80, degrades over the longest period whereas p(FAD:SA) 70:30, the most amorphous copolymer, degrades over the shortest time. However, unlike the CPP-CPP bond which is less reactive than either the CPP-SA or SA-SA bond [1], there is no evidence that the FAD-FAD bond is any less reactive than the FAD-SA or SA-SA bond.

The acidic degradation peak grows faster in the outer erosion zone than in the inner zone for both p(FAD:SA) 50:50 (Figure 4.7b) and p(FAD:SA) 70:30. This would point more towards a surface eroding phenomenon rather than one of bulk erosion. However, this trend is less clear in the p(FAD:SA) 20:80 where there is no significant difference in hydrolysis between the outer and inner zone. Perhaps the outer zone of the p(FAD:SA) 20:80 contains crystalline regions which are more resistant to degradation. However, the meeting of the two outer zones (13 days) at the center correlates well with the disappearance of the anhydride peak (13 days) and 85% SA erosion from the p(FAD:SA) 20:80 device.

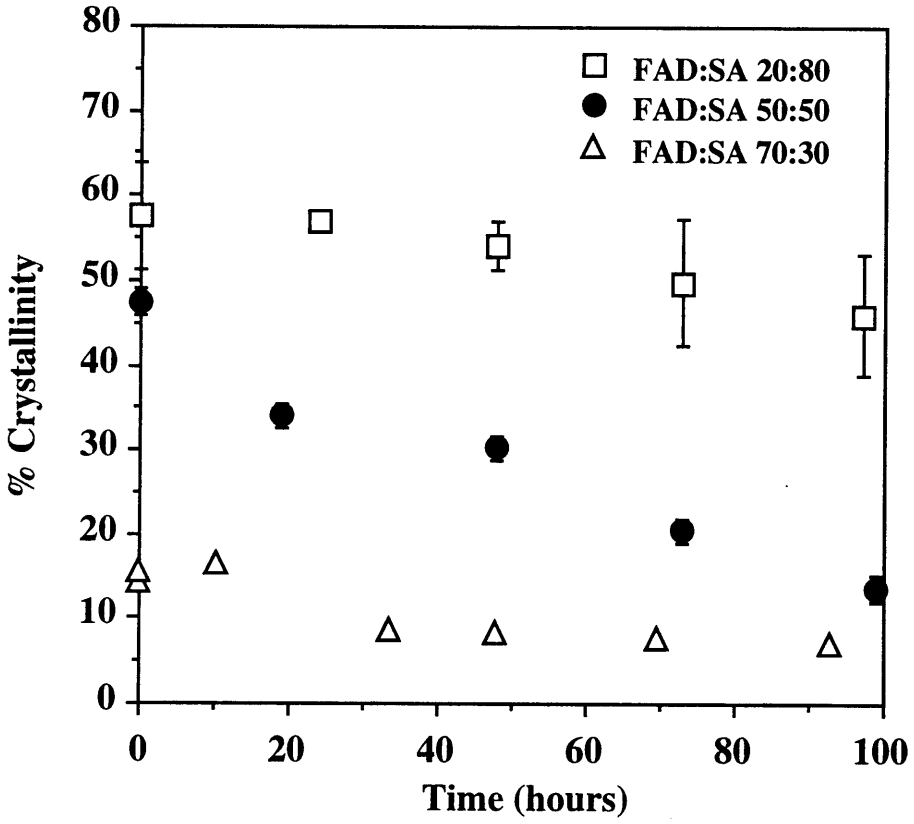

Figure 4.5 %Crystallinity changes with erosion. Crystallinity was calculated from the heat of fusion as described in Section 4.2.2.4. Data with error bars represent an average of two experiments; error bars represent the spread of the data

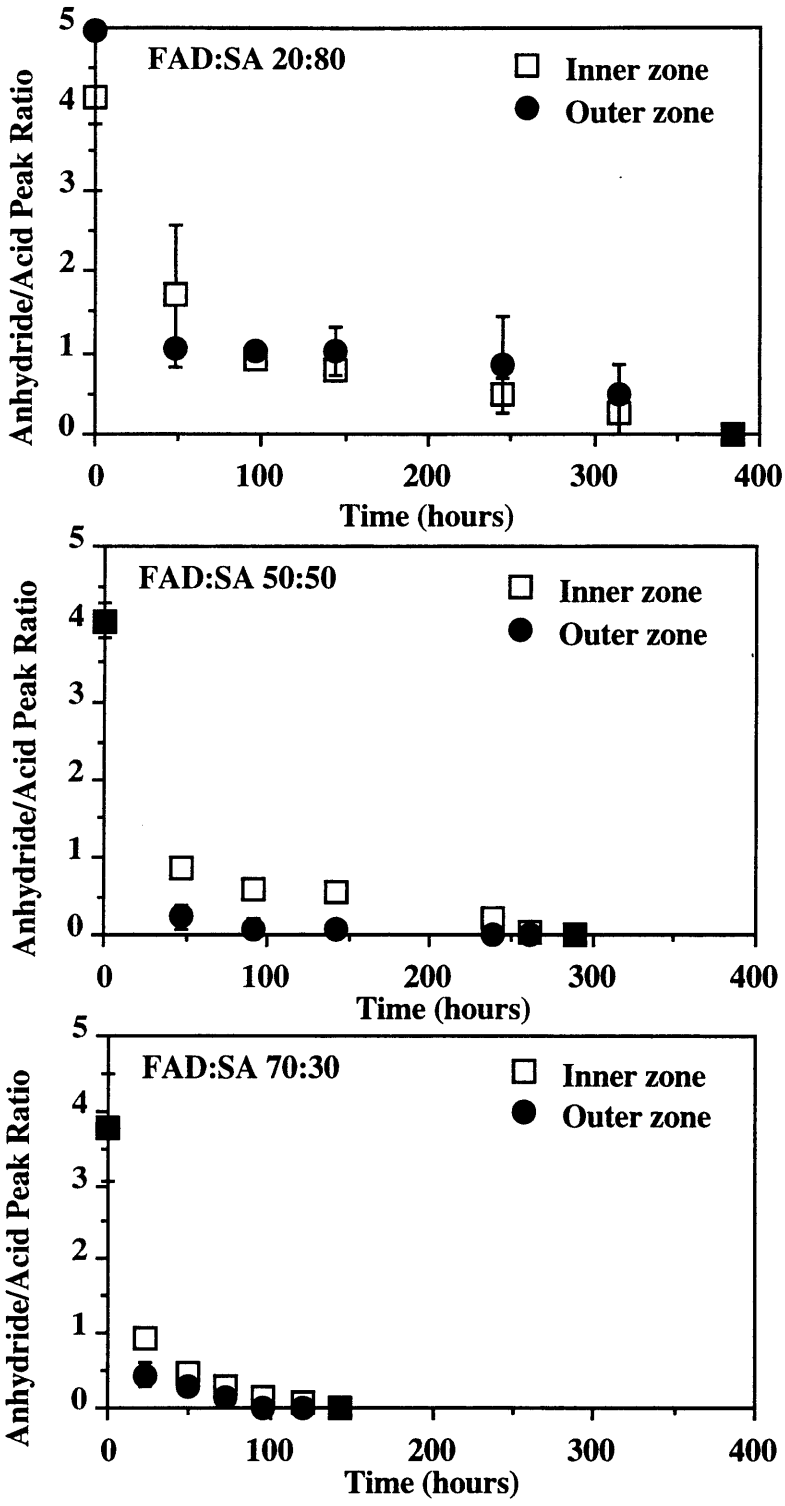

Figure 4.6 Ratio of anhydride bond peak to acidic degradation product peak with erosion for p(FAD:SA) 20:80, p(FAD:SA) 50:50, and p(FAD:SA) 70:30 copolymer discs of 2.7 ± 0.1 mm thickness. Data with error bars represent an average of two measurements; error bars represent the spread of the data.

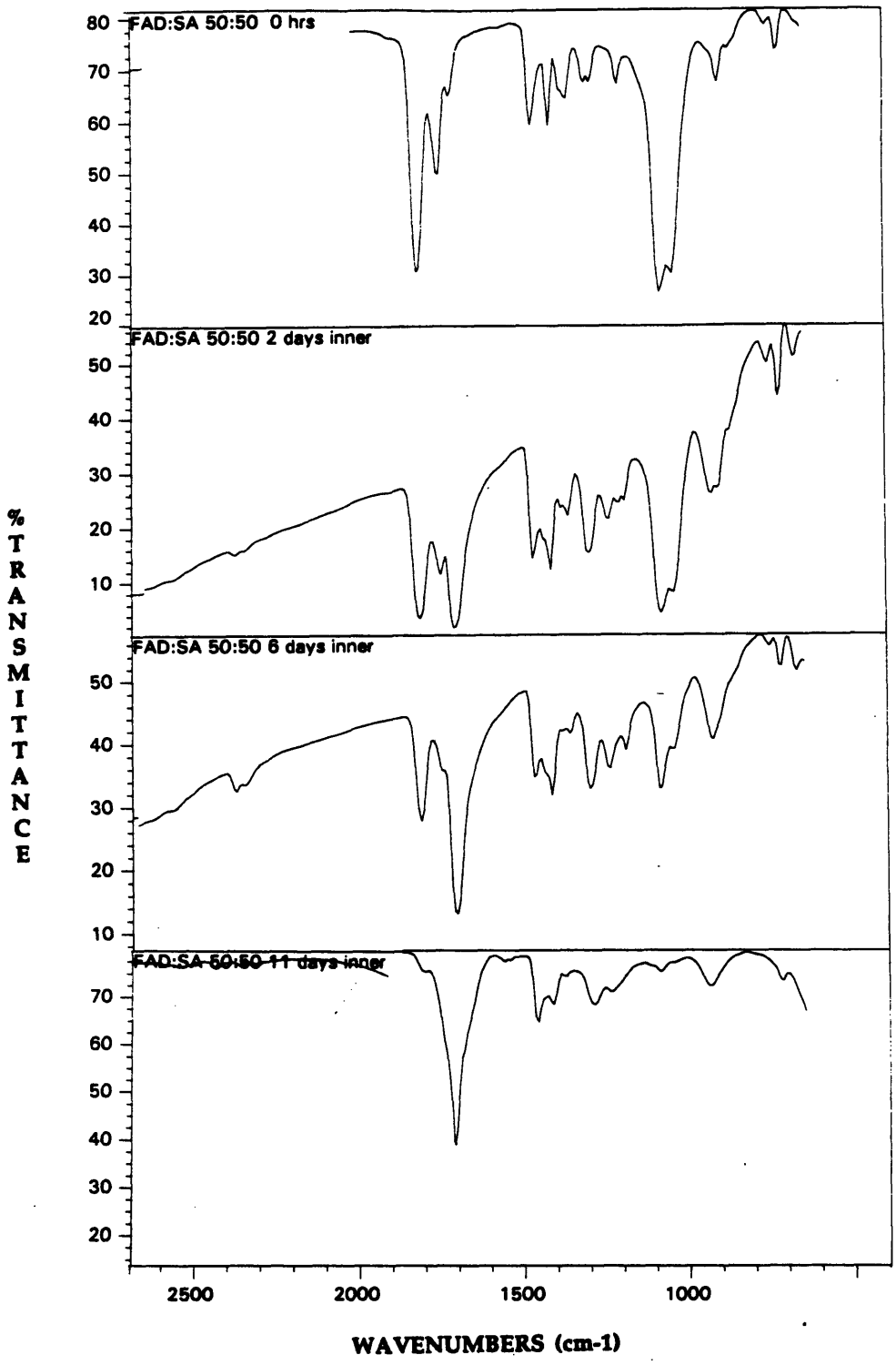

Figure 4.7a Hydrolysis of anhydride bonds in p(FAD:SA) 50:50 during erosion (as determined by infrared spectroscopy). Copolymer discs are of initial 14 ± 0.1 mm diameter, 2.7 ± 0.1 mm thickness. The anhydride bond has a characteristic doublet occuring at 1800-1850 and 1740-1790 cm^{-1}. The carboxylic acid peak is at 1700-1725 cm^{-1}

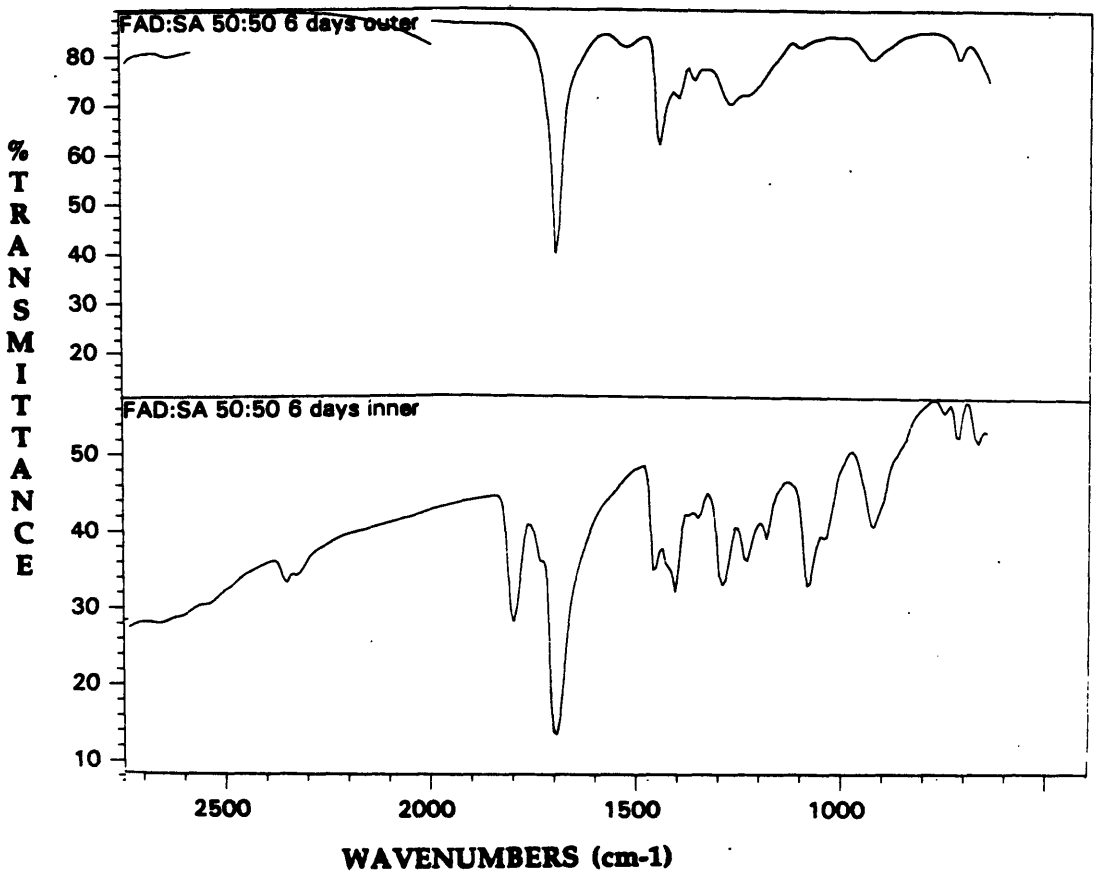

Figure 4.7b Hydrolysis of anhydride bonds in outer zone compared to inner zone of p(FAD:SA) 50:50 during erosion.

We also need to explain why anhydride bond hydrolysis in p(FAD:SA) 20:80 is only slightly slower than in p(FAD:SA) 50:50. Perhaps the greater hydrophobicity of p(FAD:SA) 50:50 somewhat counterbalances the higher crystallinity of p(FAD:SA) 20:80 so that the difference in degradation is less than expected. However, p(FAD:SA) 50:50 erodes over a longer period than p(FAD:SA) 20:80, indicating that the higher FAD content of p(FAD:SA) 50:50 is playing a role in slowing SA release.

Correlating anhydride bond hydrolysis with appearance of SA in solution provides a good example of how important diffusion of the monomer/oligomer through the erosion zone may be (Figure 4.8). Although the anhydride bonds of p(FAD:SA) 70:30 have completely hydrolyzed in 5 days, only 55% of the SA has appeared in solution. P(FAD:SA) 50:50 is completely hydrolyzed in 11 days, and only 55% of the SA has appeared in solution. The FAD content of the outer zone may be a diffusional barrier to the interior product diffusing out. In contrast for higher SA content copolymers, p(FAD:SA) 20:80 is completely degraded in 13 days and almost all of the SA (90%) has appeared in solution. The more porous p(FAD:SA) 20:80 erosion zone may provide less of a barrier to the SA diffusing out compared to p(FAD:SA) 50:50 and p(FAD:SA) 70:30 erosion zones of higher (more insoluble) FAD content. The structure/composition of this erosion zone (which is related to copolymer monomer composition) does play an important role in overall erosion of the polymer device.

Another method to quantify degradation is by determining the decrease in copolymer molecular weight (MW) with time. The p(FAD:SA) 50:50 MW decreases substantially within the first 24 hours (Figure 4.9, Table A.6). This is consistent with infrared spectroscopy data which indicates some anhydride bond hydrolysis in the inner zone during that time. The sharp decline correlates with the lag period before SA detection in solution. This may be due to the time required for SA to solubilize and diffuse into the buffer medium. Studies have also investigated the MW changes of p(FAD:SA) 20:80 and p(FAD:SA) 70:30 with degradation (Figure 4.10, Table A.7). Regardless of initial MW, all polymers decrease to <5000 daltons in less than 24 hours. However, the p(FAD:SA) 70:30 MW dropped the most quickly, consistent with the fast anhydride bond hydrolysis.

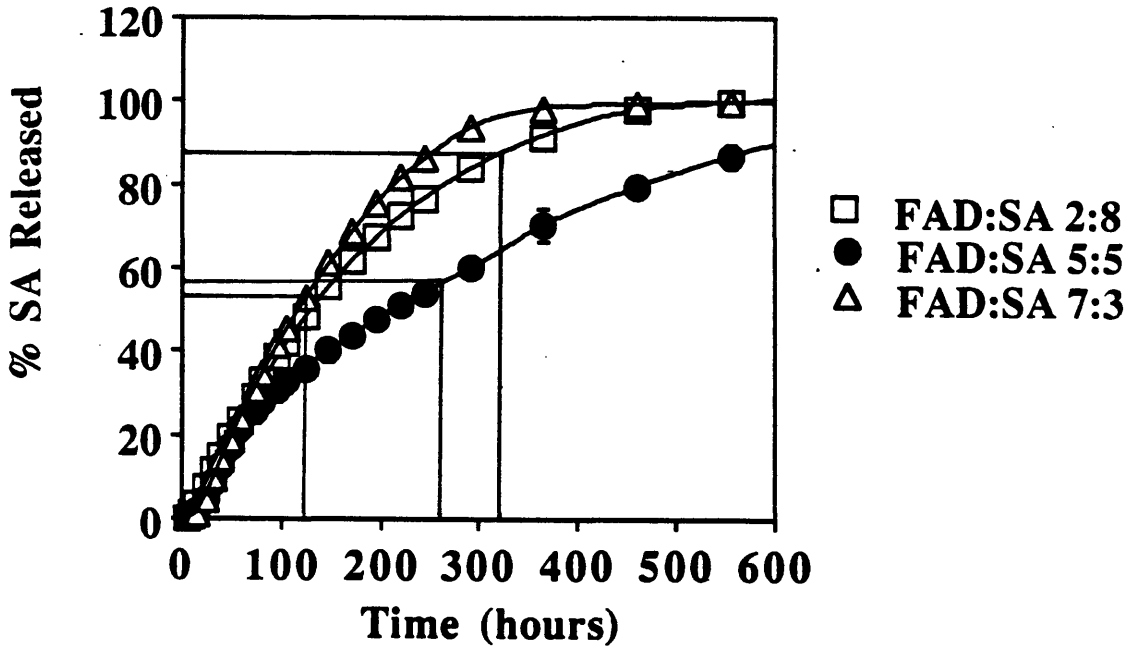

Figure 4.8 Correlation of anhydride bond hydrolysis (degradation) with overall erosion process (appearance of SA in solution). Solid lines connect time of complete anhydride hydrolysis with %SA erosion from disc. Data with error bars represent an average of two measurements; error bars represent the spread of the data.

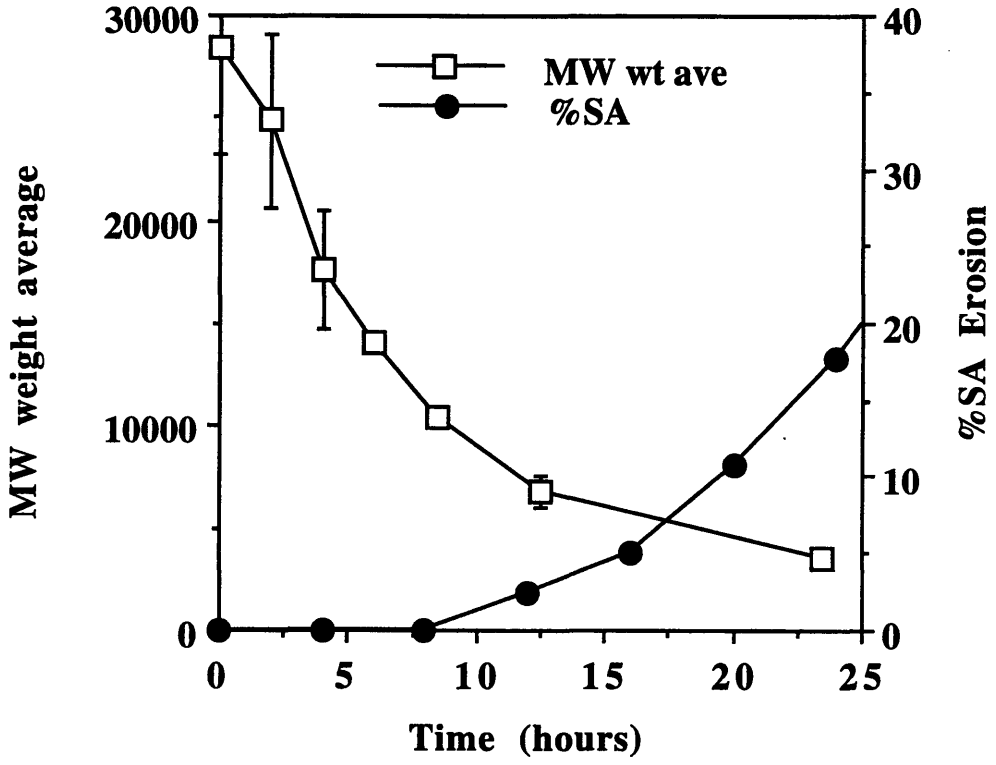

Figure 4.9 Relation of molecular weight decrease of p(FAD:SA) 50:50 with %SA erosion. Data with error bars represent an average of two measurements; error bars represent the spread of the data.

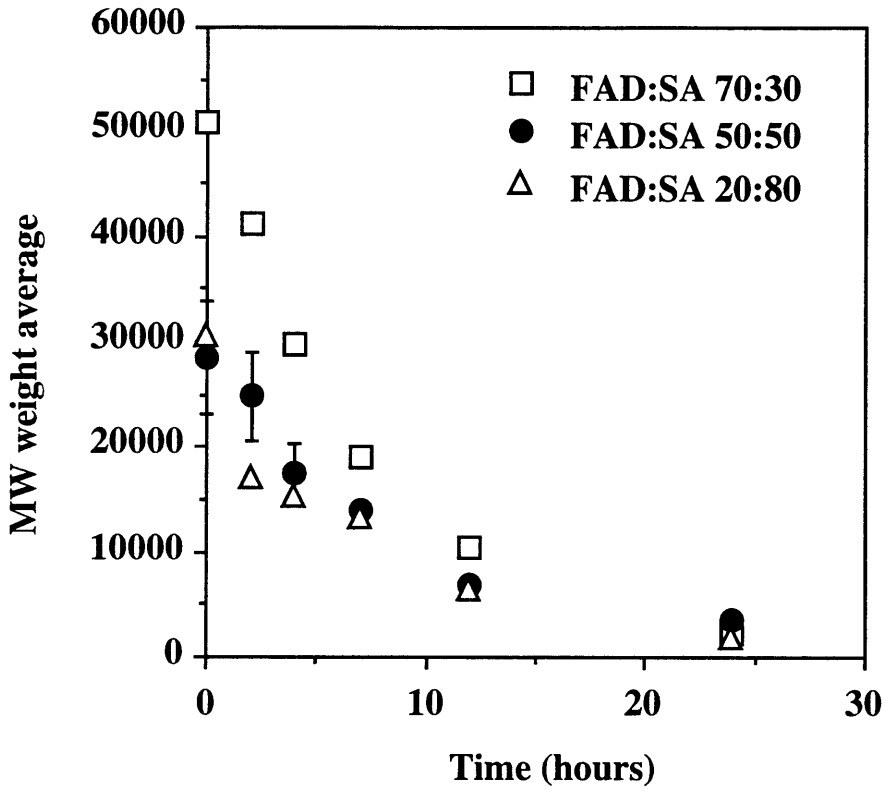

Figure 4.10 Effect of p(FAD:SA) monomer ratio on molecular weight decrease with erosion. Data with error bars represent an average of two measurements; error bars represent the spread of the data.

4.3.5 Water uptake

Thus, although the anhydride bonds are hydrolyzing faster at the disc surface, there does appear to be some degradation occurring in the polymer matrix interior. Therefore, we determined to what extent water penetration occurred in the polymer matrix interior. Karl Fischer water content results indicate very little unreacted water in the polymer bulk during polymer degradation. During the erosion process, the most hydrophilic copolymer, p(FAD:SA) 20:80, never exceeded 5 wt% water in the bulk (see Table A.10). The more hydrophobic polymers p(FAD:SA) 50:50 and p(FAD:SA) 70:30 never exceeded 3 wt% and 1 wt% water in the interior during the erosion period. This indicates that there was very little free water in the polymer bulk. However, tritiated water studies (which measures both reacted and unreacted water) indicate water does penetrate through the entire disc thickness within 24 hours. Water that penetrates must react almost instantaneously with the anhydride bond. This is in contrast with a purely bulk eroding system, where the hydrolysis reaction is often slower than water uptake, resulting in large percentages of water (sometimes up to 60 wt% [26]) in the polymer bulk.

4.3.6 Disc thickness

Further evidence of the p(FAD:SA) copolymer exhibiting certain surface eroding characteristics are found if we examine the effect of device thickness on polymer erosion. Studying the effect of device thickness on erosion often indicates whether the process is primarily one of surface or bulk erosion. The erosion of a surface eroding polymer would only be dependent on the discs's total surface area, and not on the disc volume (or thickness). On the other hand, a bulk eroding system would be dependent on device volume (or thickness). An example of a system degrading primarily by bulk erosion is the p(LGA) copolymer. The rate of appearance of glycolic acid of the 100 mg device is almost exactly half of the 200 mg device. This is consistent with a system primarily degrading by bulk erosion[1]. On the other hand, the rate of SA erosion from p(FAD:SA) polyanhydrides devices is independent of disc thickness early in the erosion profiles (Figure 4.11, Table A.8). Initially discs of different thicknesses show similar SA erosion rates, indicating that the eroding zone is moving inward at approximately the same rate for all devices. However, erosion rates drop off as the erosion fronts meet at the disc center. Therefore, thicker devices exhibit longer periods of SA release.

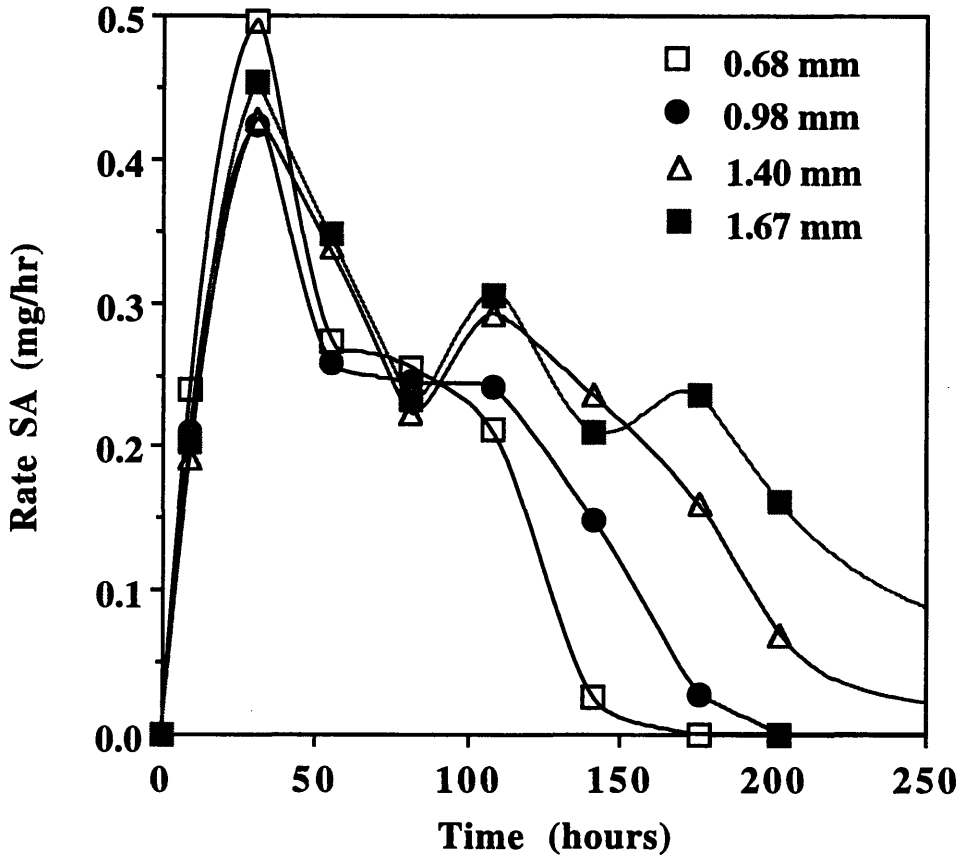

Figure 4.11 Effect of disc thickness on SA erosion rate of p(FAD:SA) 50:50. Plot shown is one set of data representative of two experiments.

4.3.7 Mass transfer effects

Finally, polymer erosion studies have been conducted at various shaking rates to gain a fuller understanding of how mass transfer affects polymer degradation. The shaking rate affects the convective forces carrying monomers away from the polymer matrix. This in turn affects the concentrations of these products at the polymer matrix surface, ultimately affecting product diffusion out of the matrix interior. Results indicate that there is no significant effect of shaking rate on SA erosion (Figure 4.12, Table A.9). For both p(FAD:SA) 20:80 and p(FAD:SA) 50:50, there is no significant difference in SA erosion at 60 and 120 RPM. Discs not shaken at all (0 RPM) appeared to erode only a little more slowly. Apparently external mass transfer effects do not significantly affect polymer erosion.

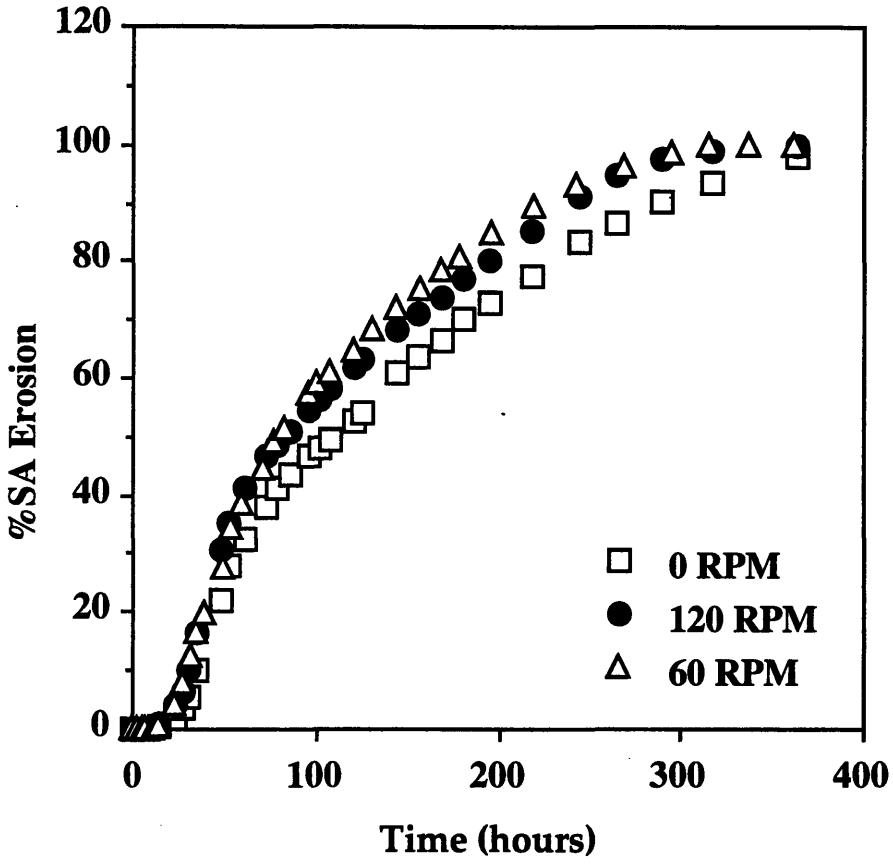

Figure 4.12 Effect of shaking rate on %SA erosion of p(FAD:SA) 50:50. Plot shown is one set of data representative of two experiments.

4.4 CONCLUSIONS

Studies investigating the erosion of the p(FAD:SA) polyanhydride show some surface eroding characteristics. These include the presence of an erosion zone, a distinct area where mass loss occurs. This erosion zone moves inward linearly with time from the surface of the polymer matrix. As the erosion zone progresses, disc thickness also decreases. Degradation occurs first in this outer zone, as demonstrated by infrared spectroscopy. The presence of the erosion zone plays an important role in erosion and drug release because any water or monomer must diffuse through this eroded layer.

Evidence of other certain surface eroding characteristics are present when the effect of device thickness on erosion was examined. The erosion rate of polymer matrices is independent of disc thickness (or volume) until the erosion zones reach the disc center (and then thicker devices erode over a longer period of time). In addition, studies indicate that the water wt% in the polymer interior never exceeded 5% during erosion (in contrast to bulk eroding systems where there are much higher water percentages in the bulk).

The p(FAD:SA) 50:50 eroded over the longest period. It was thought that increasing the more hydrophobic monomer (FAD) of the copolymer may result in slower erosion due to further inhibition of water penetration. However, further increases up to 70 wt% actually decreased the erosion period. DSC results indicate that higher FAD content copolymers were more amorphous, resulting in faster polymer degradation. IR analysis confirmed much faster hydrolysis of the anhydride bond in the p(FAD:SA) 70:30 than in higher SA content copolymers which were more crystalline.

It is apparent that choice of monomers plays a role in the copolymer physical properties and erosion characteristics. It affects copolymer crystallinity, anhydride bond hydrolysis, and monomer dissolution and diffusion out of the polymer matrix. These processes all contribute to the overall polymer erosion pattern. It has been shown that the p(FAD:SA) degradation period cannot be extended to months or years by increasing the FAD component. However, the FAD monomer, which is practically insoluble in water, does appear to slow the diffusion of molecules through the erosion zone of the polymeric device.

CHAPTER 5

RELEASE OF MODEL DRUGS[b]

[b] Results of this chapter are published in [27]

5.1 INTRODUCTION

In this chapter, underlying polymer erosion is correlated with drug release from p(FAD:SA). We also investigate how drug release can be varied by changing polymer composition. The monomer ratio of the copolymer can affect certain properties of the polymer, such as hydrophobicity and crystallinity, which in turn affects the release of drug. In addition, we examine the role of drug solubility, loading, and size on release from the p(FAD:SA). One hydrophilic model drug (Acid Orange 8), one hydrophobic model drug (Rhodamine B Base), and model macromolecules (Dextran Mw=20k and 150k) were studied. It is usually more difficult to control release of hydrophilic drugs because of their affinity for water, which results in faster release. In contrast, hydrophobic drugs may result in more sustained release over a longer period of time.

Finally, we introduce a method of drug incorporation which reduces the drug's "burst effect" from the polymer. In most cases, this "burst effect" is undesirable because an uncontrollable significant portion of the drug is released immediately at the beginning of the release period. This is often seen when a hydrophilic drug is incorporated into a polymer by mixing particles of drug with particles of polymer (or melted polymer). The "burst effect" is the result of drug granules at the surface of the polymer quickly dissolving when immersed in solution. Usually the larger the drug particle size, the larger the "burst". Our method involves forming an emulsion [28] of the drug and polymer in solution. With this emulsion method, extremely tiny particles can be incorporated into the polymer very homogeneously, thus reducing the "burst effect".

5.2 EXPERIMENTAL METHODS

5.2.1 Copolymer composition studies/loading

5.2.1.1 Materials

Copolymer discs of p(FAD:SA) of weight% p(FAD:SA) 20:80 (Mw = 15,000), p(FAD:SA) 50:50 (Mw = 35,000) and p(FAD:SA) 70:30 (Mw = 39,000) loaded with 3% Acid Orange 8 (Sigma Chemicals) and p(FAD:SA) 50:50 (Mw = 35,000) with loadings of 1, 3, 7, and 10% A.O. were received as a gift from Scios-Nova Pharmaceuticals. The polymer was loaded with A.O. by the mix method as described in [5]. The discs were 225 ± 10 mg, 14 mm diameter, and 1.7 ± 0.1 mm thick.

5.2.2 Comparison of drug incorporation methods for water soluble drugs

5.2.2.1 Materials

The p(SA) homopolymer (Mw = 10,000), p(FAD:SA) 20:80 (Mw = 9,000) and p(FAD:SA) 50:50 (Mw = 12,000) was synthesized according to Section 4.2.1, and received as a gift from Scios-Nova Pharmaceuticals (Baltimore, MD). Acid Orange 8 (A.O.) and Rhodamine B Base (RhBB) were obtained from Sigma Chemicals Co (St. Louis, MO).

5.2.2.2 Emulsion method

An emulsion method [28] previously developed for making drug loaded microspheres, was adapted for this study. For 3% A.O. loading: 100 mg p(FAD:SA) was dissolved in 2 ml methylene chloride (Mallinckrodt, analytical grade) and 3 mg A.O. was dissolved in 0.2 ml deionized water. The two solutions were then vortexed, emulsified by probe sonication (Model VC-250, Sonic & Materials Inc. at output 4) for 30 seconds and placed into liquid nitrogen for 30 minutes. The solvent was evaporated overnight in the lyophilizer (Labconco, Freeze Dryer 8).

5.2.2.3 Mix method

The p(FAD:SA) polymer was reduced to powder by mechanical grinding and

sieving (<250 mm). The A.O. was sieved to 53 mm. The two powders were then mixed together with a mortar and pestle.

5.2.3 Role of drug solubility

Rhodamine B Base (RhBB) was mixed with p(FAD:SA) dissolved in methylene chloride to form a homogeneous solution (cosolution method). The solvent was then allowed to evaporate in a vacuum hood, leaving a film of p(FAD:SA) incorporated with RhBB. A.O. was incorporated into p(FAD:SA) 50:50 using the emulsion method. Drug incorporation methods were chosen to give the most uniform drug distribution in the polymer matrix.

5.2.4 Disc fabrication

The drug/polymer powder mixture from the emulsion, mix, and cosolution methods were molded (at 120°C for 20 minutes) into 70 mg discs using teflon molds of 8 mm diameter.

5.2.5 Determination of polymer molecular weights

Polymer molecular weight was determined on a Perkin-Elmer gel permeation chromatography (GPC) system consisting of the Series 10 pump and the 3600 data station with the LC-25 refractive index detector. Samples were eluted in chloroform through a PL gel 5-mm mixed column (Polymer Laboratories) at a flow rate of 0.9 ml/min at 23°C. Polymer molecular weights were determined relative to polystyrene standards (Polysciences).

5.2.6. Polymer erosion and drug release studies

The discs were placed into 20 ml of 0.1 M phosphate buffer (pH 7.4) at 37°C (Precision gravity convection incubator model 4EG) with agitation at 120 RPM (Lab-line shaker). At timed intervals, the entire buffer volume was sampled and 20 ml of fresh buffer was added to the sample vial to approximate perfect sink conditions. Polymer erosion was monitored by analyzing the sampled buffer solutions for SA content by reverse phase ion-pair high pressure liquid chromatography (Hewlett Packard 1090 Series II). The column used was a poly(styrene-divinylbenzene) reversed phase HPLC column (Hamilton, PRP-1), and the mobile phase consisted of acetonitrile in aqueous 0.05 mol/L tetrabutylammonium phosphate (Waters, Pic- A).

SA was detected by UV at λ=210 nm . The run time was 10 minutes at a flow rate of 1.2 ml/min and 100 μL injection volume. The release of drug was determined by a Perkin Elmer 553 UV/VIS Spectrophotometer at λ = 490 nm for A.O. and λ = 544 nm for RhBB. Unless noted in figure caption, every time point corresponded to one sample measurement.

5.2.7 Determination of drug solubility

Either A.O. or RhBB was added to 0.1 M pH 7.4 phosphate buffer solution at 25°C and 37°C. The solution at 37°C was then allowed to cool down to room temperature. Filtered samples were taken over a 24 hour period, and the sample drug concentration was determined by UV/VIS Spectroscopy (Perkin Elmer 553). The drug solubility was taken to be the equilibrium concentration of both the 25°C and cooled 37°C solution (which were the same). The A.O. solubility was determined to be 26 mg/ml and RhBB solubility determined to be 1.25 mg/ml.

5.2.8 Light Microscopy

Cross sections were obtained using a razor blade from 3% A.O. loaded (by the emulsion method) p(FAD:SA) 20:80 at different stages of erosion. The sections were examined under a light microscope (Wild Makroskop M420, Heerbrugg, Switzerland) at 40x.

5.2.9 Dextran studies

200 mg of p(FAD:SA) 50:50 copolymer was dissolved in 1 ml of methylene chloride. For 9% loading; 20 mg of FITC-dextran (Mw = 20k or 150K) was dissolved in 100μl of water. The solvent and aqueous solutions were then combined together in a test tube and vortexed (at speed 7) for 30 seconds, emulsified by probe sonication at output 7 for 30 seconds (test tube was placed in ice bath), dropped into liquid nitrogen, and then lyophilized overnight. The droplet size in emulsion was measured by putting a drop of the emulsion onto a glass size and examining under a Nikon Diaphot microscope (Micro Video Instruments; Avon, MA). The drug/polymer mixture was compressed into disc form using a Carver press at 1000 psi for 10 minutes at room temperature. The release of FITC-dextran was determined by a Perkin Elmer 553 UV/VIS Spectrophotometer at λ = 494 nm.

5.3 RESULTS AND DISCUSSION

5.3.1 Visualization studies

The results from light microscopy cross sections indicate that there is a drug depleted outer zone which grows wider with time. The zone of p(FAD:SA) 50:50 (Figure 5.1) appears as a clear, viscous, adhesive substance surrounding the device. In contrast, the p(FAD:SA) 20:80 zone (Figure 5.2) is more similar to the zone present in the p(CPP:SA), which is white, fragile, and porous. [1]

The diffusing front, defined as the moving front of the zone, advances inward with time. This front is where the drug has begun to diffuse outward. The eroding front, which is the degrading surface of the polymer, also moves inward with time. However, the eroding front moves at a much slower rate than the diffusion front, presumably due to the slower dissolution of the polyanhydride degradation products. The structure and copolymer composition of the outer zone is important because any monomer and/or drug must diffuse through this zone to reach the surface of the polymer matrix.

5.3.2 Drug Release

5.3.2.1 Copolymer composition

Copolymer composition has a significant effect on A.O. drug release (see Figure 5.3, Table A.11). A.O. release from p(FAD:SA) 50:50 formulated from the mix method extends over a longer time period than release from p(FAD:SA) 20:80 and p(FAD:SA) 70:30. (The %A.O. release is normalized to the total amount of A.O. released). The A.O. release profiles are consistent with the underlying SA erosion in that the p(FAD:SA) 50:50 also erodes over a longer period than the other p(FAD:SA) copolymers (see Figure 5.4, Table A.11).

Differences in A.O. release rates may be attributed to differing underlying erosion rates among the different p(FAD:SA) copolymers. We can gain further insight into understanding the difference in A.O. release rates by examining the relationship between drug release and polymer erosion (See Figure 5.5). A.O. release precedes the p(FAD:SA) 20:80 polymer erosion, which seems reasonable due

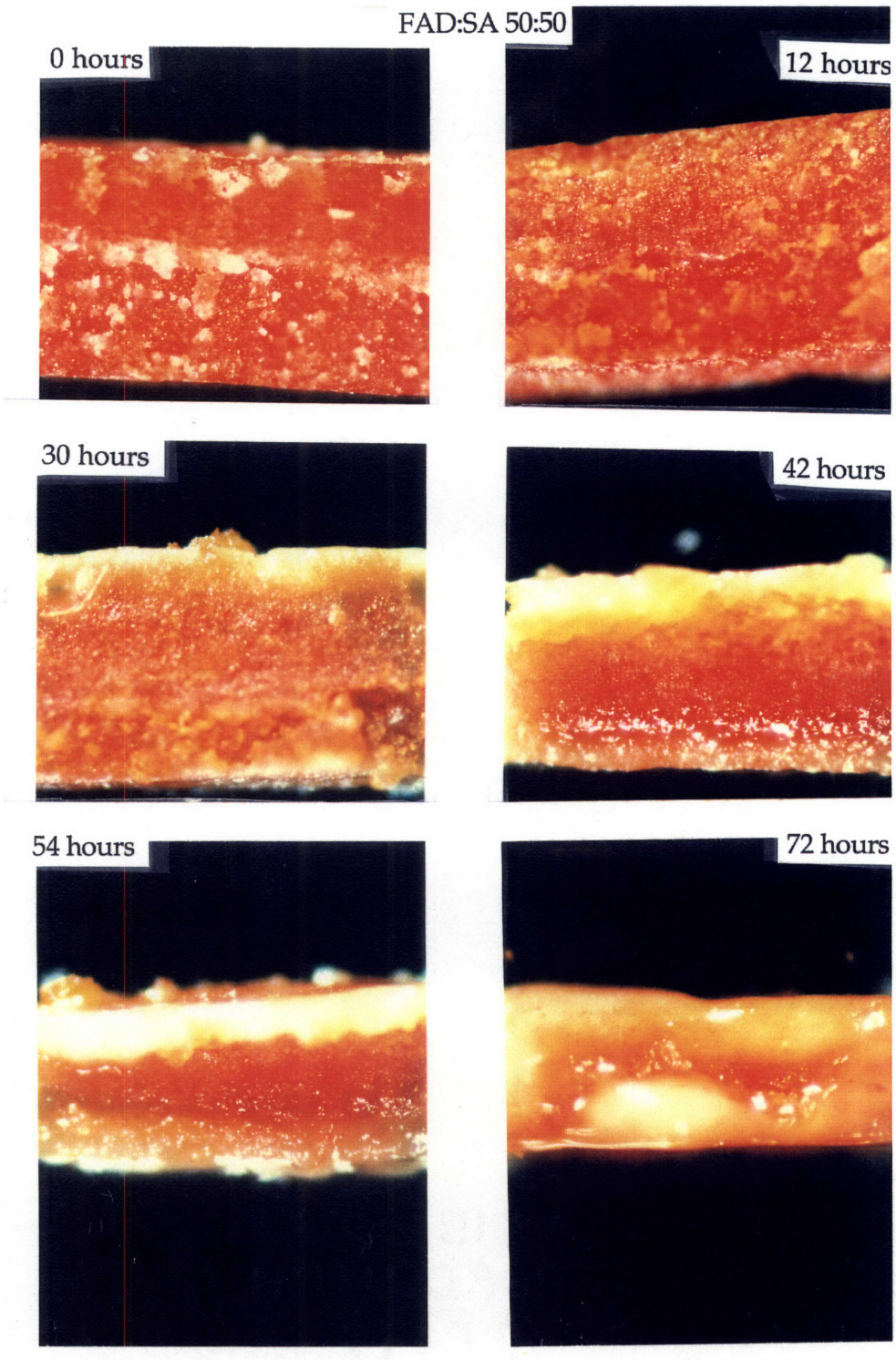

Figure 5.1 Light microscopy cross sections of 3% A.O. loaded p(FAD:SA) 50:50 (initial thickness 1.25 mm) of 40x magnification at indicated time intervals.

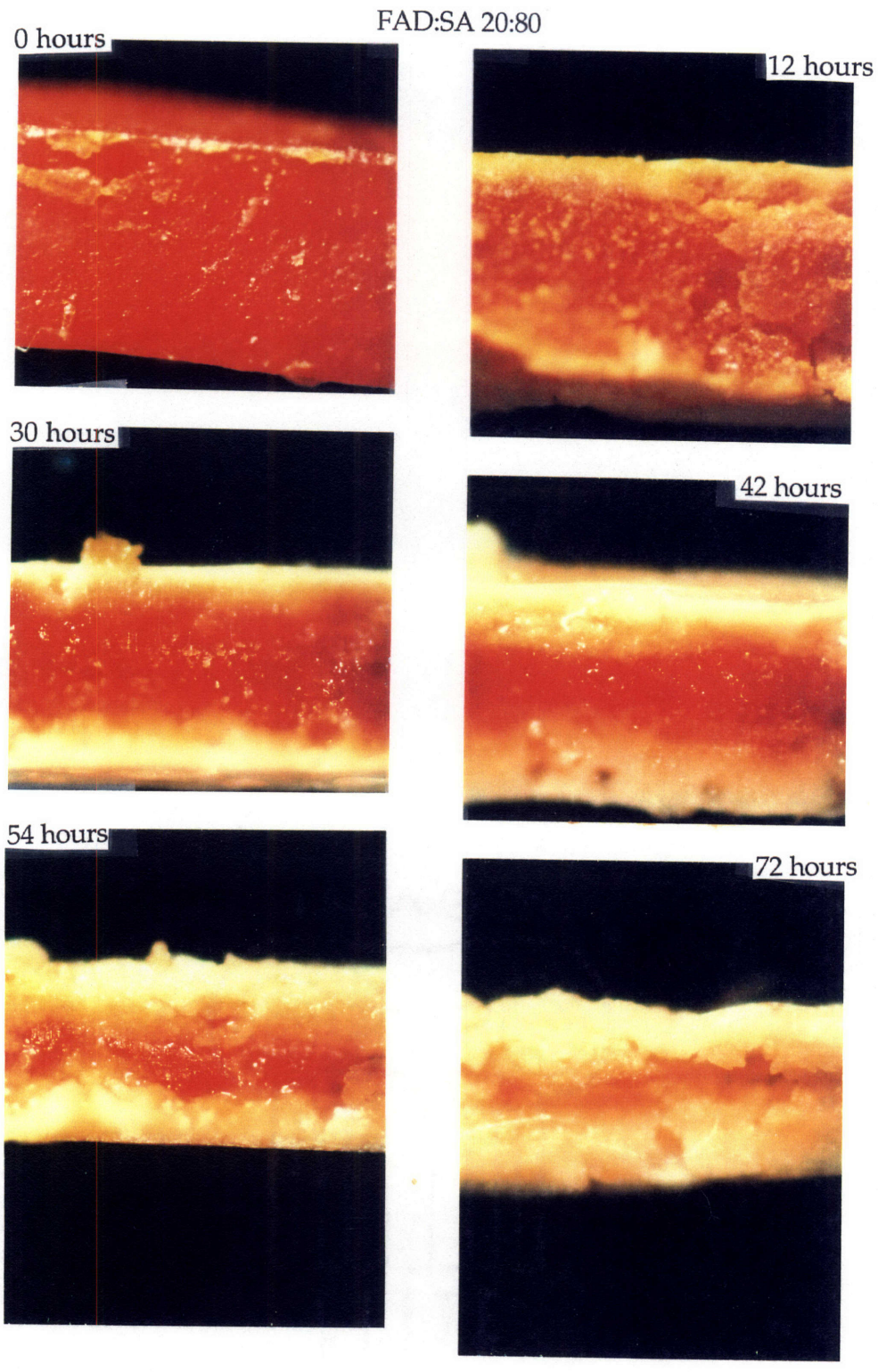

Figure 5.2 Light microscopy cross sections of 3% A.O. loaded p(FAD:SA) 20:80 (initial thickness 1.25 mm) of 40x magnification at indicated time intervals.

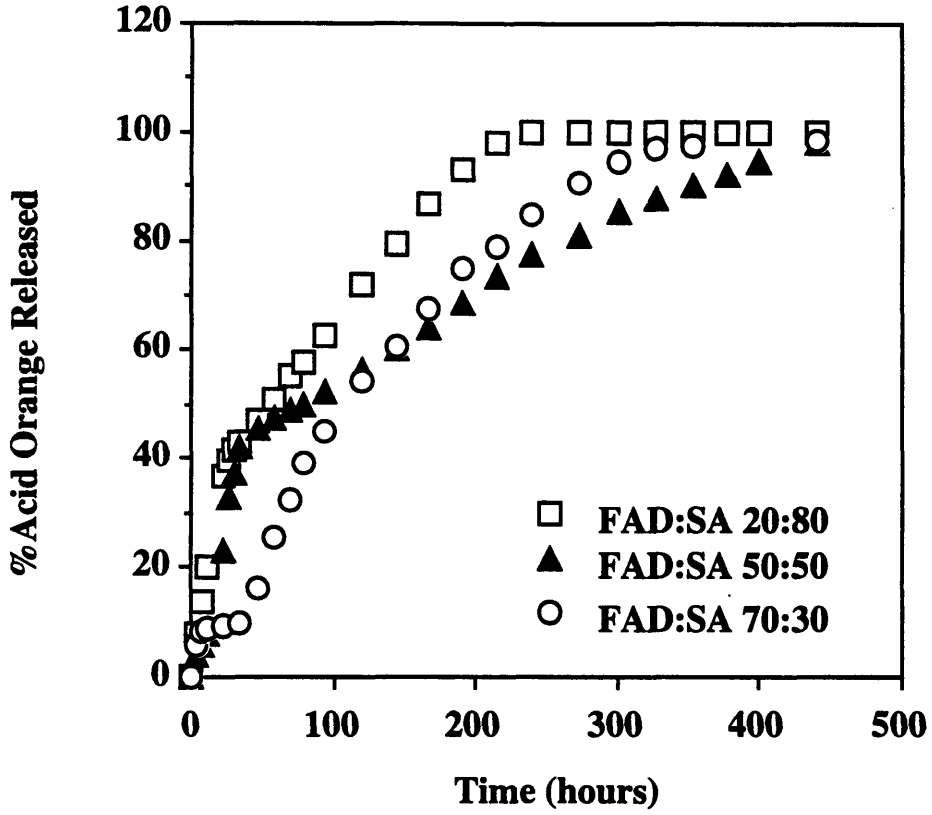

Figure 5.3 Effect of p(FAD:SA) monomer ratio on %A.O. release. A.O. was loaded by melting the polymer at 70°C, and then adding in the drug and mixing well. The homogenous mixture was then cast into rods 14 mm in diameter using a rubber mold. The rods were then cut into discs of initial weight 200 mg, initial thickness 1.7± 0.1 mm. Polymer compositions used were p(FAD:SA)20:80, p(FAD:SA) 50:50 and p(FAD:SA) 70:30 at a loading of 3% A.O. Plot shown is one set of data representative of two experiments.

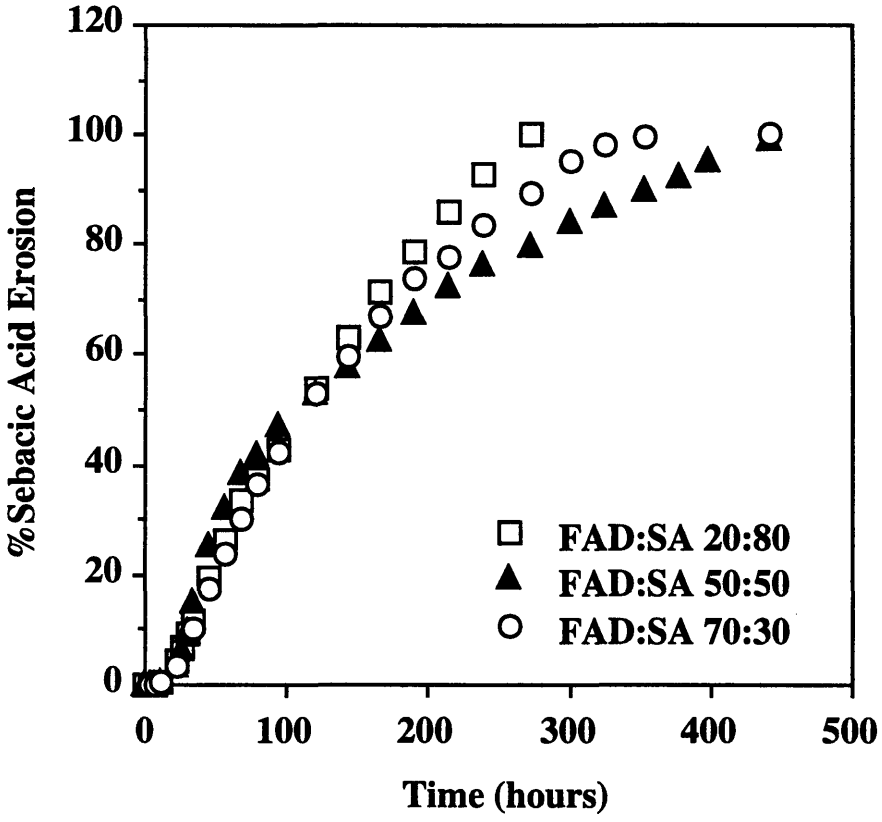

Figure 5.4 Effect of FAD:SA monomer ratio on SA erosion.
Polymer-drug matrices were formulated as in Figure 5.3.
Plot shown is one set of data representative of two experiments.

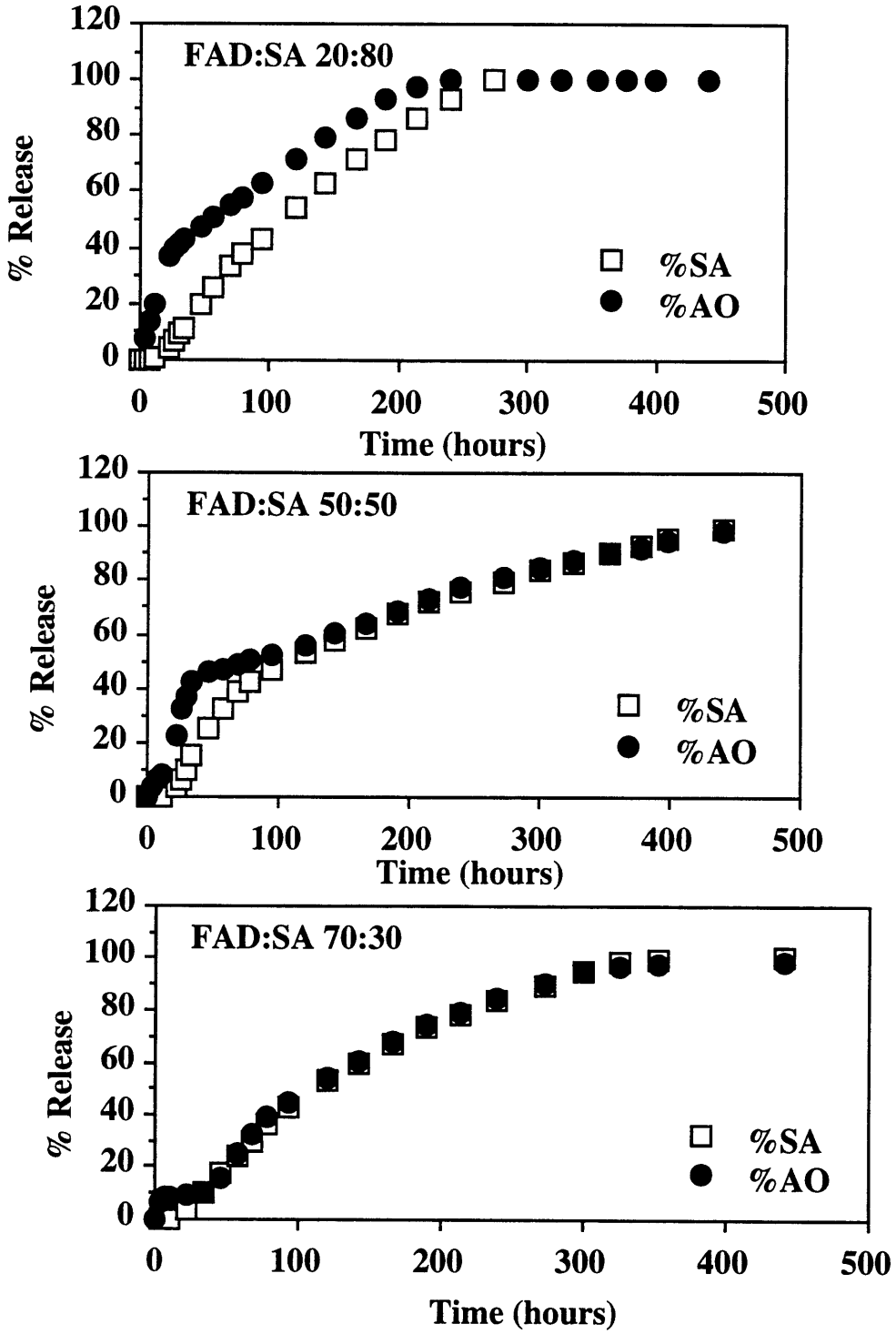

Figure 5.5 Correlation of %A.O. release with underlying %SA erosion of 3% loaded p(FAD:SA) 20:80, p(FAD:SA) 50:50, and p(FAD:SA) 70:30. Polymer-drug matrices were formulated as in Figure 5.3. Plot shown is one set of data representative of two experiments.

to A.O.'s higher solubility and lower entanglement within the matrix compared to the SA. On the other hand, A.O. release from the p(FAD:SA) 50:50 and p(FAD:SA) 70:30 (after the initial burst effect) follows SA erosion at lower drug loadings (1-3%). This closer correlation between drug release and polymer erosion may be due to the higher FAD content of the outer zone that the A.O. molecule must diffuse through in p(FAD:SA) 50:50 and p(FAD:SA) 70:30. As a result, A.O. release through the more porous erosion zone of the p(FAD:SA) 20:80 is faster than A.O. release from the copolymers of higher FAD content, p(FAD:SA) 50:50 and p(FAD:SA) 70:30.

A.O. release profiles from both p(FAD:SA) 20:80 and p(FAD:SA) 50:50 formulated by the mix method begin with a large "burst" and then exhibit relatively constant release for the rest of the time period. Part of this early release is most likely due to the "burst effect" seen in devices prepared by the mix method. The "burst" is the result of drug granules at the surface of the polymer quickly dissolving when immersed in solution. Some of this initial surge could also be attributed to the hydrophilic nature of A.O., which may be attracting water into the matrix, and the greater drug concentration gradient in the initial period. These factors could result in higher rates of A.O. release early in the time period.

5.3.2.2 Drug loading

The hydrophilicity and water attraction of A.O. is consistent with the effect of drug loading on A.O. release from drug-polymer matrices formulated by the mix method (see Figure 5.6, Table A.12). The 10% A.O. loaded device is depleted earliest, followed by the 7% loaded disc. The drug release profiles at the higher loadings precede SA erosion. On the other hand, drug release from the 1% and 3% loaded devices follows SA erosion very closely. These devices also released drug over the longest time. The faster drug depletion of higher loaded devices may be due to the greater amount of hydrophilic drug present. On the other hand, there does not seem to be a significant effect of A.O. drug loading on SA erosion at low drug loadings (see Figure 5.7, Table A.12). The blank polymer (0% loading) erosion profile shows little difference in erosion compared to those devices at low A.O. loadings. However, as one increases the loading up to 10% A.O., there is an increase in erosion rate.

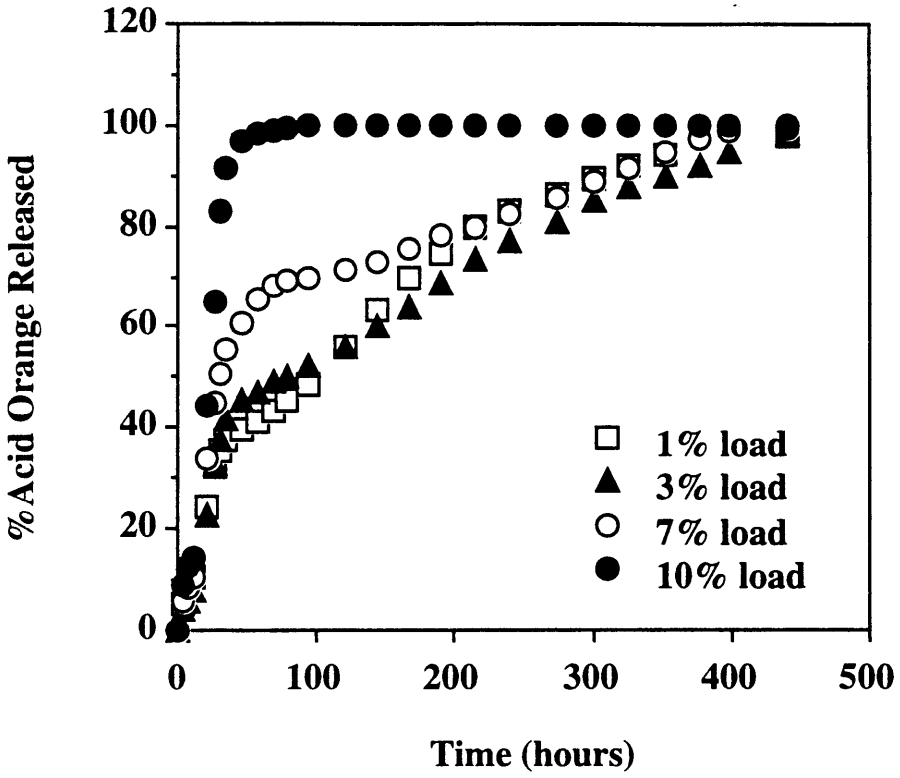

Figure 5.6 Effect of A.O. drug loading on %A.O. release from p(FAD:SA) 50:50. Polymer-drug matrices were formulated as in Figure 5.3. Plot shown is one set of data representative of two experiments..

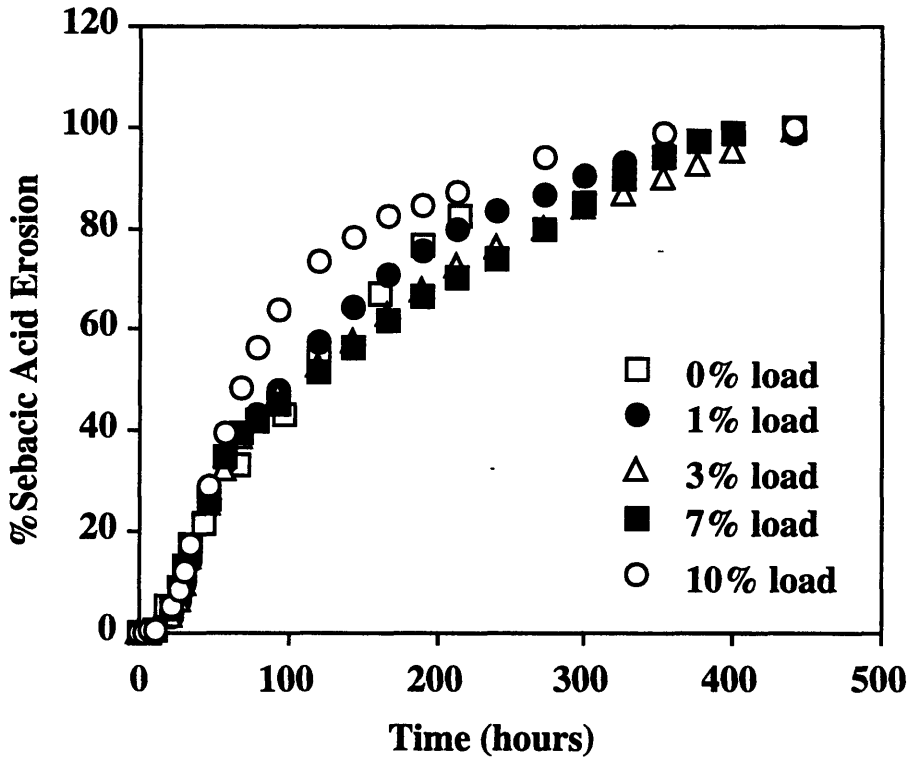

Figure 5.7 Effect of A.O. drug loading on %SA erosion of p(FAD:SA) 50:50. Polymer-drug matrices were formulated as in Figure 5.3. Plot shown is one set of data representative of two experiments.

5.3.2.3 Reduction of burst effect

Since 40% of the A.O. is released within the first 50 hours (and an even higher percentage is released at higher A.O. loadings), it would be extremely desirable to reduce this "burst effect". We believed we could accomplish this by changing our drug incorporation procedure. Since it is thought that the burst effect is mainly the result of large drug particles at the disc surface going directly into the releasing medium, we believed that by reducing drug particle size and increasing the homogeneity of the drug-polymer mixture, we could reduce the burst effect. We decided to try an emulsion method, which involves forming an emulsion of the drug with the polymer solvent mixture. We found that the emulsion method of drug incorporation greatly minimizes the A.O.'s "burst effect" from the surface of the polymer (see Figure 5.8a, Table A.13). The p(SA) device prepared by the mix method releases 25% of the total A.O. within the first 2 hours after immersion into buffer. This is in comparison to only 4% A.O. release from the p(SA) emulsion prepared disc. SA erosion is unaffected by the type of drug incorporation method (emulsion vs. mix) used (see Figure 5.8b, Table A.13). We also found that the droplet size in the drug-polymer emulsion affects the size of the burst. It was measured that the smaller the droplet size in the emulsion, the smaller the initial burst (see Figure 5.8c, Table A.16).

The reduction of this "burst effect" enables the p(SA) incorporated by the emulsion method to release the drug at a more constant rate over a longer time, and also minimizes the danger of a toxic burst occurring at the start of the release. We can also now determine the effect of copolymer composition on A.O. drug release without this initial "burst effect" affecting our results (see Figure 5.9a, Table A.14). Here, we can see that A.O. release from p(FAD:SA) 50:50 is slower than A.O. release from the higher content SA copolymers over the entire release period. Comparing A.O. release with the underlying SA erosion, we notice again that A.O. release precedes SA erosion for p(FAD:SA) 20:80 , and follows more closely the SA erosion in p(FAD:SA) 50:50 (see Figure 5.9b, Table A.14).

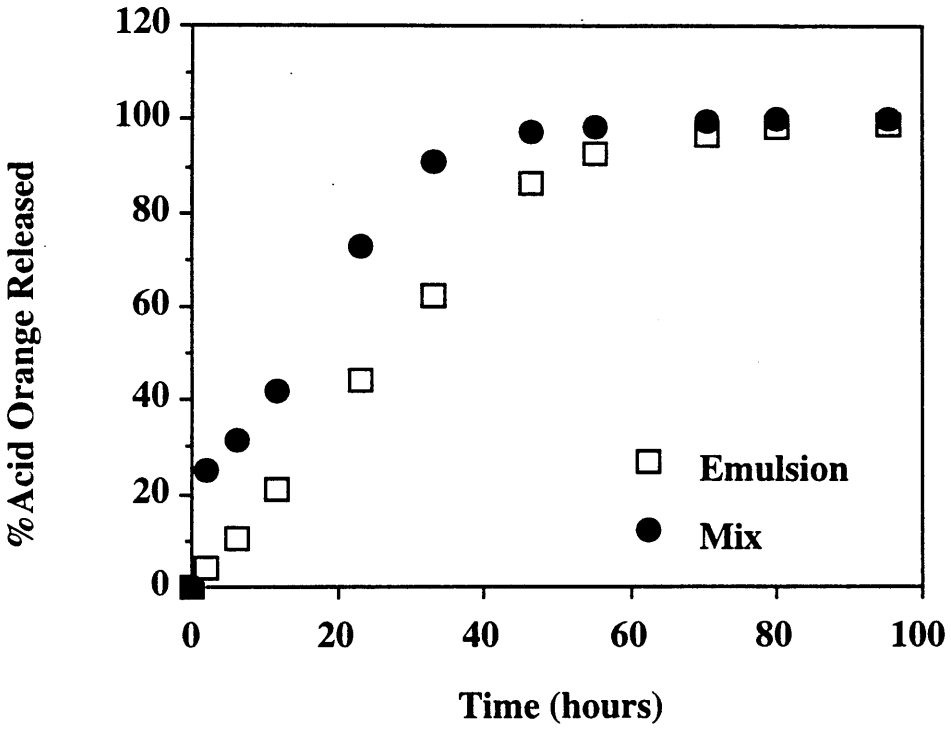

Figure 5.8a Effect of drug incorporation on %A.O. release from 3% A.O. loaded p(SA). The emulsion method was compared to the mix method of drug incorporation. (Both are described in the materials and methods section). 70 mg discs were fabricated by melting the polymer - drug powder in teflon molds of 8 mm diameter. Plot shown is one set of data representative of two experiments.

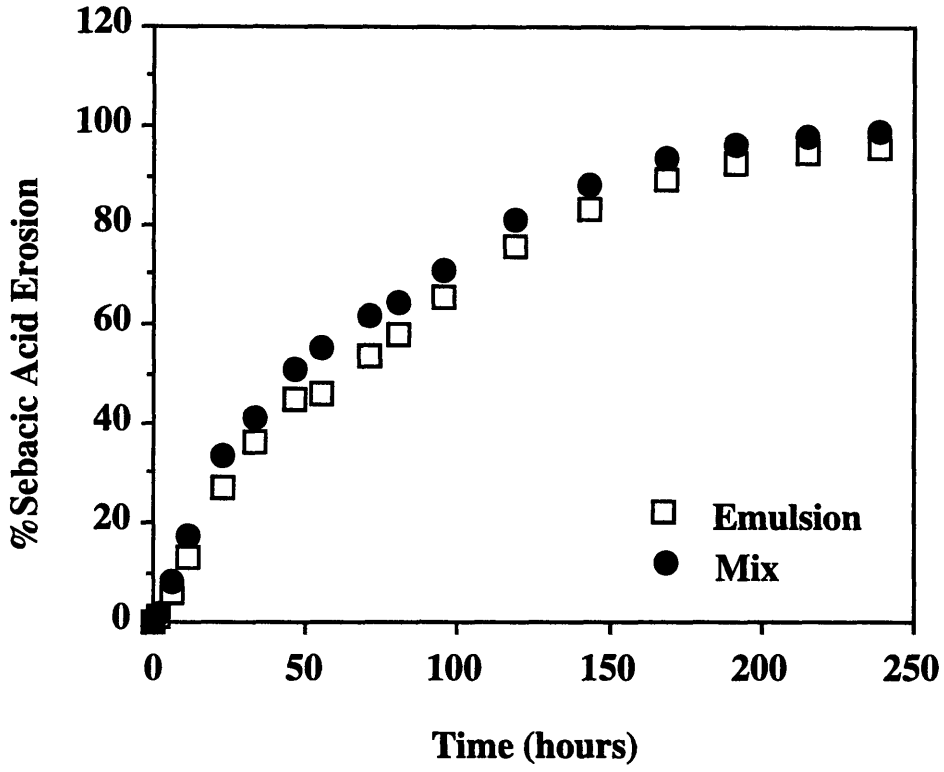

Figure 5.8b Effect of drug incorporation method (emulsion vs mix) on %SA erosion from 3% A.O. loaded p(SA). Plot shown is one set of experimental data.

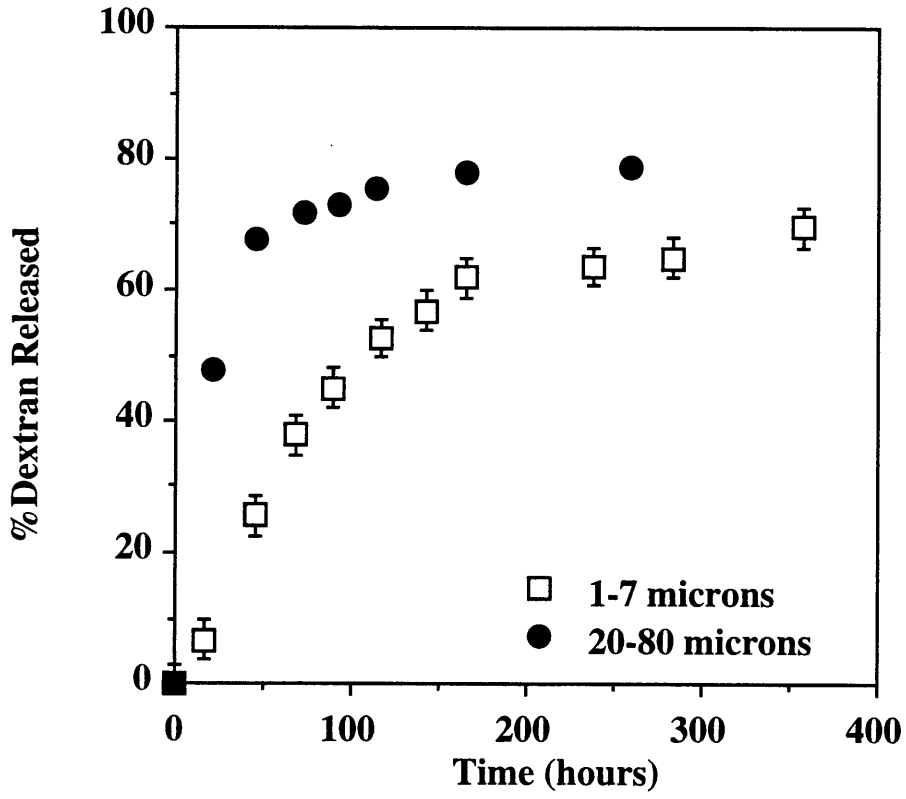

Figure 5.8c Effect of droplet size in emulsion during drug incorporation on dextran (Mw=20,000) release from 10% loaded p(FAD:SA) 20:80. Data with error bars represent an average of two measurements; error bars represent the spread of the data.

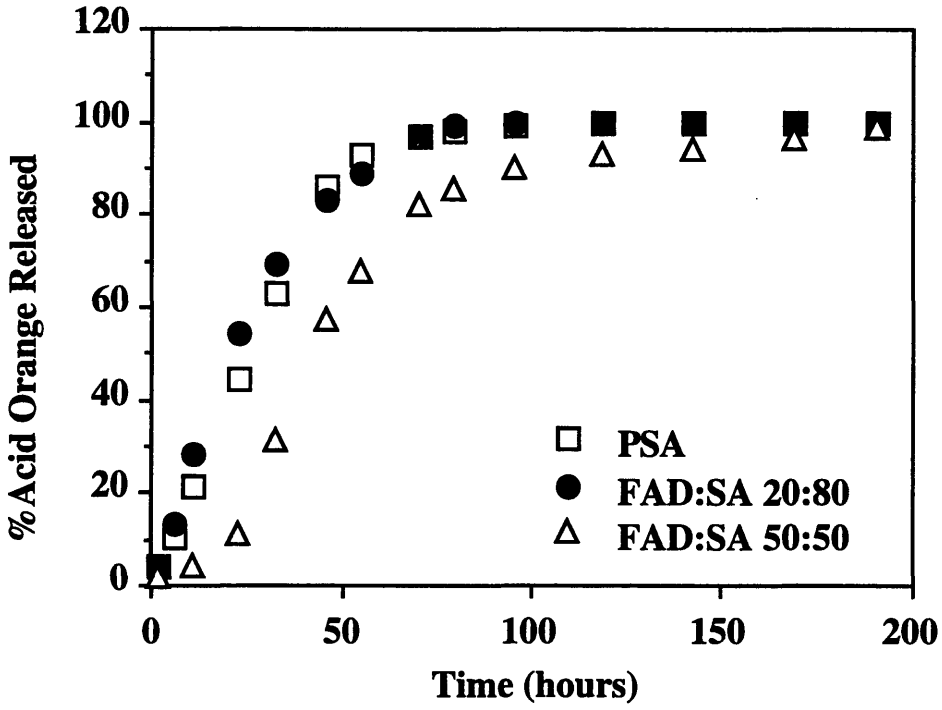

Figure 5.9a Effect of p(FAD:SA) monomer ratio on A.O. drug release from 3% A.O. loaded polymer-drug matrices fabricated by the emulsion method. Devices were of 8 mm diameter, 1.3 mm thickness. Plot shown is one set of data representative of two experiments.

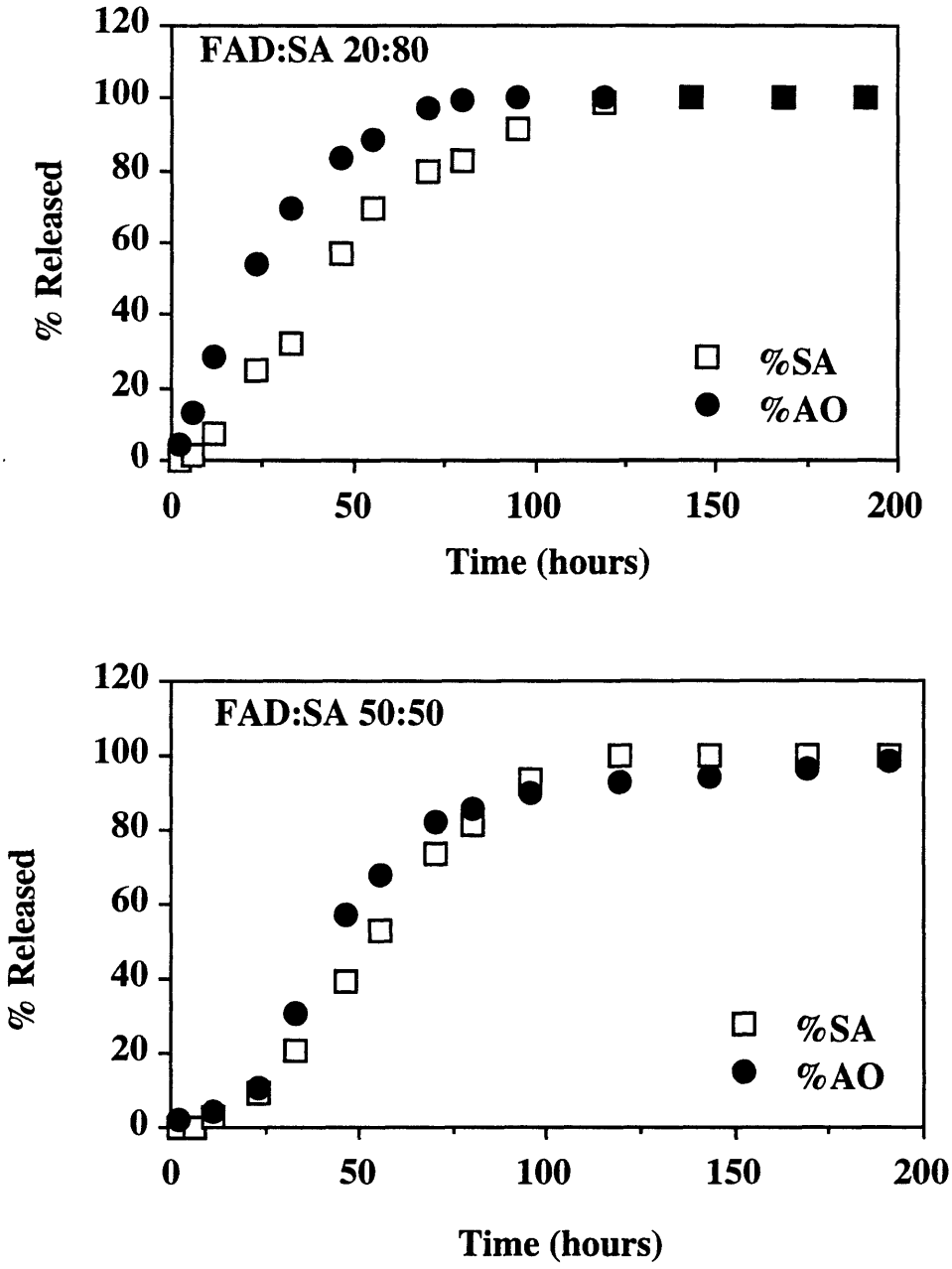

Figure 5.9b Correlation of %A.O. release with underlying %SA erosion for 3% loaded p(FAD:SA) 20:80 and p(FAD:SA) 50:50. Polymer-drug matrices were formulated by the emulsion method. Plot shown is one set of data representative of two experiments.

5.3.2.4 Drug solubility

Because of the hydrophilicity of A.O., it would be beneficial to follow the release of a more hydrophobic drug to determine the importance of drug solubility on release characteristics. We have examined the release of the more hydrophobic dye, Rhodamine B Base, from the p(FAD:SA) copolymer (see Figure 5.10, Table A.15). (The %RhBB release is normalized to the total amount of RhBB released). Results were compared with A.O. release from p(FAD:SA) formulated by the emulsion method at the same loading (3%). Results indicate that Rhodamine B Base (RhBB) releases much slower than the A.O. from both the p(FAD:SA) 20:80 and p(FAD:SA) 50:50. This slower release is expected based on the relative hydrophobicities of the two dyes. However, we must also take into consideration the different functionalities of the two dyes which may have different interactions with the polymer matrix. (eg. possible hydrophobic interactions between RhBB and p(FAD:SA) copolymer). In addition, we must take into account that slightly different methods of drug incorporation were used (emulsion for A.O. vs. cosolution for RhBB). The methods were chosen to give the most uniform drug distribution in the polymer matrix for each case (water soluble vs. insoluble drug).

The monomer ratio of the p(FAD:SA) copolymer has less effect on the release of RhBB as compared to A.O. (see Figure 5.11, Table A.15). Results correlating drug release with underlying polymer erosion indicate that RhBB release actually lags the SA erosion (see Figure 5.12). The low solubility of the drug and hydrophobic interactions with the polymer may be rate limiting in it's release. The release of RhBB also appears independent of device loading (see Figure 5.13, Table A.15). This is in contrast to A.O. release, where higher loadings resulted in faster drug depletion of the device. Since RhBB is less hydrophilic than A.O., it probably attracts less water into the polymer matrix (and even polymer erosion may be slower). Higher RhBB loadings do not deplete faster than lower loadings.

The studies thus far have looked at the release of small model drugs. We were also interested in investigating the release of large macromolecules. Dextrans of Mw = 20k and Mw = 150k were chosen as models. Macromolecular size affected release from p(FAD:SA) 50:50 (150k dextran released slower than 20k dextran). At 150 hours, the p(FAD:SA) 50:50 had released 50% of the 20k dextran, compared to only 35% release of the 150k dextran (see Figure 5.14, Table A.16). In addition,

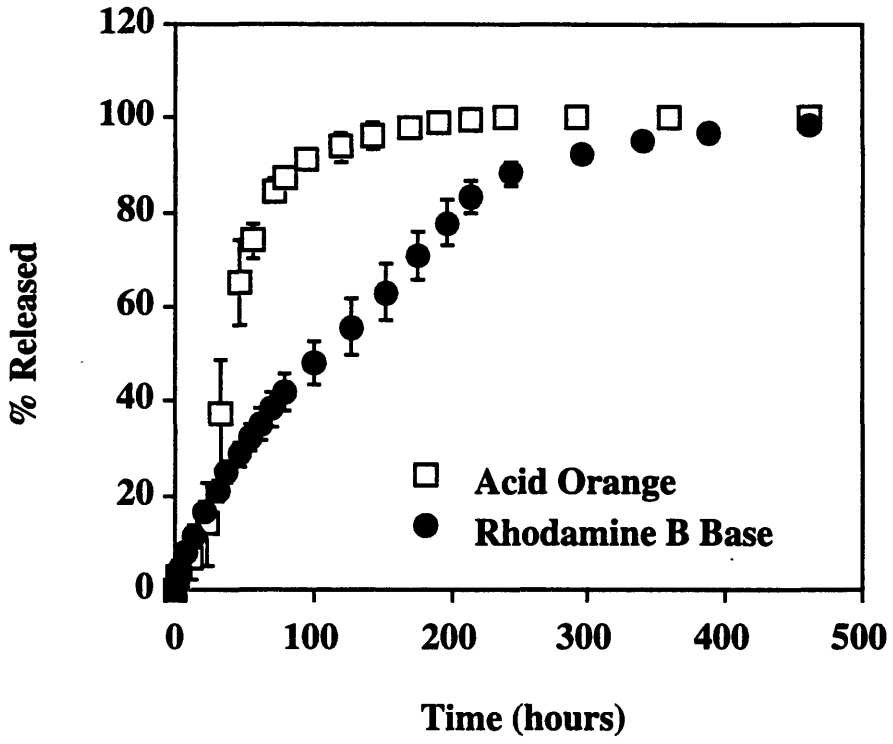

Figure 5.10 Effect of drug solubility on release from 3% loaded p(FAD:SA) 50:50. A.O. release was compared to Rhodamine B Base (RhBB), a more hydrophobic model drug. The emulsion method was used to incorporate A.O., and cosolution method was used to incorporate RhBB. (Both are described in the materials and methods section) Data with error bars represent an average of two measurements; error bars represent the spread of the data.

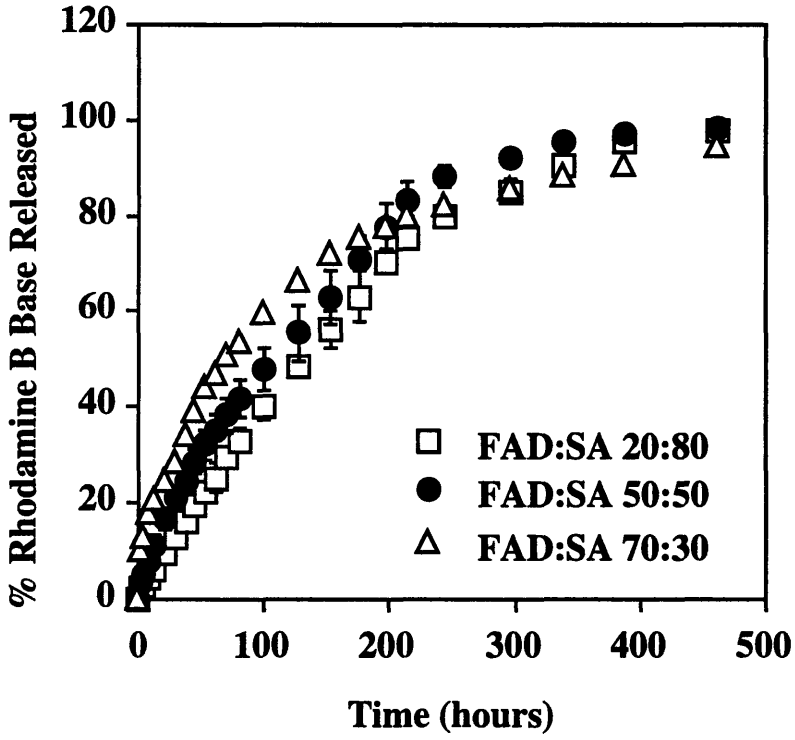

Figure 5.11 Effect of copolymer composition on %RhBB release. The RhBB was incorporated by the cosolution method. Polymer compositions used were p(FAD:SA) 20:80, p(FAD:SA) 50:50, and p(FAD:SA) 70:30 at a loading of 3% RhBB. Data with error bars represent an average of two measurements; error bars represent the spread of the data.

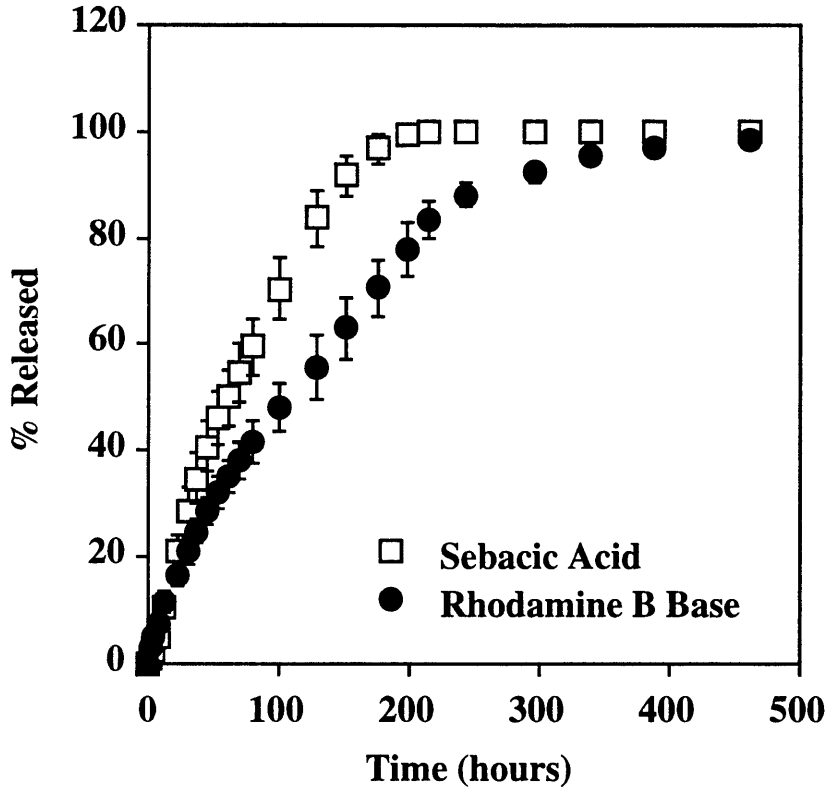

Figure 5.12 Correlation of %RhBB release with underlying SA erosion of 3% loaded p(FAD:SA) 50:50. Data with error bars represent an average of two measurements; error bars represent the spread of the data.

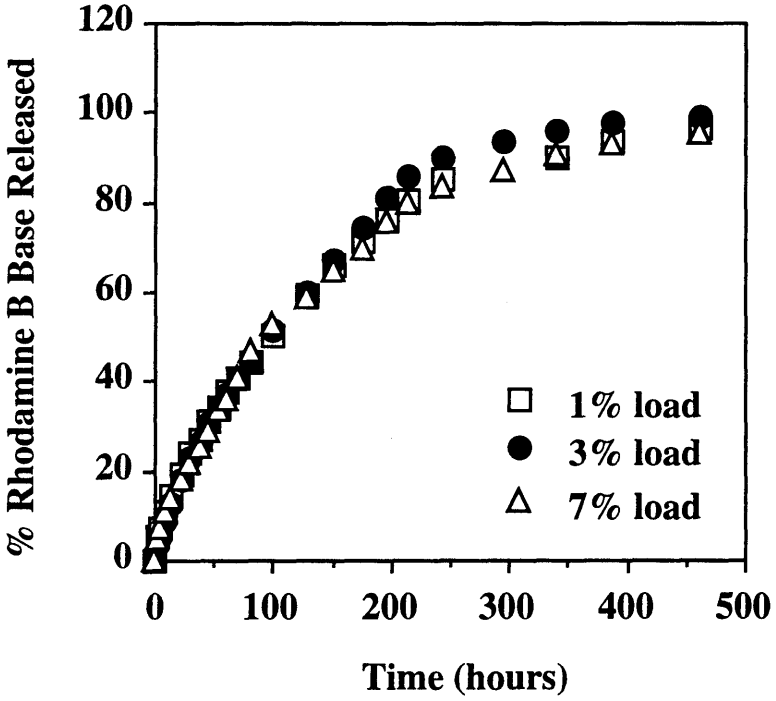

Figure 5.13. Effect of drug loading on % RhBB release from p(FAD:SA) 50:50. Plot shown is one set of experimental data.

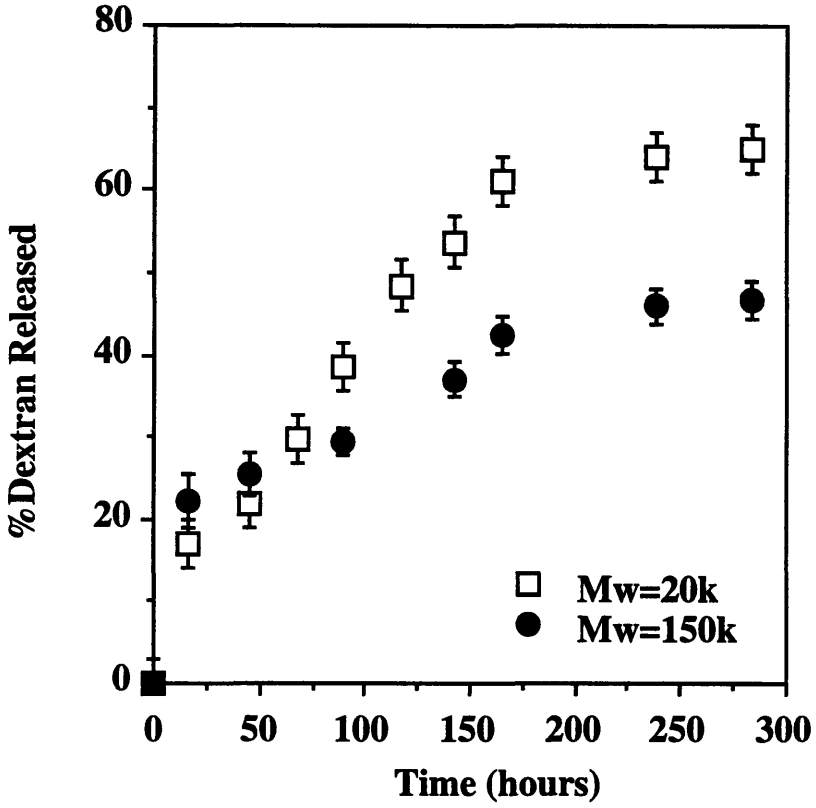

Figure 5.14 Effect of FITC-Dextran size on release from p(FAD:SA) 50:50. Discs were 9% loaded by the emulsion method, 50 mg, and 1.0 mm thick. Data with error bars represent an average of two measurements; error bars represent the spread of the data.

only about 40% of the total 150k dextran incorporated was released, indicating that more than half was still entrapped in the polymer matrix. The smaller macromolecule (20k dextran) showed more complete release (60% of the initial load was released).

5.4 CONCLUSIONS

Studies investigating the release of model drugs from p(FAD:SA) polyanhydrides were also described. Acid Orange (A.O.) release was affected by method of drug incorporation, monomer composition and drug loading. Higher A.O. loaded devices were depleted before lower loaded ones. We were also able to vary release by changing the monomer ratio of the p(FAD:SA) copolymer. A.O. release from p(FAD:SA) 50:50 extended over a longer time period than release from p(FAD:SA) 20:80 and p(FAD:SA) 70:30, which was consistent with the underlying polymer erosion.

We also correlated drug release with underlying polymer erosion. Results indicated that A.O. release followed SA erosion (after the initial burst effect) for the p(FAD:SA) 50:50 and p(FAD:SA) 70:30. On the other hand, A.O. release preceded SA erosion for p(FAD:SA) 20:80. It appeared that the A.O. molecule found less hindrance through the more porous erosion zone of the higher SA content copolymers. The FAD monomer, which is practically insoluble in water, may slow the diffusion of molecules through the erosion zone of the polymeric device.

A.O. release studies using the mix method of drug incorporation illustrated the problem of the initial "burst" of hydrophilic drugs. 40% of the total A.O. (even greater percentages at high A.O. loadings) was released within the first 50 hours. We eliminated this undesirable "burst effect" by using a new drug incorporation method which forms an emulsion of the drug and polymer in solution. With this emulsion method, extremely tiny particles can be incorporated into the polymer very homogeneously, thus greatly reducing the "burst effect". We were able to decrease the initial A.O. burst during the first two hours of release from 25% to 4% of the total A.O. using the emulsion method. Using discs prepared from this emulsion method, we can more clearly see the effect of copolymer composition on A.O. drug release.

The effect of drug solubility and size on release was also studied. The release of A.O. was compared with Rhodamine B Base (RhBB), a more hydrophobic drug. Results indicated that RhBB released slower than A.O., and was less affected by

loading and copolymer composition. The RhBB release lagged behind the SA erosion from the matrix. The low solubility and hydrophobic interactions of the dye may be rate limiting in it's release. The release of large macromolecules was also investigated. Dextrans of Mw = 20k and Mw = 150k were chosen as models. Macromolecular size affected release from p(FAD:SA) 50:50, where 150k dextran released slower than 20k dextran.

CHAPTER 6

PROTEIN RELEASE

6.1 INTRODUCTION

In the previous chapter, we described the release of small molecular weight model drugs (Mw = 300 - 400) from p(FAD:SA). However, it would also be desirable to be able to deliver large macromolecules such as proteins and hormones. Protein delivery is a challenging problem because one must maintain the protein's native structure through fabrication and release. Loss of native conformation not only leads to loss of biological activity, but also increases susceptibility to further problems such as covalent or non-covalent aggregation. In addition, the large variety of functional groups present in proteins amplifies the number of chemical processes which may lead to potential inactivation (eg. oxidation, deamidation, β-elimination, disulfide scrambling, hydrolysis, isopeptide bond formation, and aggregation) [21].

Our approach is to incorporate the protein in a polymeric matrix that could potentially protect the protein from solvent induced denaturation and proteolytic enzymes [20] until it is released in a controlled and sustained manner at the desired application site. We chose to study the enzymes β-chymotrypsin (Mw = 25,000) and horseradish peroxidase (Mw = 44,000) (see Figure 6.1 [29]) as our model proteins. These enzymes were chosen so that enzymatic activity could be monitored through each step of the device fabrication and release period. Dextran was chosen as a stabilizer due to preliminary results by [30] suggesting that rHSA (recombinant human serum albumin) lyophilized with dextran delayed aggregation.

6.1.2 Objectives

The goals of this chapter are to:

1) Monitor enzyme activity through disc fabrication
2) Monitor enzyme activity during controlled release
3) If there is any activity loss, determine why it occurs

```
                5                  10         carb    15                  20                  25
Glu-Leu-Thr-Pro-Thr-Phe-Tyr-Asp-Asn-Ser-Cys-Pro-Asn-Val-Ser-Asn-Ile-Val-Arg-Asp-Thr-Ile-Val-Asn-Glu-

               30                  35                  40                  45                  50
Leu-Arg-Ser-Asp-Pro-Arg-Ile-Ala-Ala-Ser-Ile-Leu-Arg-Leu-His-Phe-His-Asp-Cys-Phe-Val-Asn-Gly-Cys-Asp-

               55      carb        60                  65                  70                  75
Ala-Ser-Ile-Leu-Leu-Asp-Asn-Thr-Thr-Ser-Phe-Arg-Thr-Glu-Lys-Asp-Ala-Phe-Gly-Asn-Ala-Asn-Ser-Ala-Arg-

               80                  85                  90                  95                  100
Gly-Phe-Pro-Val-Ile-Asp-Arg-Met-Lys-Ala-Ala-Val-Glu-Ser-Ala-Cys-Pro-Arg-Thr-Val-Ser-Cys-Ala-Asp-Leu-

               105                 110                 115                 120                 125
Leu-Thr-Ile-Ala-Ala-Gln-Gln-Ser-Val-Thr-Leu-Ala-Gly-Gly-Pro-Ser-Trp-Arg-Val-Pro-Leu-Gly-Arg-Arg-Asp-

               130                 135                 140                 145                 150
Ser-Leu-Gln-Ala-Phe-Leu-Asp-Leu-Ala-Asn-Ala-Asn-Leu-Pro-Ala-Pro-Phe-Phe-Thr-Leu-Pro-Gln-Leu-Lys-Asp-

               155         carb    160                 165                 170                 175
Ser-Phe-Arg-Asn-Val-Gly-Leu-Asn-Arg-Ser-Ser-Asp-Leu-Val-Ala-Leu-Ser-Gly-Gly-His-Thr-Phe-Gly-Lys-Asn-

               180                 185 carb            190                 195         carb    200
Gln-Cys-Arg-Phe-Ile-Met-Asp-Arg-Leu-Tyr-Asn-Phe-Ser-Asn-Thr-Gly-Leu-Pro-Asp-Pro-Thr-Leu-Asn-Thr-Thr-

               205                 210             carb 215            220                 225
Tyr-Leu-Gln-Thr-Leu-Arg-Gly-Leu-Cys-Pro-Leu-Asn-Gly-Asn-Leu-Ser-Ala-Leu-Val-Asp-Phe-Asp-Leu-Arg-Thr-

               230                 235                 240                 245                 250
Pro-Thr-Ile-Phe-Asp-Asn-Lys-Tyr-Tyr-Val-Asn-Leu-Glu-Glu-Gln-Lys-Gly-Leu-Ile-Gln-Ser-Asp-Gln-Glu-Leu-

               carb                260                 265         carb    270                 275
Phe-Ser-Ser-Pro-Asn-Ala-Thr-Asp-Thr-Ile-Pro-Leu-Val-Arg-Ser-Phe-Ala-Asn-Ser-Thr-Gln-Thr-Phe-Phe-Asn-

               280                 285                 290                 295                 300
Ala-Phe-Val-Glu-Ala-Met-Asp-Arg-Met-Gly-Asn-Ile-Thr-Pro-Leu-Thr-Gly-Thr-Gln-Gly-Gln-Ile-Arg-Leu-Asn-

               305
Cys-Arg-Val-Val-Asn-Ser-Asn-Ser

Disulfide bridges: 11-91, 44-49, 97-301, 177-209.
```

Figure 6.1 The amino acid sequence of horseradish peroxidase
carb = site of carbohydrate attachment

The first goal was to monitor enzyme activity through disc fabrication. There are many steps in the disc fabrication (see Figure 6.2) which could affect protein activity (such as exposure to organic solvent, shear from vortexing, heat from sonication, freeze-drying, compression molding). Therefore, it is important to determine which step(s) are crucial in maintaining protein activity.

The next goal was to monitor protein release from p(FAD:SA), and determine how much active the released protein is. If there are any activity losses that occur during release, we would want to determine why they occur. Size exclusion chromatography will be used to characterize the released protein. Potential problems that should be considered include protein denaturation and/or aggregation within the polymer due to a variety of factors (water penetration into polymer, interaction with hydrophobic polymer, acid denaturation from the acidic degradation products, etc.)

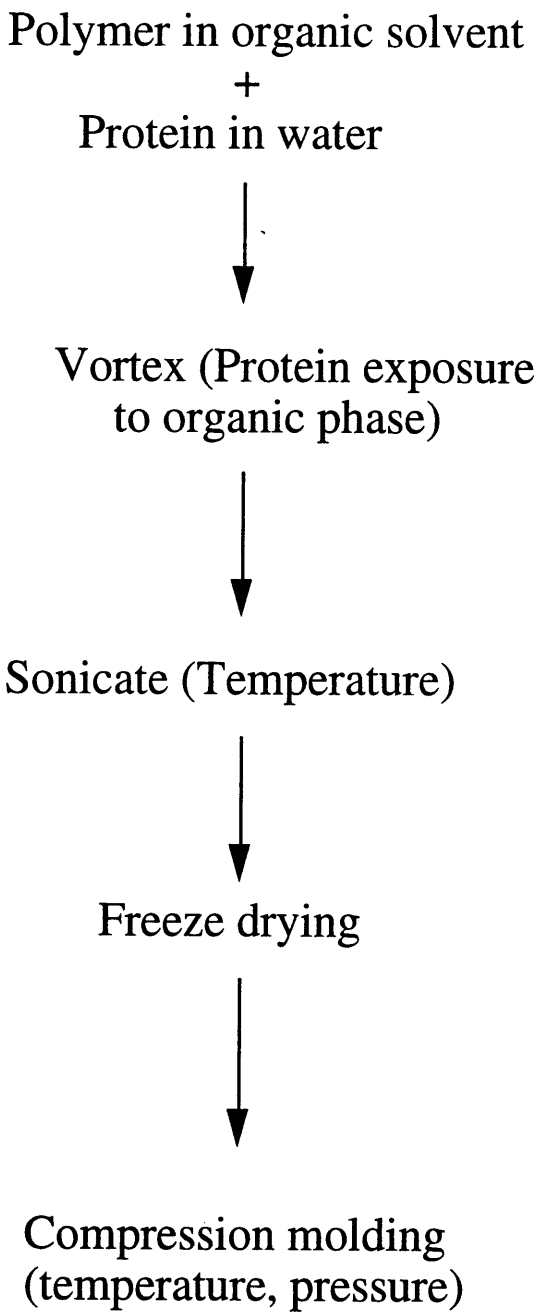

Figure 6.2 Steps in fabrication process that could affect protein activity

6.2 EXPERIMENTAL METHODS

6.2.1 MATERIALS

P(FAD:SA) of weight% 50:50 (M_W=30,000) were received as a gift from Scios-Nova Pharmaceuticals. The polymer was synthesized by melt polycondensation as described in Section 4.2.1. Horseradish peroxidase, β-chymotrypsin, benzoyl-L-tyrosine ethyl ester (BTEE), and 2,2'-Azino-bis (3-Ethylbenzthiazoline-6-Sulfonic Acid) (ABTS) substrate, and markers for isoelectric focusing were purchased from Sigma Chemicals. Bicinchoninic acid (BCA) protein assay was purchased from Pierce.

6.2.2 METHODS

6.2.2.1 Protein incorporation

200 mg of p(FAD:SA) 50:50 (by weight) polymer was dissolved in 1 ml of methylene chloride. For 9% loading; 20 mg of protein was dissolved in 100 ml of water. The solvent and aqueous solutions were then combined together in a test tube and vortexed (at speed 7) for 30 seconds, emulsified by probe sonication at output 7 for 30 seconds in ice bath, dropped into liquid nitrogen, and then lyophilized overnight.

6.2.2.2 Disc fabrication

50 mg of the protein/polymer mixture was compressed into disc form using a Carver press at 1000 psi for 10 minutes at room temperature. Compression molding (instead of melt molding) was used to avoid exposing the protein to high temperatures.

6.2.2.3 Protein release studies

Each disc was placed into 5 ml of pH 7.4 phosphate buffer and kept at 37°C and 120 RPM. At timed intervals, the entire buffer volume was sampled and 5 ml of fresh buffer was added. The protein concentrations were measured using the Bicinchoninic acid (BCA) protein assay (Pierce).

6.2.2.4 Protein activity

The activity of β-chymotrypsin and peroxidase was determined after every step in the drug incorporation and disc fabrication procedures. The enzyme activity was also measured in each sample collected during the drug release study. β-Chymotrypsin activity was defined as the reaction velocity determined by measuring an increase in absorbancy at $\lambda = 256$ nm resulting from the hydrolysis of benzoyl-L-tyrosine ethyl ester (BTEE) at 25°C [31]. Peroxidase activity was defined as the reaction velocity determined by measuring an absorbance at $\lambda = 405$ nm resulting from the oxidation of 2,2'-Azino-bis (3-Ethylbenzthiazoline-6-Sulfonic Acid) substrate (ABTS). The enzyme concentrations were measured using the BCA protein assay (Pierce).

6.2.2.5 Protein characterization

Peroxidase samples were analyzed by size-exclusion chromatography (SEC). The instrumentation used consisted of two solvent pumps (Model 510 solvent pumps; Waters), an autoinjector (WISP 712 autoinjector; Waters), and detector (490 Programmable Multiwavelength Detector; Waters), all controlled by a data station (Dec 350 data station; Digital Equipment Corporation, Maynard, MA). The chromatographic separations were performed at room temperature through a gel column (TSK gel, G3000SW, The Next Group, Southboro, MA) Filtered (Millipore, type HV, 0.45 μm filter) and degassed (helium) 0.05 M phosphate buffer (with .15 M KCl) at pH 7.4 was used as the mobile phase with a flow rate of 1.2 ml/min, at $\lambda = 210$ nm.

6.2.2.6 pH and FAD monomer studies

Peroxidase activity (0.1 mg/ml) was measured at pH = 3, 5, 6, 7.4, and 9 with FAD monomer (0.1 - 0.2 g) or without FAD monomer over a one week period.

6.2.2.7 Isoelectric Focusing

Peroxidase was focused in a gradient of pH range 3-10 (Pharmalytes pH 3-10, Sigma), and gels calibrated with the following markers: Amyloglucosidase (pI, 3.8), Ovalbumin (pI, 5.2), Carbonic Anhydrase (pI, 7.0), Myoglobin (pI, 7.6). using the method of [32]. Separation and staining were done with Coomassie brilliant blue on a BioRad Mini-Protean II Cell .

6.2.2.8 Stabilizers

Same methods as in Section 6.2.2.1 except 590 kDa dextran or 500 kDa DEAE-dextran (Diethylaminoethyl-dextran) was combined with protein at a 1:1 weight ratio.

6.3 RESULTS AND DISCUSSION

6.3.1 Fabrication results

Enzyme activity was measured after each step in the drug incorporation and fabrication. (Activity is reported as percentage of initial starting activity/mg protein). For β-chymotrypsin, the % activity after each step were: 1) exposure to organic solvent (97% ± 10%) and polymer (90% ± 10%), 2) sonicating on ice (80% ± 10%), 3) freeze drying (80% ±10%), and 4) compression molding (80% ± 10%). We were able to compression mold at room temperature due to the low T_g (3°C ± 5°C) of p(FAD:SA) 50:50. This is advantageous when the material to be incorporated (such as proteins) is heat sensitive. Final peroxidase also retained about 80% of initial activity after incorporation and fabrication. We found the importance of forming the emulsion by probe sonicating on ice. If ice was not used, peroxidase lost more than 75% of its activity. This was probably due to the heat generated by sonication, which denatured much of the enzyme.

6.3.2 Release results

β-chymotrypsin incorporated into p(FAD:SA) appeared to stabilize the enzyme early in the release period (in the first 10 hours), but not after 24 hours. Free β-Chymotrypsin (0.2 mg/ml) in pH 7.4 phosphate buffer at 37°C loses 60% of its activity in 10 hours, while β-Chymotrypsin released from p(FAD:SA) 50:50 lost only 15% of its activity in the same time period (see figure 6.3). P(FAD:SA) 20:80 lost only 35% of its activity over 10 hours. The activity differences between the two copolymers may be due to the more hydrophobic p(FAD:SA) 50:50 allowing less water to enter the polymer. It is hypothesized that water penetration into the polymer may eventually allow the enzyme with enough mobility to unfold and expose its buried hydrophobic amino acid residues to the hydrophobic polymer surface [33]. After 24 hours, both free and encapsulated β-Chymotrypsin lost almost all activity.

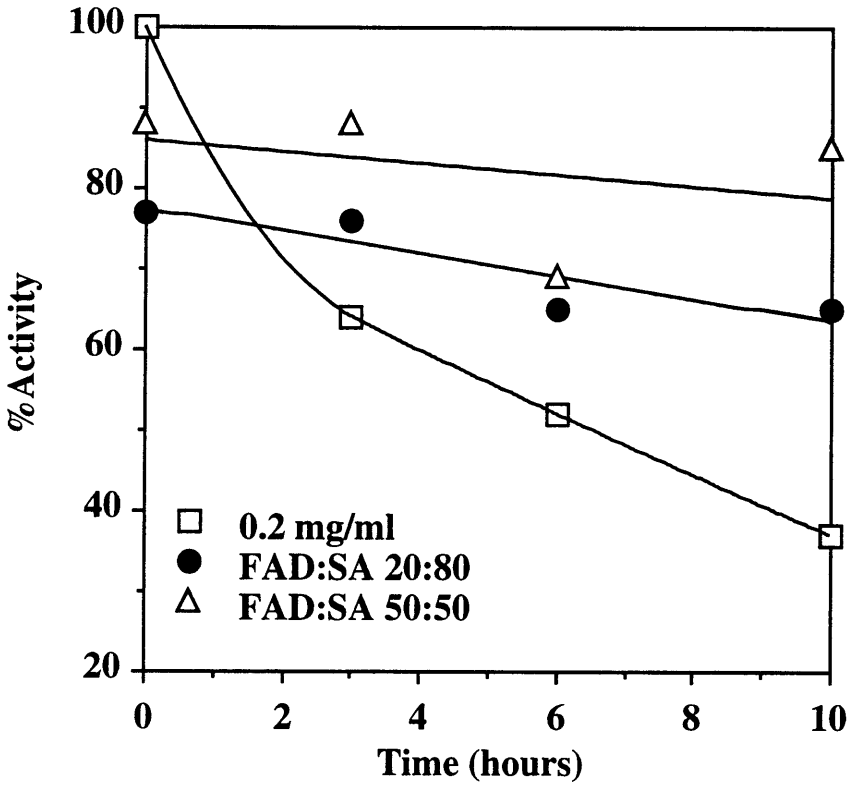

Figure 6.3 Comparison of beta-chymotryspin activity (using BTEE as a substrate) from p(FAD:SA) 20:80, p(FAD:SA) 50:50, and no polymer (0.2 mg/ml in phosphate buffer). Discs were 9% loaded, 10 mg, and 1.0 mm thick. Plot shown is one set of experimental data.

Due to the instability of β-chymotrypsin in phosphate buffer, samples were taken every 3 hours. However, a minimum concentration was also needed to measure enzyme activity. These factors made β-chymotrypsin a difficult enzyme to work with. Therefore, peroxidase was also studied because it is more stable in solution than β-chymotrypsin (free peroxidase in solution at 37°C exhibits about 10% activity loss after 24 hours, compared to 60-70% activity loss for β–chymotrypsin), and the activity assay was sensitive to low peroxidase concentrations.

Constant peroxidase release, with no burst effect, was obtained from p(FAD:SA) 50:50 over a one week period (see Figure 6.4, Table A.17). Peroxidase released from p(FAD:SA) 50:50 maintained activity (about 80%) over the first half of the release period (see Figure 6.5, Table A.18). At Day 4, peroxidase released from p(FAD:SA) was twice as active as the control (no polymer; peroxidase at a concentration of 0.07 mg/ml free in phosphate buffer), which had lost about 60% of its activity. However, peroxidase released from the polymer began to lose activity during the latter half of the release period. Starting on Day 5 (see Figure 6.6), peroxidase activity from p(FAD:SA) 50:50 dropped down to 45% of initial activity. By Day 7, it was completely inactive. Size exclusion chromatography (SEC) of release samples from Days 0 - 4 indicated only the presence of peroxidase which elutes at a characteristic retention time (R_t) of 8.8 minutes and sebacic acid which elutes at R_t = 11.6 minutes. However, starting on Day 5, a peak appeared at the void volume (R_t = 5.5 minutes) of the column, which indicated the presence of soluble aggregates. At Day 5, 35% of the peroxidase had aggregated, and activity had dropped down to 45% of initial. By Day 7, 100% of the peroxidase had aggregated, and the enzyme had lost all activity (see Figure 6.7, Table A.18). Enzyme activity loss increased with the % aggregated protein (as determined by SEC).

The most likely explanation for the enzyme activity loss is denaturation or aggregation of enzyme within the polymer over the extended time period. Water penetration into the polymer may eventually allow the enzyme with enough mobility to unfold and expose its buried hydrophobic amino acid residues to the hydrophobic polymer surface. Although it was reported in Chapter 4 that only about 5 wt% water is found in the polymer interior during erosion, this may be enough water to act as a "molecular lubricant" to increase protein flexibility, resulting in enhanced accessibility of reactive groups with consequently higher rates of irreversible covalent modification of the protein [33].

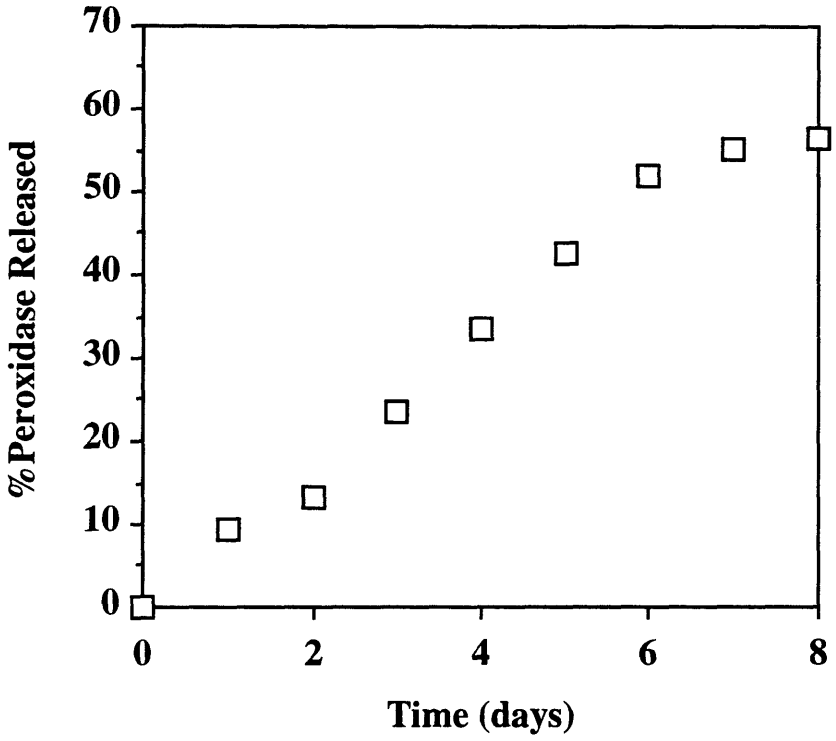

Figure 6.4 Horseradish peroxidase release from p(FAD:SA) 50:50 at 9% loading. Discs were 50 mg, and 1.0 mm thick. Plot shown is one set of data representative of three experiments.

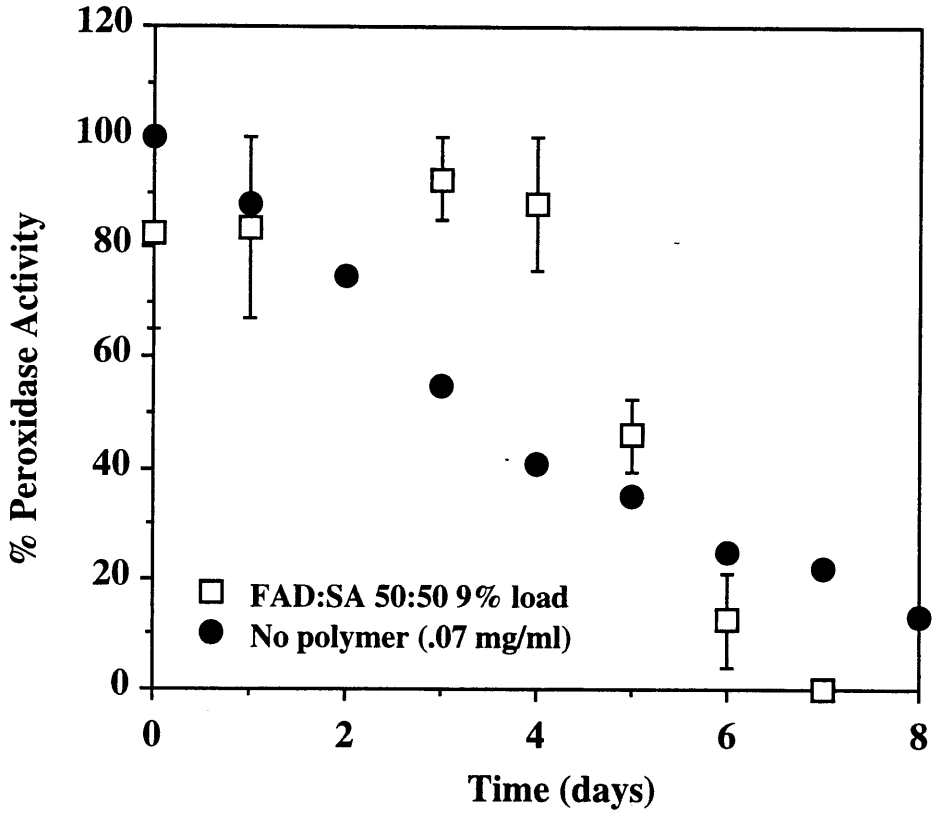

Figure 6.5 Comparision of peroxidase activity (using ABTS as a substrate) from p(FAD:SA) 50:50 and no polymer (0.07 mg/ml). Data with error bars represent an average of two measurements; error bars represent the spread of the data.

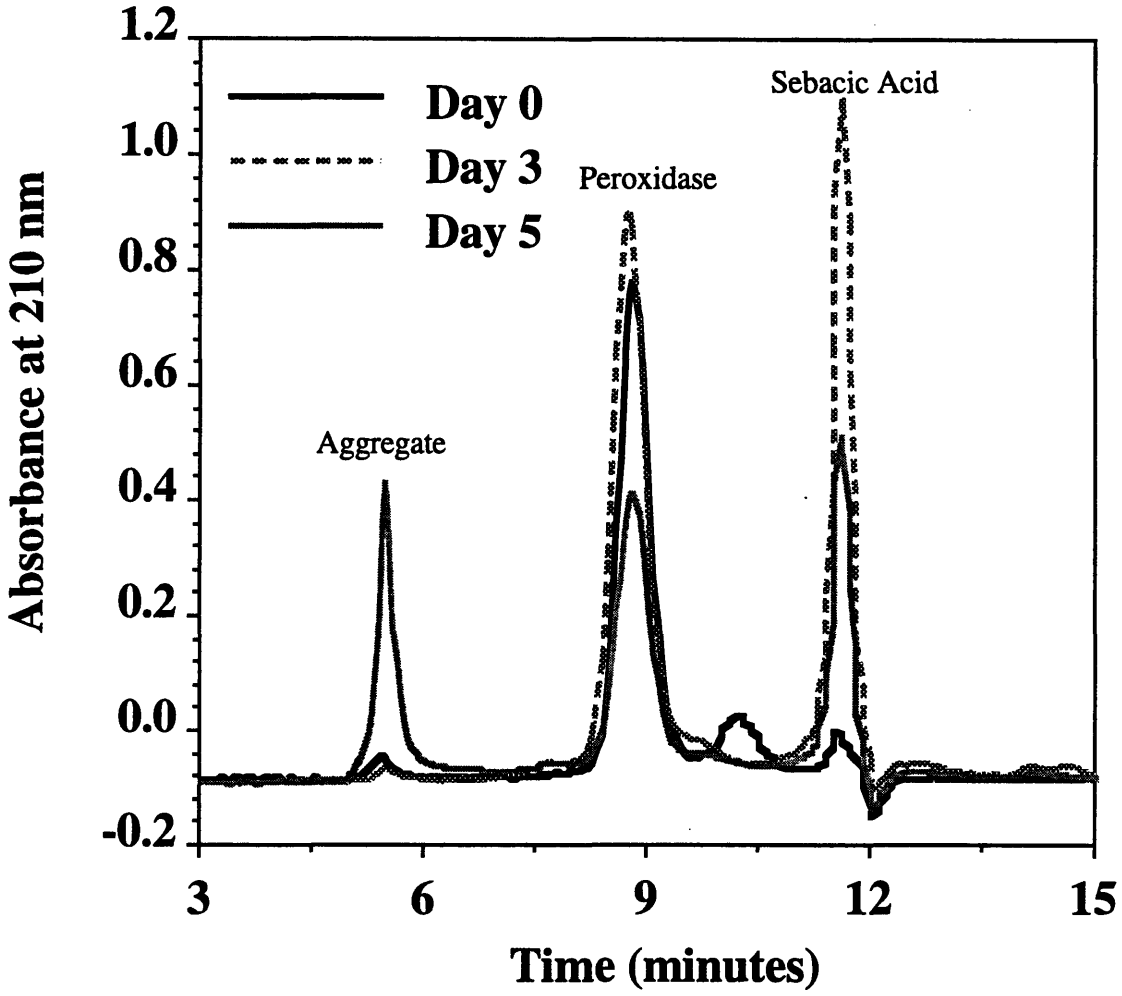

Figure 6.6 Size exclusion chromatography (SEC) of peroxidase during release. Day 0 is initial peroxidase. At Day 3; still no aggregate peak. By Day 5; presence of aggregate peak.

t = 5.5 minutes--->soluble aggregates
t = 8.8 minutes--->peroxidase peak
t = 11.6 minutes--->sebacic acid peak

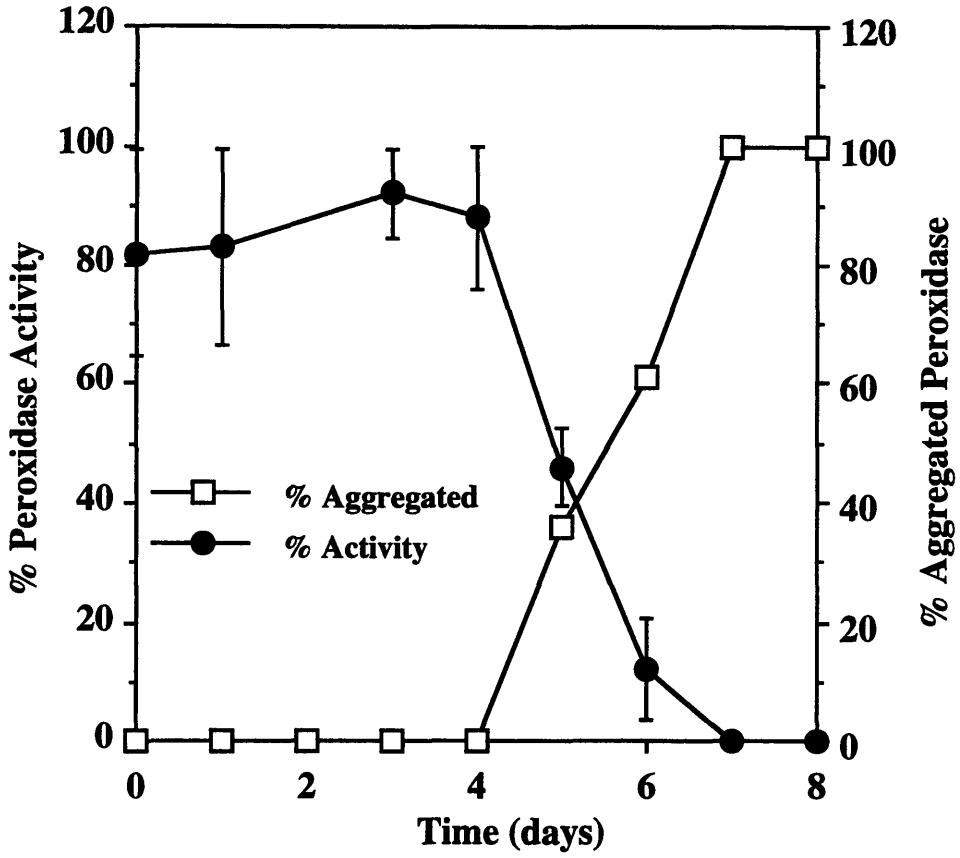

Figure 6.7 % Peroxidase aggregation (as determined by SEC) plotted with the % peroxidase activity loss during release. Data with error bars represent an average of two measurements; error bars represent the spread of the data.

Besides water penetration and surface induced hydrophobic denaturation, another factor to consider is the acidic microenvironment created by anhydride bond hydrolysis during polymer degradation. If dissolution and diffusion of SA monomer out of the polymer matrix is much slower than degradation, then there may be SA monomer build up (and hence lower pH within the polymer). The pH inside the polymer has been reported to be about pH 5 [8, 18]. We have measured that a saturated phosphate buffer solution of SA monomer is about pH 5, and a saturated unbuffered solution (water) of SA monomer is about pH 3.6. This experiment gives an indication of the acidity of the polymer interior which has been saturated with SA monomer. It has also been shown in p(CPP:SA) that monomers crystallize during erosion inside the porous network of the eroded polymer matrix [8], suggesting that certain regions within the polymer are saturated with acidic monomers.

Although acidity may be desirable in some situations (eg. insulin lyophilized from an acidic pH displays a much higher stability in the solid state [34]), acidic and alkaline denaturation of proteins is also a well-documented phenomenon in many protein stability studies [35]. Many proteins unfold at pH values less than about 5 or greater than 10. Unfolding at such extremes of pH usually occurs because the folded protein has groups buried in nonionized form that can only ionize only after unfolding. Most prevalent are His and Try residues, which tend to cause unfolding at acid and alkaline pH values, respectively [35]. Thus, the lower pH microenvironment could result in acidic denaturation of the protein. Our studies have shown that there is more complete peroxidase release from p(FAD:SA) 50:50 (60% of total peroxidase incorporated) compared to p(FAD:SA) 20:80 (30% of total incorporated). Also, much of the peroxidase released from p(FAD:SA) 20:80 does not occur until the polymer disc has fallen apart. P(FAD:SA) 20:80 theoretically should have a more acidic polymer interior when compared to p(FAD:SA) 50:50 due its higher sebacic acid content (which contributes to lowering the pH). Therefore, there may be less complete peroxidase release from p(FAD:SA) 20:80 due to protein aggregation or precipitation within the matrix.

Since it appears that pH may play an important role in peroxidase activity loss, the next step taken was to investigate how pH and presence of hydrophobic surfaces (such as FAD monomer) affect peroxidase stability.

6.3.3 Stability results:

We found peroxidase to have the highest retention of activity at pH 6 (see figure 6.8, Table A.19), which is at its isoelectric point (IEF of peroxidase was measured to be around pH 6; See Section 6.2.2.7 and Table A.20). After 8 days at pH 6, peroxidase has only lost 20% activity. This agrees with the theory that globular proteins are most stable near their isoelectric point [36], which is the pH at where the net charge of the protein is zero. It has been suggested that charges on the surface of globular proteins are generally arranged so that there are more favorable than unfavorable electrostatic interactions among charged groups; thus they should contribute favorably to the conformation stability [37]. As the protein moves away from its isoelectric point and becomes more charged, electrostatic interactions between like charges within the protein molecule may result in a tendency to unfold.

Peroxidase activity is decreased as we move to either extreme of its isoelectric point of pH 6. At pH 5, peroxidase has lost 75% of its activity after 8 days. At pH 3, all peroxidase activity is lost after 24 hours. Peroxidase stability is also decreased at alkaline pH. At pH 9, peroxidase has lost 90% of its initial activity by Day 8.

Although complete acid hydrolysis of protein into its amino acids is obtained under extreme conditions (6 M HCl, 24 h, 110°C), shorter exposures under less acidic conditions show preferred peptide hydrolysis at aspartic acid residues, and aspartyl-prolyl linkages are especially vulnerable [21, 38]. In addition, the deamidation of asparagine and glutamine residues, which introduces negative charges into the hydrophobic interior of the protein resulting in inactivation, takes place under strongly acidic and basic conditions. Since the pH of the polymer interior could be as low as pH 4 to 5, it is possible that peroxidase undergoes acid denaturation within the polymer. Adverse side reactions that occur under alkaline conditions include partial peptide bond hydrolysis, deamidation, β-elimination and racemization, double bond formation, destruction of amino acid residues and formation of new amino acids [21].

In addition, we found peroxidase activity reduced more quickly in the presence of FAD monomer (hydrophobic surfaces) at pH 7.4 and pH 9 (see figure 6.9, Table A.19). With the addition of FAD monomer at pH 7.4, peroxidase activity loses 80% of its activity (compared to only 20% loss at pH 7.4 without FAD monomer) after 1 day. Similar results are seen at pH 9. The results indicate that at

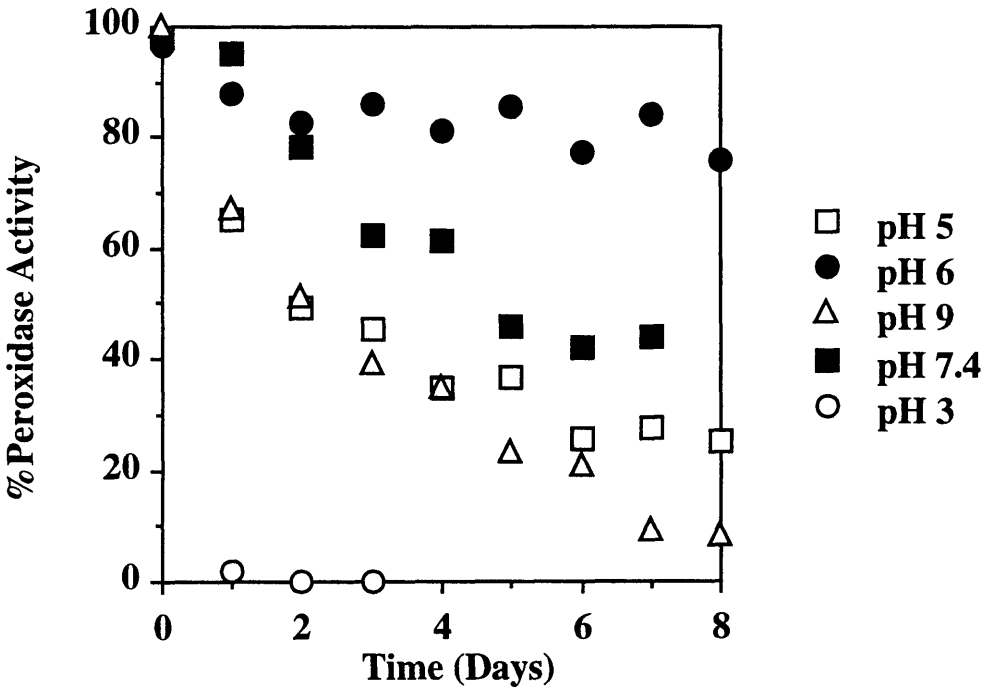

Figure 6.8 Effect of pH on peroxidase stability.
Plot shown is one set of experimental data.

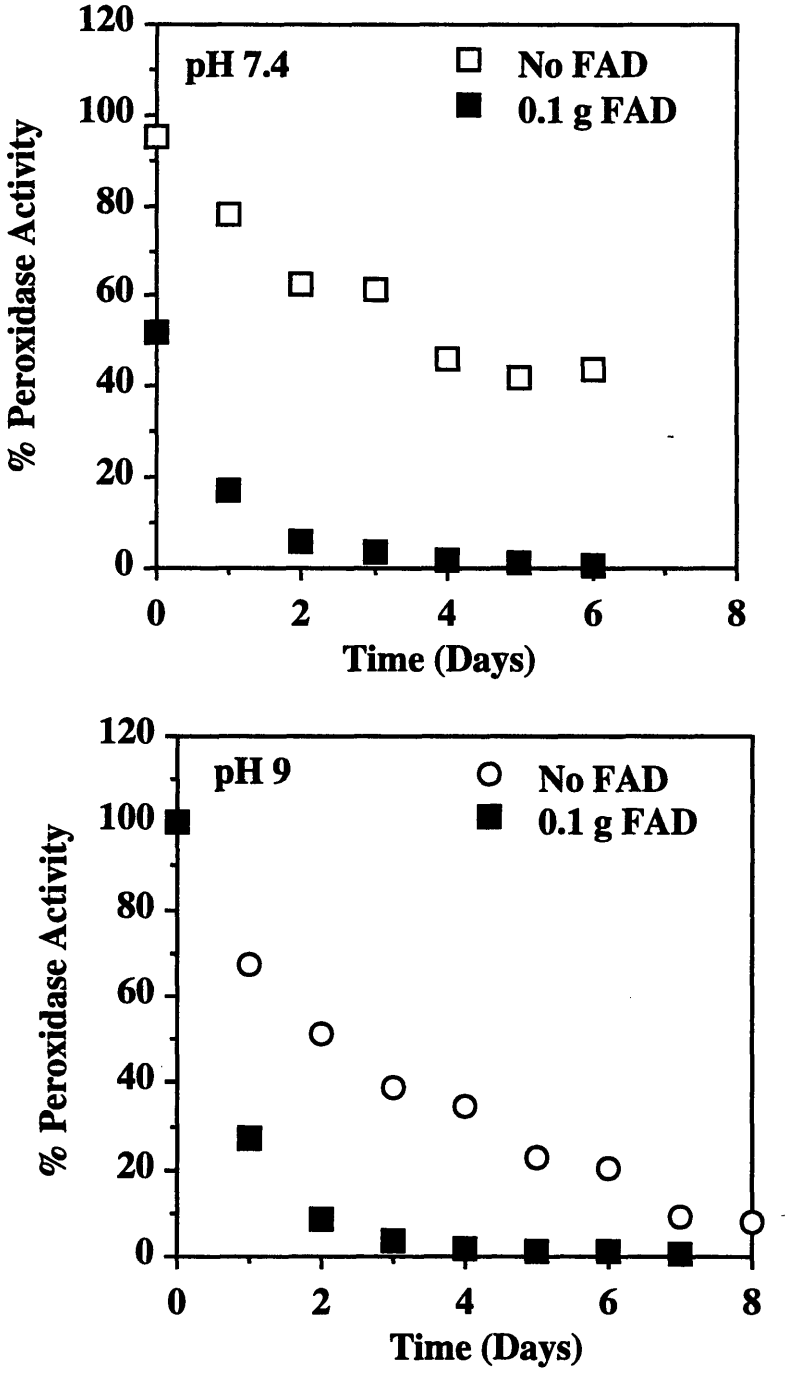

Figure 6.9 Effect of FAD monomer (hydrophobic surface) on peroxidase stability at pH 7.4 and pH 9. First plot shown is one set of data representative of two experiments. Second plot is one set of experimental data.

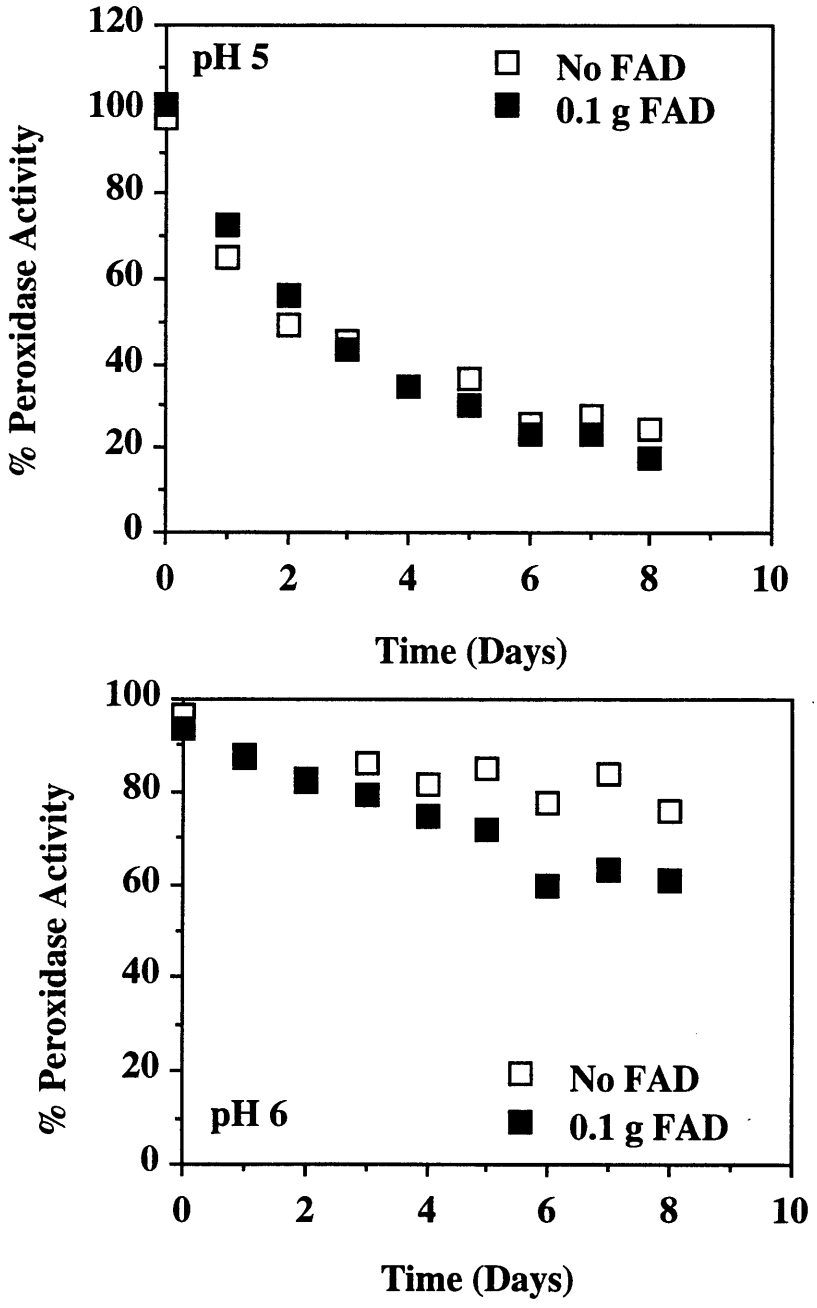

Figure 6.10 Effect of FAD monomer (hydrophobic surface) on peroxidase stability at pH 5 and pH 6. First plot shown is one set of data representative of two experiments. Second plot is one set of experimental data.

these alkaline pHs, the protein is more susceptible to surface-induced hydrophobic denaturation [39]. One possible explanation is that once far away from a protein's isoelectric point (the IEF of peroxidase is around pH 6), electrostatic interactions between like charges within the protein molecule result in a tendency to unfold [21]. In principle, this process is fully reversible, but these conformational changes may make the protein more susceptible to surface-induced hydrophobic denaturation leading to irreversible aggregation.

At lower pHs (pH 5 and pH 6) that are closer to the isoelectric point, there is less appreciable activity loss in the presence of FAD monomer (see figure 6.10, Table A.19). At pH 5, the peroxidase stability curves with and without FAD monomer are almost the same. At pH 6, the peroxidase stability curves with and without FAD are similar until Day 6, consequently peroxidase activity in the presence of FAD drops down to 60% of initial, compared to the peroxidase in the absence of FAD which was at 75%. These findings suggest that the hydrophobic surface is not providing any additional compromising interactions with the protein which lead to its unfolding and denaturation. Therefore, if the polymer interior is at a pH around 5, then most of the peroxidase activity loss is probably due to acidic denaturation and not to the presence of hydrophobic surfaces.

It is generally desirable to maintain a native protein structure in the solid state to enhance stability. The physical stability of proteins can be increased by various additives to aqueous solution, such as sugars, amino acids, and certain salts. The most ubiquitous mechanism of protection is by preferential exclusion from the protein surface [40]. However, not all of these agents are equally useful in stabilizing the folded structure during incubation in the solid state. Carpenter et al. [41] have demonstrated that only certain agents (such as saccharides) are strong lycoprotectants and it has been hypothesized that these agents stabilize the native structure through hydrogen bonding as a water substitute.

Dextran and DEAE-dextran were chosen as stabilizers (in a 1:1 dextran to protein ratio) because preliminary results by [30] suggested that rHSA (recombinant human serum albumin) lyophilized with dextran or DEAE-dextran at a 1:1 weight ratio delayed aggregation in the solid state. Unfortunately, our results demonstrated that this particular formulation did not reduce the loss in peroxidase activity during its release. It would appear that the peroxidase activity loss is due to a different

mechanism that is not slowed or stopped using dextran as a stabilizer. For example, if acidic induced denaturation was the major cause of activity loss, then preferential exclusion from the protein surface (which is the proposed mechanism for stabilizers such as dextran and other sugars, etc.) probably would not be very effective. Incorporation of a buffer or base may be more appropriate. It is also possible that higher concentrations of dextran were needed, or other types of stabilizers may be more effective. Therefore, the potential for other stabilizers has not been ruled out, and future work should include the exploration of other types of stabilizers and formulations. Carpenter et al. [41] have demonstrated that only certain agents, such as saccharides, are strong stabilizers.

6.4 CONCLUSIONS

We have shown the potential to release active protein from the biodegradable polymeric carrier p(FAD:SA). Our incorporation and fabrication procedures did not decrease protein activity. Peroxidase activity was preserved during the first half of release period, but decreased during the latter half. Size exclusion chromatography indicated the presence of aggregated protein during the latter half of the release period. It was thought that the acidic microenvironment within the polymer matrix and/or interaction with the hydrophobic polymer may play a role in the protein aggregation. Stability studies indicated that peroxidase activity was maintained at its isoelectric point of pH 6, and stability decreased at either pH extreme. This agrees with the theory that globular proteins are most stable near their isoelectric point [36]. It is hypothesized [36] that as the protein moves away from its isoelectric point and becomes more charged, electrostatic interactions between like charges within the protein molecule may result in a tendency to unfold. In addition, peroxidase activity dropped more quickly in the presence of FAD monomer (hydrophobic surfaces) at alkaline pH.

The problems of protein stability, especially in relation to the delivery of drugs using polyanhydride polymers, leads us to interesting future work. Our studies indicate that determination of the specific pathway leading to protein

inactivation (which may be different for each protein), may be beneficial to the successful development of these polymers for protein delivery. More specifically, work should involve decreasing the subtle changes in pH which appear to exacerbate the loss in peroxidase activity. Strategies are required to minimize the inactivation. Some methods which can be used to evaluate protein stability during drug delivery include chromatography (SEC and reversed-phase HPLC), optical techniques (light scattering, UV and visible absorption spectroscopy, optical rotatory dispersion, and circular dichroism, flurorescence, infrared, and Raman spectroscopy) electrophoresis, (isoelectric focusing (IEF) and sodium dodecyl sulfate-polyacrylamide gel electrophoresis (SDS-PAGE)) and activity assays [42].

One approach for stabilization would be to control the polymer microenvironment. If acidity within the polymer is a major reason leading to inactivation, then polymers composed of less acidic monomers would be desirable. In our case, since SA is the main monomer providing the acidity, then polyanhydrides composed of less SA (such as p(CPP)) should be used. Another approach would be to incorporate a buffer or base into the polymer interior.

If hydrophobic surfaces are leading to surface-induced denaturation and/or noncovalent aggregation, then less hydrophobic polymers should be used. Another idea that could be explored would be to use stabilizers that could "shield" the protein from the hydrophobic surface. Sluzky et al. [43] have used sugar based non-ionic detergents such as n-octyl-β-D-glucopyranoside and n-dodecyl-β-D-maltoside (which occupy interfacial sites) to prevent or delay insulin aggregation in solution. It is hypothesized [43] that the surfactants probably competed with insulin for interfacial sites, consequently minimizing both the number of insulin's contacts with the hydrophobic surface and the adsorption induced conformational changes. An alternative explanation to increased solution stability in the presence of surfactants was that these molecules bound to insulin, thus shielding the protein's hydrophobic moieties from the aqueous environment, reducing conformation changes at hydrophobic surfaces, or preventing interactions between destabilized molecules.

Another strategy would be to control the water content in the polymer. It was mentioned in Section 6.3.2 that water may act as a "molecular lubricant" to increase protein flexibility, resulting in enhanced accessibility of reactive groups with

consequently higher rates of deleterious processes that lead to protein inactivation [33]. For example, Costantino et al. [33] have found that the extent of bovine serum albumin (BSA) aggregation was very low (less than 10%) if there was no added aqueous buffer. As the water content was increased, the aggregation increased, reaching a maximum of about 25-30% water (over 90% aggregation). However, at water contents above this level, the aggregation actually decreased. This behavior was explained by the "dilution" effect at high water content. Therefore, to stabilize the protein from aggregation, one approach would be to keep the protein at optimal hydration levels by choosing the most suitable polymer. Water contents within the polymer bulk in vitro can range from 1 wt% in certain polyanhydrides [22] up to 60 wt% in poly(glycol-co-lactic acid) [26]. Ron et al. [20] have increased the cumulative in vitro release of bovine somatotropin from < 50% to approximately 90% by changing the polymer from p(CPP:SA) 50:50 to the very hydrophobic polymer poly[1,3-bis(*p*-carbosyphenoxy)hexane] (p(CPH)). Although not investigated, the change to a less acidic environment (p(CPP:SA 50:50) would theoretically have a more acidic polymer interior than p(CPH)) may also be responsible for decreasing aggregation and consequently increasing the cumulative release.

Another approach for stabilizing solid protein formulations is to increase the physical stability of the lyophilized protein. Dextran and DEAE stabilizers were tried in this chapter, but certainly other stabilizers (in particular sugars and polyols) should also be considered. An improvement in the release of both recombinant bovine somatotropin and zinc insulin was observed upon the addition of sucrose as an excipient in polyanhydride matrices [20]. Other strategies would be to "rigidify" [21] the native form of the protein. This could be done by increasing the intrinsic stability of the protein, using additives, immobilization, and chemical modification (See Table 1[21]).

Effectors	*Comments*
Intrinsic stability	
1. Mesophilic versus thermophilic enzymes	Rigidification of enzyme conformation
2. Site-specific mutagenesis	Replacement of labile amino acid residues
Additives	
1. Specific	Shift N $\rightleftharpoons$ U equilibrium toward native form
2. Non-specific	Neutral salts and polyhydric compounds
3. Competitors	Outcompete enzyme for inactivating agent; remove catalysts of deteriorative chemical reactions
Immobilization	
1. Multi-point attachment of enzyme to support	Rigidification of enzyme conformation; steric hindrances prevent interaction with macromolecules, e.g. degradation by proteases
2. Partitioning effects and diffusion restrictions	Chemical and physical properties of support influence the micro-environment around the enzyme molecule
Chemical modification	
1. Cross-linking reagents	Rigidification of enzyme conformation
2. Reagents that alter ionic state or introduce steric hindrances	Modification adds, neutralizes or alters charged residues on enzyme molecule; attachment of soluble macromolecules inhibits interactions with other solutes, e.g. proteases

Table 6.1 Examples of approaches to minimize irreversible inactivation of proteins. (Table is taken from ref [21]).

CHAPTER 7

CONCLUSIONS AND FUTURE DIRECTIONS

The goals of this thesis work were accomplished by gaining a better understanding of the mechanism of polymer erosion of polyanhydride systems, using the p(FAD:SA) copolymer. We found polymer hydrophobicity, crystallinity, and diffusion (all controlled by copolymer composition) played a role in the erosion of p(FAD:SA). Also, p(FAD:SA) displayed certain surface eroding characteristics, such as material loss from the outside to the inside of the matrix, erosion rate which was not dependent on the volume of the polymer matrix, thicker samples with longer lifetimes, and low water uptake into the polymer interior.

After gaining a better understanding of the erosion of p(FAD:SA), we felt we could move onto our next objective, which was to investigate the factors controlling drug release from polyanhydride systems. Acid orange (A.O.), a hydrophilic dye, and Rhodamine B Base (RhBB), a hydrophobic dye, were used as models. We found that by reducing drug particle size in the drug incorporation method, we could decrease a drug's initial "burst" during release. The effect of copolymer composition, drug properties (solubility), and drug loading on release was also studies. A.O. release was affected by copolymer composition and initial drug loading, and exhibited faster release than the more hydrophobic dye, RhBB. Also, A.O. release correlated well with the underlying SA erosion.

Finally we moved onto the more challenging problem of releasing proteins from our polyanhydride system. The fabrication procedures were found not to significantly affect the activity of the proteins incorporated. Peroxidase was released over a one week period, and enzyme activity was retained over the first half of release. However, activity dropped over the second half and protein stability studies suggest that polymer hydrophobicity and the acidic environment within the polymer during release may have contributed to the loss of protein activity.

From this thesis work, we have a better understanding of the erosion and drug release from p(FAD:SA) *in vitro*. Future work can move onto the more complex *in vivo* system (which would be the ultimate destination of the polymer).

Wu et al. [44] have compared the *in vivo* vs. *in vitro* erosion of p(CPP:SA), but aside from biocompatibility, little has been done with p(FAD:SA). There are many other factors that must be taken into account *in vivo*, such as the action of proteolytic enzymes, proteins, phagocytic cells, imperfect sink conditions, mass transfer, etc. on erosion and release. Other concerns would include a foreign body response to the implant, which may involve the formation of a granuloma or fibrous capsule around the implant. This could affect water diffusion in and/or drug release out of the polymer. The extent of drug distribution into tissues would also need to be considered. For example, the diffusion and elimination of drugs in brain tissue has been studied [45, 46]. This thesis work also lays out a foundation for which a mathematical model which could predict the erosion and drug release from p(FAD:SA). Such approaches taken by Goepferich et al. [17] could be pursued.

As mentioned in Chapter 6, the problems of protein stability, especially in relation to the delivery of drugs using polyanhydride polymers, leads us to interesting future work. Our studies indicate that determination of the specific pathway leading to protein inactivation (which may be different for each protein), may be beneficial to the successful development of these polymers for protein delivery. Strategies are then required to minimize the inactivation. Approaches could include modifying the polymer, adding stabilizers to the protein formulation, or actually altering the protein itself [21]. Stabilization strategies are discussed in detail in Chapter 6. The results of this thesis work have given us better insight into what type of concerns need to be addressed when designing controlled release systems for drug and protein delivery.

REFERENCES

[1] Tamada, J., and Langer, R., "Erosion Kinetics of Hydrolytically Degradable Polymers", *Proc. Natl. Acad. Sci.*, **90,** 552-556, 1993.

[2] Langer, R., "Polymer-Controlled Drug Delivery Systems", *Accounts of Chemical Research*, **26,** 537-542, 1993.

[3] Tamada, J., and Langer, R., "The Development of Polyanhydrides for Drug Delivery Applications", *J. Biomat. Sci. Polymer Edn.*, **3,** 315-353, 1992.

[4] Brem, H., Piantadosi, S., Burger, P., Walker, M., Selker, R., Vick, N., Black, K., Sisti, M., Brem, S., Mohr, G., Muller, P., Morawetz, R., Schold, S., "Intraoperative Controlled Delivery of Chemotherapy by Biodegradable Polymers: Safety and Effectiveness for Recurrent Gliomas Evaluated by a Prospective, Multi-Institutional Placebo-Controlled Clinical Trial", *Lancet*, Submitted.

[5] Domb, A., and Maniar, M, "Absorbable Biopolymers Derived from Dimer Fatty Acids", *J. Polym Sci*, **31,** 1275-1285, 1993.

[6] Domb, A., "Personal communication", 1994.

[7] Brem, H., Domb, A., Lenartz, D., Dureza, C., Olivi, A., and Epstein, J., "Brain biocompatibility of a biodegradable controlled release polymer consisting of anhydride copolymer of fatty acid dimer and sebacic acid", *J. Controlled Release*, **19,** 325-330, 1992.

[8] Goepferich, A., and Langer, R., "The Influence of Microstructure and Monomer Properties on the Erosion Mechanism of a Class of Polyanhydrides", *J. Polym. Sci.*, 2445-2458, 1992.

[9] Albertsson, A.C. and Lundmark, S., "Synthesis, Characterization and Degradation of Aliphatic Polyanhydrides", *Br. Polym. J.*, **23,** 205-212, 1990.

[10] Lewis, D.H., Biodegradable Polymers as Drug Delivery Systems, Eds. M. Chasin and R. Langer, Marcel Dekker, New York, 1990.

[11] Heller, J., Sparer, R., and Zentner, G., Biodegradable Polymers as Drug Delivery Systems, Eds. M. Chasin and R. Langer, Marcel Dekker, 121-162, New York, 1990.

[12] Tamada, J., and Langer, R., "Mechanism of the Erosion of Polyanhydride Drug Delivery Systems", *Proceed. Intern. Symp. Control. Rel. Bioact. Mater.*, **17,** 156-157, 1990.

[13] Leong, K.W., Brott, B.C., and Langer, R., "Bioerodible polyanhydrides as drug-carrier matrices. I. Characterization, degradation, and release characteristics", *J. Biomed. Mater. Res.*, **19,** 941-955, 1985.

[14] Ron, E., Mathiowitz, E., Mathiowitz, G., Domb, A., and Langer, R., "NMR Characterization of Erodible Copolymers", *Macromolecules*, **24,** 2278-2282, 1991.

[15] Mathiowitz, E., Ron, E., Mathiowitz, G., Amato, C., and Langer, R., "Morphological Characterization of Bioerodible Polymers 1. Crystallinity of Polyanhydride Copolymers", *Macromolecules*, **23,** 3212-3218, 1990.

[16] Tamada, J., Sawka, M., and Langer, R., "Probing the Nature of the Erosion of Polyanhydrides", 1991.

[17] Gopferich, A., and Langer, R., "Modeling of Polymer Erosion", *Macromolecules*, **26,** 4105-4112, 1993.

[18] Laurencin, C.T., "Novel Bioerodible Polymers for Controlled Release Analyses of In Vitro/In Vivo Performance and Characterization of Mechanism", *Doctoral Thesis*, 1987.

[19] Leong, K.W., D'Amore, P., Marletta, M., and Langer, R., "Bioerodible polyanhydrides as drug-carrier matrices. II. Biocompatibility and chemical reactivity", *J. Biomed. Mater. Res*, **20,** 51-64, 1986.

[20] Ron, E., Turek, T., Mathiowitz, E., Chasin, M., Hageman, M., and Langer. R., "Controlled Release of Polypeptides from Polyanhydrides", *Proc Natl Acad Sci*, **90,** 4176-4180, 1993.

[21] Volkin, D., and Klibanov, A., Protein Function: A Practical Approach Chapter 1: Minimizing protein inactivation, Ed. T. Creighton, Oxford University Press, Oxford, England, 1-24, 1990.

[22] Shieh, L., Tamada, J., Chen, I., Pang, J., Domb, A., and Langer, R., "Erosion from a New Family of Biodegradable Polyanhydrides", *J. Biomed. Mat. Res*, In Press.

[23] Mathiowitz, E., Amato, C., Dor, Ph., and Langer, R., "Polyanhydride Microspheres: 3. Morphology and Characterization of Systems Made by Solvent Removal", *Polymer*, **31,** 547-555, 1990.

[24] Hiemenz, P.C., Polymer Chemistry, Dekker, 235-244, New York, 1984.

[25] Bassett, D.C., Principles of Polymer Morphology, Cambridge University Press, 22-28, Cambridge, 1981.

[26] Shah, S.S., Cha, Y., and Pitt, C.G., "Poly(glycolic acid-co-DL-lactic acid): diffusion or degradation controlled drug delivery", *J. Controlled Release*, **18,** 261-270, 1992.

[27] Shieh, L., Tamada. J., Tabata, Y., Domb, A., and Langer, R., "Drug release from a new family of biodegradable polyanhydrides", *J. Controlled Release*, **29,** 73-82, 1994.

[28] Tabata, Y., and Langer, R., "Polyanhydride Microspheres that Display Near-Constant Release of Water-Soluble Drugs", *Pharm Research*, **10,** 391-399, 1993.

[29] Welinder, K.G., "Covalent Structure of the Glycoprotein Horseradish Peroxidase", *FEBS Letters*, **72,** 19-23, 1976.

[30] Costantino, "Unpublished results", 1994.

[31] Worthington, C., Worthington Enzyme Manual, Freehold, N.J., 1988.

[32] Creighton, T.E., Protein Structure: A Practical Approach, Eds. D. Rickwood and B.D. Hames, Oxford University Press, 23-63, Oxford, 1989.

[33] Costantino, H.R., Langer, R., and Klibanov, A., "Solid-Phase Aggregation of Proteins Under Pharmaceutically Relevant Conditions", *J. Pharm Sci*, in press.

[34] Costantino, H.R., Langer, R., and Klibanov, A., "Moisture-Induced Aggregation of Lyophilized Insulin", *Pharm Research*, **11,** 21-29, 1994.

[35] Creighton, T.E., Proteins: Structure and Molecular Properties, W.H. Freeman and Company, New York, 1993.

[36] Pace, C.N., "Conformation stability of globular proteins", *Trends Biochem Sci*, **15,** 14-17, 1990.

[37] Wada, A., and Nakamura, H., *Nature*, **293,** 757-758, 1981.

[38] Kenley, R., and Warne, N., "Acid-Catalyzed Peptide Bond Hydrolysis of Recombinant Human Interleukin 11", *Pharm Research*, **11,** 72-76, 1994.

[39] Andrade, J.D., and Hlady, V., "Protein Adsorption and Materials Biocompatibility", *Adv. Polymer Science*, **79,** 1-63, 1985.

[40] Timasheff, S.N., Stability of Protein Pharmaceuticals. Part B. In Vivo Pathways of Degradation and Stategies for Protein Stabilization, Eds. T. Ahern and M. Manning, Plenum, 265-286, New York, 1992.

[41] Carpenter, J., Prestrelski, S., Anchordoguy, T., Arakawa, T., Formulation and Delivery of Proteins and Peptides, Eds. J. Cleland and R. Langer, American Chemical Society, 134-147, Washington, D.C., 1994.

[42] Hanson, M., and Rouan, S., Formulation of Protein Pharmaceuticals, Eds. T. Ahern and M. Manning, Plenum, 209-233, New York, 1993.

[43] Sluzky, V., Klibanov, A., and Langer, R., "Mechanism of Insulin Aggregation and Stabilization in Agitated Aqueous Solutions", *Biotech and Bioeng*, **40,** 895-903, 1992.

[44] Wu, M., Tamada, J., Brem, H., and Langer, R., "In vivo versus in vitro degradation of controlled release polymers for intracranial surgical therapy", *Journal of Biomedical Materials Research*, **28,** 387-395, 1994.

[45] Lapin, G., Polymeric Site-Specific Pharmacotherapy, Ed. A. Domb, John Wiley & Sons Ltd., 69-94, Chichester, England, 1994.

[46] Radomsky, M., Polymeric Site-Specific Pharmacotherapy, Ed. A. Domb, John Wiley & Sons Ltd., 46-68, Chichester, England, 1994.

APPENDIX

Table A.1 Erosion Front Progression of p(FAD:SA) 20:80

Time (Days)	Erosion Front 1 (%)	Time (Days)	Erosion Front 2 (%)
0.0	0.0	0.0	0.0
1.0	9.0	2.0	34.0
2.0	23.0	4.0	46.0
3.0	37.0	7.0	62.0
4.0	45.0	9.0	71.0
5.0	52.0	11.0	85.0
7.0	70.0	13.0	100.0
13.0	100.0		

Table A.2 Effect of p(FAD:SA) monomer ratio on %SA erosion

Time (hours)	%SA 2:8 #1	%SA 2:8 #2	%SA 5:5 #1	%SA 5:5 #2	%SA 7:3 #1	%SA 7:3 #2
0	0.0	0.0	0.0	0.0	0.0	0.0
4	0.3	0.2	0.2	0.2	0.3	0.0
9	0.9	1.1	0.8	0.4	0.7	0.0
15	3.0	3.6	1.9	1.4	1.7	0.9
24	7.1	8.1	5.1	4.4	5.4	4.1
32	10.8	11.7	9.0	8.2	10.7	8.0
39	14.1	15.6	12.8	11.6	15.3	12.6
49	18.4	19.9	18.5	15.8	19.8	18.1
59	22.6	24.2	23.1	19.4	24.2	23.3
73	28.0	29.6	27.0	23.6	31.0	29.9
82	32.3	33.4	29.8	25.6	35.3	34.3
96	37.3	39.2	32.7	28.5	41.3	40.8
106	41.1	43.0	34.6	30.9	45.6	45.0
124	47.0	48.7	37.5	34.1	52.7	52.2
148	55.2	55.6	41.7	38.3	60.9	60.9
172	61.5	62.0	45.1	42.3	68.7	68.5
196	66.9	67.4	48.9	46.0	75.5	74.9
220	71.8	72.6	52.2	49.7	82.1	80.4
244	76.3	76.6	55.2	52.7	86.9	84.7
292	84.2	82.9	61.2	58.6	94.1	93.1
364	93.1	89.6	72.8	67.2	98.0	98.0
460	99.4	96.1	80.8	77.4	99.0	99.3
555	100.0	99.4	88.5	84.6	99.4	99.6
1824	100.0	100.0	100.0	100.0	100.0	100.0

Table A.3 Copolymer crystallinity as a function of copolymer composition

Mole% SA	Weight% SA	Hfus1 (J/g)	%Crystal 1	Hfus 2 (J/g)	%Crystal 2
100.0	100.0	120.0	67.0	120.0	67.0
92.0	80.0	89.0	53.0	102.0	62.0
73.0	50.0	55.5	42.0	69.6	53.0
54.0	30.0	17.6	18.2	16.2	16.7

Table A.4 %Crystallinity changes with erosion

Time (hours)	%Cryst 5:5 #1	%Cryst 5:5 #2	Time (hours)	%Cryst 7:3	Time (hours)	%Cryst 2:8 #1	%Cryst 2:8 #2
0.0	53.0	42.0	0.0	14.3	0.0	53.0	62.0
19.0	34.6	33.5	0.0	15.5	24.0	57.0	57.0
48.0	30.4	30.0	10.5	16.5	48.0	52.0	56.0
73.0	20.9	19.9	33.5	8.7	73.0	44.5	55.0
99.0	12.6	14.5	48.0	8.1	97.0	41.0	51.0
119.0	14.5	12.6	69.5	7.4			
			93.0	6.9			
			117.5	2.8			

Table A.5 Ratio of anhydride bond peak to acidic degradation peak with time in outer (out) and inner (in) zone of p(FAD:SA) copolymers

Time (hrs)	In 2:8 #1	In 2:8 #2	Out 2:8 #1	Out 2:8 #2	Time (hrs)	In 5:5 #1	In 5:5 #2	Out 5:5 #1	Out 5:5 #2	Time (hrs)	In 7:3 #1	In 7:3 #2	Out 7:3 #1	Out 7:3 #2
0.0	5.0	3.3	5.0	3.3	0.0	3.9	4.2	3.9	4.2	0.0	3.1	4.5	3.1	4.5
24.0	1.9		1.6		23.5	1.0		0.5		23.0	1.0	0.9	0.6	0.3
48.0	1.7	1.1	1.0	1.0	47.5	0.9	0.9	0.4	0.1	49.0	0.6	0.4	0.3	0.2
72.0	1.5		1.3		72.0	0.8		0.2		72.0	0.3	0.2	0.2	0.1
96.0	1.0	0.8	1.0	0.9	92.0	0.6	0.5	0.2	0.0	96.0	0.3	0.0	0.0	0.0
120.0	1.0		1.0		119.0	0.7		0.1		120.0	0.1	0.0	0.0	0.0
144.0	0.9	0.6	1.0	0.6	142.5	0.6	0.5	0.1	0.0	144.0	0.0	0.0	0.0	0.0
168.0	0.8		0.8		166.5	0.4		0.1						
191.0	0.8		0.7		190.5	0.2		0.0						
215.0	0.7		0.8		214.5	0.2		0.0						
244.5	0.6	0.3	0.9	0.0	238.0	0.2	0.3	0.0	0.0					
314.5	0.5	0.0	0.5	0.0	261.5	0.0	0.1	0.0	0.0					
383.5	0.0	0.0	0.0	0.0	288.5	0.0	0.0	0.0	0.0					
483.0	0.0	0.0	0.0	0.0										

Table A.6 Molecular weight decrease of p(FAD:SA) 50:50 with %SA erosion

Time (hours)	MW wt ave #1	MW wt ave #2	Time (hours)	%SA Erosion
0.0	32173.0	24771.0	0.0	0.0
2.0	27867.0	21869.0	4.0	0.0
4.0	19599.0	15627.0	8.0	0.0
6.0	13952.0	14253.0	12.0	2.4
8.5	10475.0		16.0	5.0
12.5	6249.0	7351.0	20.0	10.7
23.5	3343.0	3538.0	24.0	17.8
			28.0	26.5
			32.0	36.1

Table A.7 Molecular weight changes with degradation of p(FAD:SA) copolymers

Time (hours)	Mw wt 7:3	MW wt 5:5 #1	Mw wt 5:5 #2	MW wt 2:8
0	50950	24771	32173	30606
2	41101	21869	27867	17159
4	29744	15627	19599	15344
7	19171	14253	13952	13259
12	10424	7351	6249	6267
24	2352	3538	3343	1848

Table A.8 Effect of disc thickness (mm) on Rate SA (mg/hr)

Time (hours)	Rate SA 0.68	Rate SA 0.98	Rate SA 1.4	Rate SA 1.67	Rate SA 2.7
0	0.000	0.000	0.000	0.000	0.000
9	0.240	0.209	0.192	0.204	0.153
31	0.496	0.424	0.428	0.454	0.484
55	0.274	0.258	0.337	0.347	0.417
81	0.255	0.245	0.222	0.233	0.395
108	0.212	0.241	0.292	0.306	0.206
141	0.025	0.149	0.235	0.210	0.213
176	0.000	0.029	0.160	0.236	0.157
203	0.000	0.000	0.069	0.161	0.161
708	0.000	0.000	0.005	0.012	

Table A.9 Effect of shaking rate on %SA erosion of p(FAD:SA) 50:50

Time (hours)	0 RPM	120 RPM	Time (hours)	60 RPM
2.0	0.0	0.0	3.0	0.0
4.0	0.0	0.0	5.5	0.0
6.0	0.0	0.0	7.5	0.0
8.0	0.0	0.0	12.0	0.2
14.0	0.3	0.8	15.0	0.4
23.5	1.8	3.9	23.0	3.9
27.5	3.5	6.2	27.5	7.6
31.0	5.7	10.3	31.5	12.2
35.5	10.2	16.3	35.5	16.7
47.5	22.2	30.9	39.0	19.6
53.0	27.8	35.3	49.0	27.7
61.5	32.7	41.3	54.0	34.2
73.0	37.8	46.6	60.0	38.3
79.0	41.2	48.5	71.0	44.2
85.5	43.5	50.7	77.5	48.8
96.0	46.6	54.4	83.0	51.3
102.0	48.3	56.4	96.0	57.1
108.0	49.6	58.0	101.0	58.9
120.5	52.8	62.0	108.0	61.0
125.5	54.0	63.2	121.0	64.7
144.0	60.7	68.3	131.5	68.4
155.5	63.5	70.9	144.0	71.7
168.0	66.4	73.9	156.5	75.3
180.5	69.9	76.8	168.0	78.4
195.5	72.9	80.2	179.0	80.8
218.5	77.2	85.4	196.5	84.8
244.0	83.3	91.2	219.5	89.2
264.5	86.6	94.8	243.0	93.1
289.0	90.1	97.4	269.0	96.3
317.0	93.3	99.1	295.0	98.6
363.5	97.8	100.0	315.0	99.8
438.5	100.0	100.0	338.0	100.0
483.0	100.0	100.0	361.5	100.0

Table A.10 Water content (measured by Karl Fischer tritration) of p(FAD:SA) copolymers during erosion

Time (hours)	% Water 5:5	Time (hours)	% Water 2:8	% Water 7:3	Time (hours)	%Water 7:3	%Water 5:5
0.0	0.00	0.0	0.00	0.00	0.0	0.00	0.00
73.0	0.90	10.5	0.22	0.12	24.0	0.21	0.44
99.0	0.97	24.0	0.39	0.21	49.0	0.15	0.77
119.0	1.00	33.5	0.53	0.30	72.0		0.36
166.5	1.47	48.0	0.60	0.59	96.5	0.88	1.62
192.0	1.26	69.5	1.38	0.50	119.0	1.34	3.07
216.0	1.18	93.0		0.72	144.0		0.75
243.0	2.47	117.5	3.94	1.79	169.0		0.87
265.0	1.86	169.5	3.89				
		240.0	3.79				

Table A.11 Acid Orange (AO) release and Sebacic Acid (SA) erosion from p(FAD:SA) copolymers

Time (hours)	%AO 2:8	%SA 2:8	%AO 5:5	%SA 5:5	Time (hours)	%AO 7:3	%SA 7:3
0.0	0.0	0.0	0.0	0.0	0.0	0.0	0.0
3.0	8.0	0.0	4.0	0.0	3.0	6.1	0.0
7.0	13.8	0.1	5.9	0.0	7.0	8.1	0.0
11.0	20.1	0.6	7.7	0.4	11.0	8.8	0.4
22.0	36.7	4.5	22.9	3.2	22.0	9.4	3.4
26.0	39.7	7.0	32.9	6.4	34.0	9.9	10.0
30.0	41.5	9.1	37.4	9.6	46.0	16.1	17.5
34.0	43.0	11.5	42.0	14.9	57.0	25.3	24.0
46.0	47.1	19.5	45.7	25.2	68.5	32.3	30.0
57.0	50.8	26.3	47.3	32.2	78.5	39.2	36.4
68.5	55.3	33.3	48.9	38.6	94.0	44.9	42.5
78.5	58.0	37.6	50.1	42.0	120.0	54.3	53.0
94.0	62.7	42.8	52.5	47.0	143.0	60.5	59.8
120.0	71.8	54.1	56.2	53.0	166.0	67.8	67.1
143.0	79.3	63.3	60.1	57.7	190.0	74.8	73.7
166.0	86.6	71.4	64.1	62.7	214.0	79.0	77.9
190.0	93.0	78.5	68.7	67.7	239.5	84.5	83.5
214.0	97.9	86.0	73.3	72.2	273.0	90.4	89.6
239.5	100.0	92.9	77.4	76.2	300.0	94.7	95.0
273.0	100.0	99.9	81.0	79.8	326.0	96.9	98.2
300.0	100.0	100.0	85.2	83.9	353.0	97.5	99.4
326.0	100.0	100.0	87.5	86.8	441.0	98.5	100.0
			89.9	89.8	537.0	99.1	100.0
			92.2	92.5	720.0	100.0	100.0
			94.7	95.2			
			98.1	99.2			
			99.2	100.0			

Table A.12 Acid Orange (AO) release and Sebacic Acid (SA) erosion from p(FAD:SA) copolymers at different AO loadings

Time (hrs)	%AO 1%	%SA 1%	Time (hrs)	%AO 3%	%SA 3%	%AO 7%	%SA 7%	Time (hrs)	%AO 10%	%SA 10%	Time (hrs)	%SA 0%
0.0	0.0	0.0	0.0	0.0	0.0	0.0	0.0	0.0	0.0	0.0	0.0	0.0
3.0	5.5	0.0	3.0	4.0	0.0	5.8	0.0	3.0	9.2	0.0	18.0	5.3
11.0	10.8	0.5	7.0	5.9	0.0	8.4	0.0	7.0	12.5	0.3	43.0	21.8
22.0	24.5	3.0	11.0	7.7	0.4	10.5	0.5	11.0	14.4	0.5	66.0	33.4
26.0	32.2	6.3	22.0	22.9	3.2	33.7	4.9	22.0	44.2	5.2	96.0	43.5
30.0	35.6	9.8	26.0	32.9	6.4	44.7	9.2	26.0	64.9	8.6	120.0	54.2
34.0	37.3	14.3	30.0	37.4	9.6	50.7	13.0	30.0	83.1	12.3	162.0	67.0
46.0	39.8	26.3	34.0	42.0	14.9	55.5	17.5	34.0	91.6	17.4	190.0	76.6
57.0	41.1	33.6	46.0	45.7	25.2	60.9	26.6	46.0	96.7	29.3	215.0	82.5
68.5	43.2	39.7	57.0	47.3	32.2	65.8	35.1	57.0	98.3	39.7	1200.0	100.0
78.5	45.4	43.3	68.5	48.9	38.6	68.3	39.6	68.5	99.1	48.7		
94.0	48.6	48.0	78.5	50.1	42.0	69.3	42.5	78.5	99.4	56.4		
120.0	56.2	57.8	94.0	52.5	47.0	69.8	45.4	94.0	99.7	63.9		
143.0	63.7	64.6	120.0	56.2	53.0	71.2	52.0	120.0	99.9	73.3		
166.0	69.8	70.7	143.0	60.1	57.7	72.8	56.3	143.0	100.0	78.5		
190.0	74.7	75.4	166.0	64.1	62.7	75.5	61.6	166.0	100.0	82.6		
214.0	79.8	80.0	190.0	68.7	67.7	78.0	66.6	190.0	100.0	84.7		
239.5	83.1	83.3	214.0	73.3	72.2	80.0	70.2	214.0	100.0	87.3		
273.0	86.4	86.6	239.5	77.4	76.2	82.6	74.2	273.0	100.0	94.0		
300.0	89.6	90.3	273.0	81.0	79.8	85.5	79.6	353.0	100.0	99.0		
326.0	91.9	93.1	300.0	85.2	83.9	89.0	85.3	441.0	100.0	100.0		
353.0	94.1	95.0	326.0	87.5	86.8	91.6	89.7	720.0	100.0	100.0		
441.0	97.6	98.8	353.0	89.9	89.8	94.4	94.1					
537.0	99.0	100.0	377.0	92.2	92.5	97.1	97.2					
720.0	100.0	100.0	399.0	94.7	95.2	98.6	98.8					
			441.0	98.1	99.2	99.4	100.0					
			537.0	99.2	100.0	99.8	100.0					
			720.0	100.0	100.0	100.0	100.0					

Table A.13 Effect of drug incorporation method (emulsion vs mix) on AO release and %SA erosion from p(SA)

Time (hours)	%AO emul	%SA emul	%AO mix	%SA mix
0.0	0.0	0.0	0.0	0.0
2.0	4.0	1.1	25.3	1.8
6.0	10.3	5.9	31.5	8.0
11.5	21.1	13.2	42.0	17.2
23.0	44.2	27.2	73.1	33.6
33.0	62.6	36.2	91.1	41.3
46.5	86.0	44.7	97.2	50.8
55.3	92.6	46.1	98.3	54.9
70.5	96.9	53.3	99.5	61.8
80.0	98.2	57.9	100.0	64.5
95.5	99.3	65.3	100.0	71.0
119.0	100.0	75.5	100.0	81.0
143.0	100.0	83.3	100.0	88.0
169.0	100.0	89.0	100.0	93.3
191.0	100.0	92.5	100.0	96.3
215.0	100.0	94.4	100.0	97.8
239.0	100.0	95.9	100.0	98.8

Table A.14 Acid Orange (AO) release and Sebacic Acid (SA) erosion from p(FAD:SA) copolymers fabricated by the emulsion method

Time (hours)	%AO 5:5	%SA 5:5	Time (hours)	%AO 2:8	%SA 2:8	%AO p(SA)
0.0	0.0	0.0	0.0	0.0	0.0	0.0
2.0	1.8	0.0	2.0	4.1	1.6	4.0
11.5	4.2	2.7	6.0	13.4	7.5	10.3
23.0	10.9	9.3	11.5	28.3	25.0	21.1
33.0	30.9	20.4	23.0	54.3	32.1	44.2
46.5	56.9	39.6	33.0	69.3	57.1	62.6
55.3	67.7	52.5	46.5	83.1	69.2	86.0
70.5	81.9	73.5	55.3	88.8	79.6	92.6
80.0	85.5	81.7	70.5	97.1	82.4	96.9
95.5	89.8	93.5	80.0	99.5	91.5	98.2
119.0	92.7	100.0	95.5	100.0	99.0	99.3
143.0	94.1	100.0	119.0	100.0	100.0	100.0
169.0	96.2	100.0	143.0	100.0	100.0	100.0
191.0	98.6	100.0	169.0	100.0	100.0	100.0
215.0	99.3	100.0	191.0	100.0	100.0	100.0
239.0	100.0	100.0	215.0	100.0	100.0	100.0

Table A.15 Rhodamine B Base (RhBB) release and Sebacic Acid (SA) erosion from p(FAD:SA) copolymers at different RhBB loadings

Time (hrs)	RhBB 2:8 3% 1	RhBB 2:8 3% 2	SA 2:8 3% 1	SA 2:8 3% 2	RhBB 5:5 1%	SA 5:5 1%	RhBB 5:5 3% 1	RhBB 5:5 3% 2	SA 5:5 3% 1	SA 5:5 3% 2	RhBB 5:5 7%	SA 5:5 7%	RhBB 7:3 3%	SA 7:3 3%
0.0	0.00	0.00	0.00	0.00	0.00	0.00	0.00	0.00	0.00	0.00	0.00	0.00	0.00	0.00
2.5	1.82	2.26	1.44	1.25	5.19	0.78	3.78	2.60	1.55	0.89	5.05	5.06	10.12	3.17
4.5	2.59	3.06	2.29	11.83	7.40	1.88	5.56	4.02	2.68	1.86	7.15	7.47	12.97	5.40
8.5	3.96	4.60	4.96	14.44	10.68	4.78	8.74	6.73	5.94	4.53	10.71	13.63	17.71	10.61
13.0	5.75	6.61	9.23	18.17	14.28	9.72	12.72	9.88	11.47	9.29	13.55	19.42	20.76	16.87
22.0	8.85	10.37	17.24	24.90	19.27	19.83	18.20	15.11	23.35	18.53	18.05	27.97	24.56	27.36
30.0	12.23	13.74	24.33	30.63	23.80	27.48	22.76	19.46	31.91	25.31	21.70	33.45	28.28	33.32
37.5	15.33	17.15	30.69	35.30	27.01	32.96	26.53	23.10	38.24	31.34	25.47	37.89	34.30	43.39
45.5	18.28	20.77	36.56	40.16	31.04	38.95	30.50	26.74	44.12	37.36	28.83	42.94	39.23	53.94
54.0	21.15	24.03	41.49	44.70	34.48	43.96	34.17	30.06	49.63	42.55	33.34	47.40	43.87	63.78
61.0	23.22	27.37	45.15	48.47	37.61	47.99	37.37	32.86	53.71	46.35	36.30	50.68	47.16	67.67
70.0	27.78	31.05	51.13	52.89	40.79	53.58	40.73	35.76	58.70	50.96	40.50	55.62	50.53	73.60
80.0	31.49	34.83	56.19	57.03	44.45	59.56	44.49	38.85	63.40	55.99	46.85	60.27	53.78	79.78
100.0	38.14	41.85	63.71	64.17	50.50	71.79	51.37	44.89	74.52	66.28	52.81	69.54	59.76	89.02
128.0	46.77	50.07	74.48	72.83	59.15	82.30	59.89	51.56	87.53	80.10	58.80	83.30	66.58	96.74
152.0	53.76	59.02	81.25	78.98	65.98	90.39	67.13	59.08	94.46	89.09	64.87	91.31	71.95	100.00
175.0	59.42	67.07	85.82	83.49	71.66	94.75	74.48	67.00	98.80	94.87	69.84	96.67	75.33	100.00
197.0	69.75	71.45	90.28	85.49	76.37	97.43	81.18	74.31	100.00	98.77	75.70	99.50	77.78	100.00
215.0	75.03	75.26	91.78	87.87	80.34	98.83	85.81	80.97	100.00	100.00	79.59	100.00	79.98	100.00
243.0	80.78	78.89	93.60	90.53	84.90	100.00	89.77	86.43	100.00	100.00	83.15	100.00	82.10	100.00
296.0	86.71	83.21	96.05	92.89	90.09	100.00	93.50	91.05	100.00	100.00	87.26	100.00	85.17	100.00
339.0	91.64	89.72	98.37	94.56	93.65	100.00	96.17	94.18	100.00	100.00	90.76	100.00	88.28	100.00
387.5	95.38	95.28	99.58	95.44	96.66	100.00	97.81	96.15	100.00	100.00	93.22	100.00	90.60	100.00
462.0	97.95	97.60	99.92	95.86	98.88	100.00	98.97	97.52	100.00	100.00	95.63	100.00	94.51	100.00
1155.0	99.35	99.62	100.00	100.00	100.00	100.00	99.62	98.17	100.00	100.00	97.49	100.00	97.86	100.00
1323.0	99.97	99.95	100.00	100.00	100.00	100.00	99.99	99.96	100.00	100.00	99.04	100.00	100.00	100.00

Table A.16 Effect of droplet size (1-7 microns [S]) vs 20-80 microns [L]) in emulsion on dextran (20k and 150k) release from p(FAD:SA) copolymers

Time (hours)	2:8 20k S #1	2:8 20k S #2	5:5 20k S #1	5:5 20k S #2	5:5 150k S #1	5:5 150k S #2	Time (hours)	2:8 20k L #1	2:8 20k L #2	5:5 20k L #1	5:5 20k L #2
0	0.0	0.0	0.0	0.0	0.0	0.0	0	0.0	0.0	0.0	0.0
17	7.6	5.6	14.3	19.6	25.6	19.0	21	46.8	49.1	62.7	53.0
45	26.3	25.0	19.3	24.3	28.0	23.0	46	67.3	68.6	70.1	63.2
68	38.9	36.7	27.4	32.0			72	71.2	72.2	77.4	74.1
89	46.9	43.2	35.4	41.5	31.0	27.6	93	72.6	73.3	78.6	77.3
117	55.4	49.9	45.4	51.5			114	75.9	75.1	79.6	79.6
142	59.8	53.9	51.5	55.9	39.2	34.9	165	78.2	77.5	82.8	83.2
165	64.3	59.4	60.9	61.2	44.7	40.3	259	79.1	78.5	83.6	84.1
238	65.8	61.6	64.7	63.1	48.0	43.9	427	80.5	80.0	85.9	86.6
283	67.2	62.9	65.9	64.2	48.9	44.4	670	81.7	81.2	86.4	87.1
357	71.8	67.6	69.1	67.0	51.2	45.3					
792	78.8	76.4	78.9	75.7	59.9	49.8					

Table A.17 Peroxidase release and SA erosion from 9% loaded p(FAD:SA) 50:50

Time (days)	%Peroxidase	%SA
0	0.00	0.00
1	9.20	29.68
2	13.30	61.45
3	23.50	77.06
4	33.40	91.82
5	42.60	98.95
6	51.80	99.44
7	55.30	99.58
8	56.60	100.03

Table A.18 Peroxidase activity and aggregation (SEC) from 9% loaded p(FAD:SA) 50:50 compared to control (0.07 mg/ml in buffer)

Time (days)	%Active 5:5 #1	%Aggregated #1	%Activity 5:5 #2	%Active Control
0	100	0	65	100
1	100	0	67	88
3	100	0	85	55
4	76	0	100	41
5	52	36	39	35
6	21	61	4	25
7	0	100	0	22
8	0	100	0	13

Table A.19 Effect of pH and FAD monomer (0.1 g) on %peroxidase (0.1 mg/ml) activity

Time (days)	pH 5 #1	pH 5 FAD #1	pH 5 #2	pH 5 FAD #2	pH 6	pH 6 FAD	pH 9	pH 9 FAD	pH 7.4	pH 7.4 FAD	pH 3	pH 3 FAD
0	100.0	100.0	100.0	100.0	100.0	100.0	100.0	100.0	100.0	100.0	100.0	100.0
1	65.2	72.8	62.7	62.9	87.9	87.4	67.4	27.1	95.2	51.9	2.0	1.7
2	49.2	56.2	43.6	40.6	82.5	82.4	51.4	8.6	78.2	17.1	0.0	0.1
3	45.6	43.8	32.2	33.0	86.2	79.4	39.2	3.9	62.4	5.7	0.0	0.0
4	34.7	34.7	32.5	28.9	81.4	74.5	34.9	1.9	61.3	3.5		
5	36.7	30.2	23.8	16.7	85.3	71.9	23.0	1.2	45.9	1.8		
6	25.7	23.4	21.4	13.6	77.4	59.8	20.6	1.1	41.9	1.0		
7	27.7	23.3	22.1	11.9	84.2	63.2	9.2	0.7	43.9	0.5		
8	24.9	17.5	100.0	100.0	75.7	61.1	8.0					

Table A.20 Isoelectric focusing of Type II horseradish peroxidase

Protein	Retention (mm)	Approx pI
Amyloglucosidase	4.0	3.8
Ovalbumin	7.5	5.1
Carbonic Anhydrase	22.5	7.0
Myoglobin	37.5	7.6
Peroxidase (Sigma P-8250)	13.4	5.8